

dti

**EB FROND WAVE ENERGY
CONVERTER – PHASE 2**

CONTRACT NUMBER: V/06/00204/00/00

URN: 05/865

dti

The DTI drives our ambition of 'prosperity for all' by working to create the best environment for business success in the UK.

We help people and companies become more productive by promoting enterprise, innovation and creativity.

We champion UK business at home and abroad. We invest heavily in world-class science and technology.

We protect the rights of working people and consumers. And we stand up for fair and open markets in the UK, Europe and the world.

**EB FROND WAVE ENERGY
CONVERTER – PHASE 2**

**V/06/00204/00/REP
URN 05/865**

Contractor

The Engineering Business Ltd

The work described in this report was carried out under contract as part of the DTI Technology Programme: New and Renewable Energy, which is managed by Future Energy Solutions. The views and judgements expressed in this report are those of the contractor and do not necessarily reflect those of the DTI or Future Energy Solutions.

First published 2005
© Crown Copyright 2005

Executive Summary

Project Objectives

Having demonstrated the fundamental proof of concept for the EB Frond Wave Energy Collector through the Phase one project, the next step (the Phase two project) was proposed to further assess the technical and commercial viability of the EB Frond concept through the development of the existing mathematical and physical modelling methods.

Introduction

The Engineering Business (EB) is firmly established as a developer of renewable offshore power generators. EB is a design and manufacturing company specialising in underwater equipment, having successfully developed systems to install, bury and protect subsea infrastructure in the cable and pipeline markets. Based on expertise in this environment, EB has been investigating Renewable Offshore Power Generation ideas since 1997, including the 150kW demonstrator of the Stingray tidal stream generator.

Marine renewable energy sources, including tidal stream and wave energy, have the potential to become commercially viable, although detailed investigation and technology development will be required at an accelerating pace to achieve this aim. To date, the major wave energy developments are either onshore or offshore systems. Few are targeting the nearshore environment.

The EB Frond project is the wave energy programme developed by The Engineering Business Ltd (EB), following on from an original idea conceived at Lancaster University.

EB Frond is a wave generator with a collector vane at the top of an arm pivoted near the seabed. The arm oscillates like an inverted pendulum, driven by the water particle motion in the waves. EB Frond incorporates devices which allow the pendulum motion to be tuned to the dominant frequency of the waves, and a set of hydraulic cylinders connected between the arm and the structure which deliver high-pressure oil to a hydraulic motor connected to an electrical generator. The structure is held rigidly on the seabed in a nearshore location and remains submerged at all times.

A technical and economic feasibility study (Phase one) of EB Frond conducted in 2003, with partial grant funding from the DTI, demonstrated that the EB Frond concept is technically feasible and has the potential to produce electricity at a unit energy cost comparable with published data from other technologies. However, this was little more than proof of concept and further work is required. It was identified that risks exist in extrapolating from small-scale to full size energy output, and that a phased development programme, from small-scale (1/25th), through intermediate scale (1/5th) to a full-scale demonstration device before final commercialisation should be the preferred development route. It was also recognised that, whilst sites for demonstration and commercial machines could be found, further work would be needed to characterise, identify and develop them.

Summary of Work

To meet the identified objectives, and take the EB Frond programme forward along the preferred development route, a number of specific tasks were identified for Phase two. These encompassed:

- Further small-scale (1/25th) testing to investigate of wave tank characteristics and their effect on EB Frond model testing, and investigation of the response of EB Frond to random waves, tidal range and extreme wave conditions.
- Development of a mathematical model for the EB Frond system, including its verification by a recognised external specialist and its validation against the acquired experimental data.
- Testing at an intermediate (1/6th) scale, including validation of scaling assumptions by comparison with small (1/25th) scale test results, reduction of uncertainties in scaling wave heights by extending the wave height envelope at 1/6th scale, and testing of selected survival strategy designs.
- Assessment of different survival strategies in extreme wave conditions.
- Site characterisation for full-scale systems.
- Use of the designs, test results and site characterisation to produce a robust economic model.

Physical modelling was performed at small (1/25th) scale. It was originally proposed to follow this up with testing at an intermediate (1/6th) scale, with waves simulating a full-scale crest to trough height of at least 4 metres. This would have permitted scaling factors to be confirmed, increased confidence in the engineering and economic predictions (including power output) and enabled costings to be reviewed for input to the economic model.

However, on completion of the small-scale testing, EB took the decision to place its renewable generation programme (EB Frond and Stingray) on hold until such a time that a development path incorporating commercial returns for EB could be identified. The intermediate scale testing and site characterisation was, therefore, not undertaken.

Summary of Results

The small-scale testing was undertaken in three stages in wave tanks at Newcastle and Lancaster Universities. These testing stages facilitated the evolution of the EB Frond collector design to a triangular shape. Testing of the current EB Frond design suggested that a power output of 263kW could be expected from the full-scale machine in a 3m significant wave height Pierson-Moskowitz sea-state.

A time domain mathematical model was developed by EB to model the EB Frond system. The theoretical basis of the model was verified by Professor Incecik of Newcastle University, with Professor Bradshaw (Lancaster University) validating it against the available Lancaster University linear models. Comparison of the EB time domain model, Lancaster linear model, and physical test results was undertaken by EB. In the sample test cases the EB time domain model agreed with physical results,

in terms of maximum time-averaged power predictions to within 61%, in the case of the linear model this discrepancy was 1556%. From these results Professor Atilla Incecik wrote “your mathematical method, which includes all the non-linear above terms, can represent the physical behaviour of your device accurately” and that “In conclusion the non-linear model that you have developed to predict the oscillation of the EB Frond and the energy output is the most appropriate for the design optimisation of your wave power generator.”

As indicated above, the Phase two project was stopped before the intermediate scale testing was undertaken. This reduced the scope of the project, since, in addition to the 1/6th scale model testing, this stage was also to include the site characterisation work and the majority of the survival strategy development work. Although the survival strategies could not be tank tested, some theoretical analysis and development work was undertaken.

The mathematical and physical modelling work was used to develop an economic model for the EB Frond system. Results from this economic model suggest that, with a 5MW pre-commercial demonstrator farm, the current EB Frond design could produce electricity at an overall cost of 17p/kWh.

Conclusions

The work has demonstrated that:

- In sinusoidal waves, there is good agreement between the EB time domain mathematical model predictions and physical model tests of maximum power output.
- In comparisons between the corrected linear model and the EB time domain model, agreement with the same physical tests produced a maximum power output estimation error of a 61% overestimation for the time domain model compared to an overestimation from the corrected linear model of 1556%.
- In random two dimensional waves (Pierson-Moskowitz spectra), the EB time domain model predicted average maximum power outputs, over a long period, which were less than twice the results of the physical model.
- Review of the survivability strategies could not lead to a conclusion without further physical modelling and parallel design study.
- The predicted unit cost of electricity produced by a pre-commercial 5MW demonstrator EB Frond wave farm located at a high energy wave site with 25 year machine life, assuming no contribution from ROCs, no profit element in construction, and 8% discount rate, is about 17p/kWh.
- The cost of electricity produced by EB Frond is likely to reduce in line with technology experience / cost curves published for a number of technologies.

Recommendations

EB Frond has moved forward significantly from the original Frond concept developed by Lancaster University. However, there is still a lot to learn beyond the basic tank testing and rudimentary mathematical modelling undertaken to date.

To take the EB Frond concept through to commercial reality, the following development route is proposed:

- (i) Small-scale testing – there may be a benefit from further small-scale testing to demonstrate repeatability and check less certain data points
- (ii) Intermediate-scale modelling – ideally at least 1/6th scale, if a suitable facility is available, to check performance in extreme seas and for review of scaling effects
- (iii) Site Characterisation
- (iv) Environmental Impact Appraisal
- (v) Full-scale demonstrator – ideally grid connected, to demonstrate the full scope of an EB Frond – installation, operation and maintenance, reliability, power generation and decommissioning
- (vi) Full-scale pre-commercial demonstrator farm – grid connected

CONTENTS

1	INTRODUCTION	1
1.1	The EB Frond Project	1
1.1	The EB Frond Principle	1
1.2	Background to Phase Two	1
1.3	Phase Two Objectives	1
2	SMALL-SCALE TESTING	3
2.1	Objectives and Test Philosophy	3
2.2	Test Sequence	3
2.3	Model Evolution	3
2.4	Test Frame	4
2.4.1	Support Frame	4
2.4.2	Power Take-Off System	5
2.4.3	Restoring Force System	7
2.5	Wave Tanks	8
2.5.1	Newcastle	8
2.5.2	Lancaster	9
2.6	Experimental Procedure	12
2.6.1	Maximum Time-Averaged Power Output	12
2.6.2	Power to Restoring Force Ratio	13
2.6.3	EB Frond Efficiencies	13
2.7	Experiments	14
2.7.1	Newcastle University	14
2.7.2	Lancaster University Visit One	16
2.7.3	Lancaster University Visit Two	21
3	TEST RESULTS	27
3.1	Newcastle	27
3.1.1	Wave Amplitude Variation	27
3.1.2	Freeboard Variation	27
3.1.3	Wave Incidence Angle Variation	28
3.1.4	Collector Thickness Change	29
3.1.5	Sea Spectra	29
3.1.6	Comparison with Phase One Test Results	29
3.2	Lancaster First Set of Results	30
3.2.1	Thickness Variation	30
3.2.2	Width Variation	32
3.2.3	Draught Variation	34
3.2.4	Added Mass Interchange	36
3.2.5	Radiussed Collector	36

3.2.6	Half Cylindrical Collector	37
3.2.7	Cylindrical Collector	38
3.2.8	Wave Period Variation	38
3.2.9	Summary	40
3.3	Lancaster Second Set of Results	41
3.3.1	Comparison of Half Cylindrical and Triangular Collectors	41
3.3.2	Buoyancy	42
3.3.3	Freeboard	43
3.3.4	Pierson-Moskowitz Seas	44
4	MATHEMATICAL MODELLING	49
4.1	Philosophy and Objectives of Modelling	49
4.2	Choice of Model	49
4.3	Workings of Model	50
4.3.1	Introduction	50
4.3.2	Overview	50
4.3.3	Time Domain Calculations	50
4.3.4	Non-Time Domain Calculations	56
4.4	General Testing Process	57
4.4.1	Natural Period Tests	57
4.4.2	Radiation Damping Coefficient Tests	58
4.4.3	Maximum Power Output Tests	58
4.4.4	Water Torque Amplitude Tests	59
4.5	Validation Process	60
5	ANALYSIS AND INTERPRETATION	61
5.1	Newcastle	61
5.1.1	Wave Amplitude Variation	61
5.1.2	Freeboard Variation	61
5.1.3	Wave Incidence Angle Variation	61
5.1.4	Collector Thickness Change	61
5.1.5	Sea Spectra	61
5.2	Implemented Improvements in Experimental Operation	62
5.2.1	PTO System	62
5.2.2	Restoring Force System	62
5.2.3	Wave Tank	62
5.2.4	EB Frond Natural Period	63
5.2.5	Calculation of Maximum Possible Power	63
5.2.6	Summary of Limitations	63
5.3	Lancaster First set of results	64
5.3.1	Thickness Variation	64
5.3.2	Width Variation	64
5.3.3	Draught Variation	64
5.3.4	Added Mass Interchange	65
5.3.5	Radiussed Collector	65
5.3.6	Half Cylindrical Collector	65
5.3.7	Cylindrical Collector	65

5.3.8	Wave Period Variation	66
5.3.9	Summary	66
5.4	Lancaster Second Set of Results	66
5.4.1	Comparison of Half Cylindrical and Triangular Collectors	66
5.4.2	Buoyancy	66
5.4.3	Freeboard	66
5.4.4	Pierson-Moskowitz Seas	67
5.5	Full-Scale Power predictions	67
5.6	Testing Limitations Specific to the Lancaster Results	69
5.7	Mathematical and Physical Model Comparisons	69
5.7.1	Newcastle	69
5.7.2	Lancaster First Set of Results	70
5.7.3	Lancaster Second Set of Results	74
5.7.4	Conclusions and Limitations	79
5.8	Possibility of Achieving Maximum Theorised Point Absorber Power Output	80
5.9	Repeatability and Level of Confidence in Results	80
6	SURVIVABILITY	83
6.1	Introduction	83
6.1.1	Collector Head	84
6.1.2	Collector Arm	85
6.1.3	Base	86
6.1.4	Summary	86
6.2	Breaking and Freak Waves	86
6.2.1	Breaking Waves	86
6.2.2	Freak Waves	88
6.2.3	Wave Structure Interaction	88
6.2.4	Tidal Effects	88
6.3	Possible Damage and Failure Scenarios	89
6.4	Survival Strategies	89
6.4.1	Free to Swing	90
6.4.2	Fixed to Seabed	90
6.4.3	Lowering Collector from Surface	91
6.4.4	Reduction in Collector Volume/Area	92
6.4.5	Inflatable Collector	93
6.4.6	Breakaway Collector Head	94
6.4.7	Summary of Survival Methods	94
6.5	Summary	95
7	ECONOMIC MODEL	97
7.1	Introduction	97
7.2	Energy Capture Estimates	97
7.2.1	Machine Characteristics	97

7.2.2	Site Characteristics	97
7.2.3	Wave Resource	98
7.2.4	Gross Power Capture	100
7.2.5	Energy Losses – Marine Climate	103
7.2.6	Machine and Electrical Losses	107
7.2.7	Cyclic Power Variation, Multi-Machine Outputs and Power Transmission	108
7.2.8	Summary – Nett Annual Energy Estimates	109
7.3	Capital and Operating Cost Estimates	110
7.4	Energy Cost Modelling	111
7.5	Summary	113
8	DEVELOPMENT ROUTE TO FULL-SCALE PRODUCTION	115
8.1	Limitations of Current Understanding	115
8.2	Proposed Development Route	115
9	CONCLUSIONS	117

1 INTRODUCTION

1.1 The EB Frond Project

The EB Frond project is the wave energy programme developed by The Engineering Business Ltd (EB), following on from an original idea conceived at Lancaster University.

The Engineering Business (EB) is firmly established as a developer of renewable offshore power generators. EB is a design and manufacturing company specialising in underwater equipment, having successfully developed systems to install, bury and protect subsea infrastructure in the cable and pipeline markets. Based on expertise in this environment, EB has been investigating Renewable Offshore Power Generation ideas since 1997, including the 150kW demonstrator of the Stingray tidal stream generator.

1.1 The EB Frond Principle

EB Frond is a wave generator with a collector vane at the top of an arm pivoted near the seabed. The arm oscillates like an inverted pendulum, driven by the water motion in the waves. EB Frond incorporates devices which allow the pendulum motion to be tuned to the dominant frequency of the waves, and a set of hydraulic cylinders connected between the arm and the structure which deliver high-pressure oil to a hydraulic motor connected to an electrical generator. The structure is held rigidly on the seabed in a nearshore location and remains submerged at all times.

1.2 Background to Phase Two

A technical and economic feasibility study (Phase one) of EB Frond conducted in 2003, with 75% grant funding from the DTI, demonstrated that the EB Frond concept is technically feasible and has the potential to produce electricity at a unit energy cost comparable with published data from other technologies. However, this was little more than proof of concept and further work is required. It was identified that risks exist in extrapolating from small-scale to full size energy output, and that a phased development programme, from small-scale (1/25th), through intermediate scale (1/5th) to a full-scale demonstration device before final commercialisation should be the preferred development route. It was also recognised that, whilst sites for demonstration and commercial machines could be found, further work would be needed to characterise, identify and develop them.

1.3 Phase Two Objectives

This Phase two study builds on the investigation work from Phase one, developing the mathematical modelling to cover a wider range of wave effects, and extending the physical modelling to include random and higher energy waves than were used in Phase one. The identified objectives included:

- Investigation of wave tank characteristics and their effect on model testing.
- Furthering investigation of response to random waves, tidal range and extreme wave conditions.

- Development of a mathematical model for the EB Frond system, including its verification by a recognised external specialist and its validation against experimental data.
- Testing at intermediate (1/6th) scale and validation of scaling assumptions by comparison with small (1/25th) scale test results.
- Reduction of uncertainties in scaling wave heights by extending the wave height envelope at 1/6th scale (not completed).
- Assessment of different survival strategies in extreme wave conditions
- Use of the designs, test results and site characterisation to produce a robust economic model.

Physical modelling was performed at small (1/25th) scale. It was originally proposed to follow this up with testing at an intermediate (1/6th) scale, with waves simulating a full-scale crest to trough height of at least 4 metres. This would have permitted scaling factors to be confirmed, increased confidence in the engineering and economic predictions (including power output) and enabled costings to be reviewed for input to the economic model.

This report also contains an analysis and interpretation of the results and a discussion of their implication for the project and for EB Frond technology as a whole.

2 SMALL-SCALE TESTING

2.1 Objectives and Test Philosophy

The objectives of the physical model testing of EB Frond were to investigate and understand the interaction of EB Frond with waves, both sinusoidal and random, representing different sea conditions.

A key aspect of this was the measurement of PTO from the scaled down models of potential EB Frond designs. These PTO values can then be scaled up to achieve full-scale power predictions. Imperfections in the small-scale replication of the device and environment will exist. However, with these errors borne in mind, the full-scale power predictions derived can be treated with much higher confidence than any mathematical simulations, with their inevitable simplifications and assumptions, the significance of which may be impossible to accurately quantify.

The physical modelling also serves as a validation tool for the mathematical model. Situations in which the two models disagree suggest limitations in one or other modelling techniques – generally because the mathematical modelling techniques have been used beyond the limit of their applicability.

In the past, work carried out by Lancaster University Engineering Department (LUED) had been performed at 1/33rd scale to suit their wave tank. However, EB believed that a larger scale test could be undertaken without detracting from the tank performance. The 1/25th scale was therefore selected as being the largest that could be used without invalidating the test work. At this scale the wave periods are equivalent to scale (ie 1/5th in this case). If the scale were bigger, the tank would not accurately achieve the required periods due to reasons such as tank reflections, beaching inefficiencies, etc.

2.2 Test Sequence

The Phase one testing was carried out at the LUED wave tank. For the first element of testing in Phase two, the test activities were switched from LUED (whose tank was undergoing modification at the required time) to the wave tank at Newcastle University Marine Science and Technology Department. Testing returned to LUED for the latter stages of the Phase two work, after the tank had been fully modified and represented a more suitable test facility.

2.3 Model Evolution

The fundamental EB Frond geometry is one of a collector surface mounted at the end of an oscillating arm. The original Phase one work comprised a preliminary investigation of a number of different configurations of this geometry at 1/33rd and 1/25th scale. The geometries investigated included tubular and solid constructions and square and rectangular shapes. This phase concluded that, although greater restoring forces were required, the solid rectangular constructions generated the greatest power.

The Phase two testing investigated the performance of this basic solid rectangular geometry in a wider range of sea conditions, and extended the investigation of collector shape through the testing of a number of variants on the rectangular shape. Details of model geometry and variation are given in Section 2.6

2.4 Test Frame

To enable the EB Frond models to be tested, they were positioned within the tank in a specially fabricated test frame. This comprised a support frame, a Power Take-off (PTO) system and a Restoring Force System (Figure 1). Modifications to these elements were made between the different stages of testing.



Figure 1: Test rig at Newcastle, comprising support frame, PTO and Restoring Force System

2.4.1 Support Frame

The support frame was constructed such that the model, PTO and restoring force systems could be secured to it. The EB Frond model was located centrally within the frame and was free to move about the pivot axis. The complete assembly could be rotated between tests to change its angle to incoming waves, whilst maintaining alignment with the PTO system and with the Restoring Force System, both of which were situated above water level. Spacers allowed a change of height of the model in the wave tank for tidal variation tests.

The support frame remained largely the same for all stages of testing, although it was heightened slightly for the P2 Lancaster work by lengthening the side bars to raise the top. This phase of testing also investigated changes in freeboard, accomplished by altering the pivot height of the collector head with reference to the

still water surface level. Seven pivot positions were provided in the base of the test rig as shown in Figure 2.

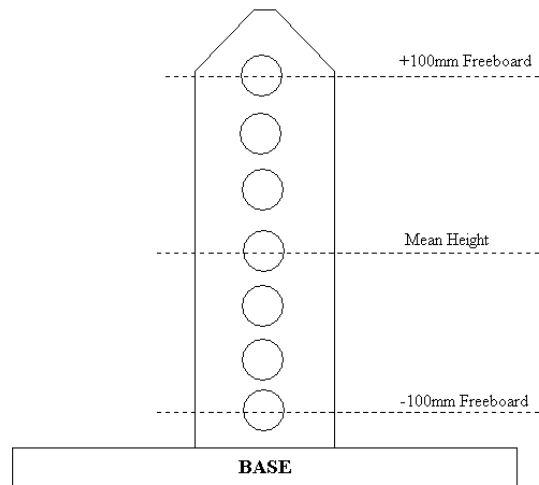


Figure 2 - Lancaster: Pivot Positions

2.4.2 Power Take-Off System

In the Phase two Newcastle tests, as with the Phase one tests, a combination of an electric motor and a dynamometer was used as the PTO system, see Figure 3 and Figure 4.

The dynamometer consisted of a horizontal beam attached to the support frame by two strain-gauged arms. A DC motor and multi-turn potentiometer were mounted on the beam and a loop of cord with a tensioning spring was wound around pulleys on the motor and potentiometer spindles. The cord was attached to the model at a slot in the blade fixed to the top of the collector. The blade movement is aligned with the plane of the cord.

The cord transmits motion from the model to the spindles of the motor and potentiometer. By using it as a generator and connecting a resistor across its terminals, the motor provides a torque resisting its rotation in either direction. The torques are resolved as forces in the cord that retard the motion of the model.

The change of electrical resistance of the potentiometer is used to measure movement of the cord, which is closely related to the collector movement. The force applied to the model is measured by the strain gauge system.

The dynamometer used in these tests had the same strain gauge and position measurement system as previously used at Lancaster in Phase one, but a new system was fitted to improve the simulation of the PTO. As before, a cord attached to the model drove a pulley on a DC motor, but a new motor / encoder arrangement was used to provide viscous damping to the cord. A Pico ADC-11 data-logger provided the interface with a computer on which the data was stored.

It is believed that, at times, the motor may have been driving the device, although not to any significant extent. In addition, the cord attached to the dynamometer was

attached to the top of the EB Frond via a two pulley system. As such, it was always extending as the EB Frond oscillated, slipping, and causing unknown effects.

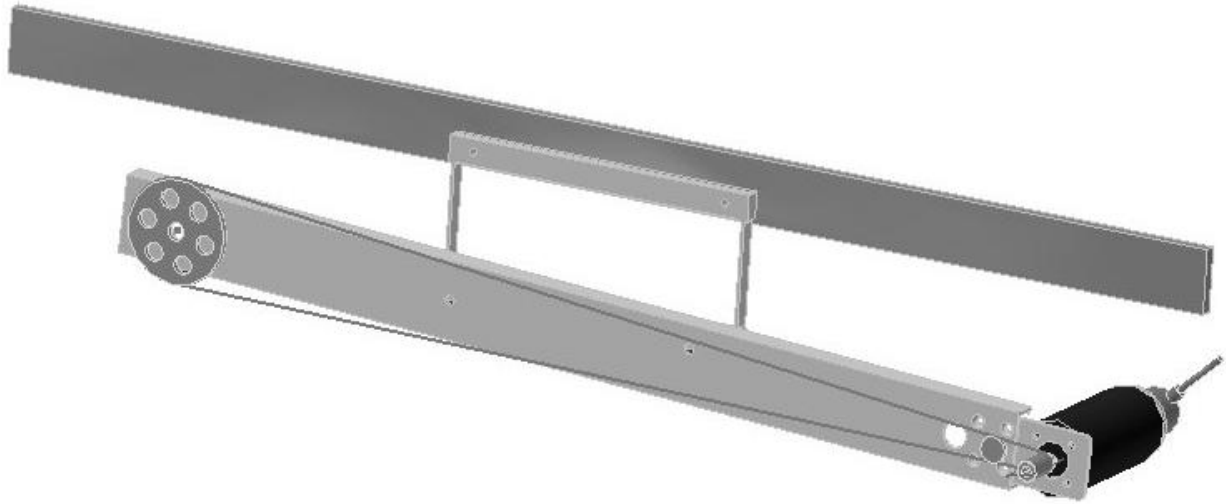


Figure 3 – Newcastle PTO system diagram

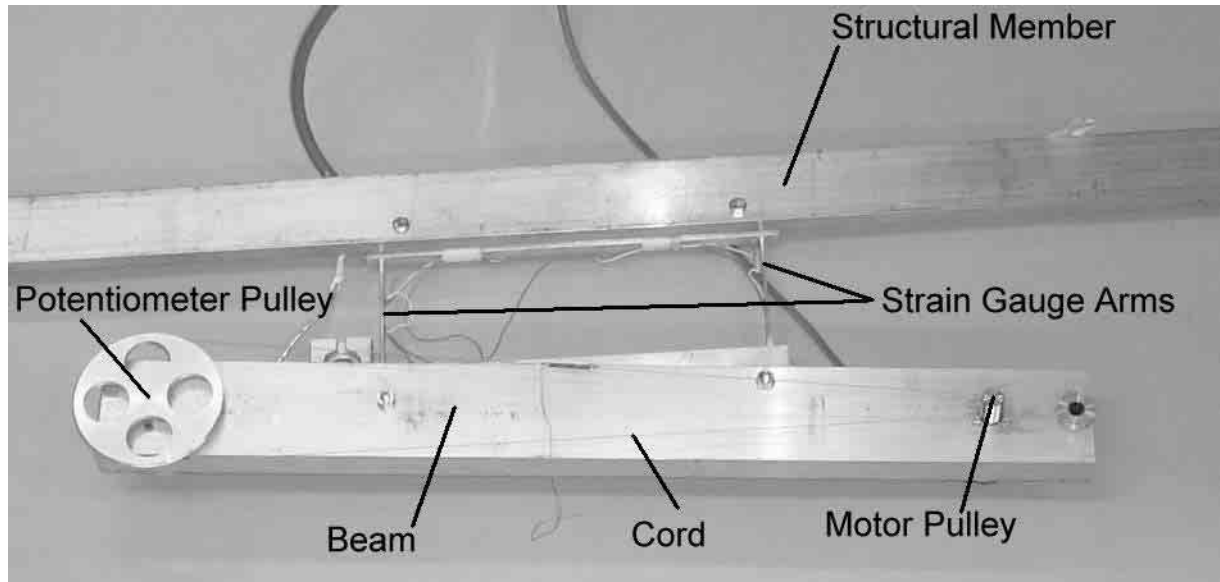


Figure 4 - Newcastle PTO system photograph

In the Lancaster Phase two testing this system was greatly improved. To allow energy to be taken from the EB Frond system the collector head was attached to a dynamometer, which comprised a toothed belt and motor (generator). Motor control was achieved through a PLC with resistance to motion being approximately proportional to instantaneous velocity of the slider (Figure 5), which was connected to the collector. This motor control system was regularly monitored to ensure the motor was behaving as intended - i.e. force proportional, and most importantly, opposite to speed. A fixed rod length, connecting the collector to the slider, was also used, which added to the improvement in test quality (Figure 6).



Figure 5 – Lancaster PTO system, toothed belt and slider



Figure 6 - Lancaster PTO system, attachment to collector

2.4.3 Restoring Force System

Vertical springs were attached to the top of the EB Frond collector, connecting it to the support frame. These springs applied upward forces on the collector. As the collector oscillates, the angle at which these spring forces act relative to the collector changes. The restoring torque is provided by buoyancy of the collector head in conjunction with the mass and stiffness of the springs. Restoring forces were adjusted and natural period calibrations were performed for each collector and each freeboard, so that any desired natural period of any EB Frond set-up could be achieved through appropriate manipulation of the restoring force system.

The Phase one arrangement at Lancaster had used extending coil springs from a fixed suspension point, which meant that the force increased with displacement of the collector, due to extensions in the springs. Problems were experienced with

spring extensions making the period change at large angles, which ruined the effect of resonance. If the EB Frond was tuned to resonate, it would be driven to large angles, the natural period of the system would then change and the resonance effects decreased, leading, once again, to smaller oscillations.

For the Newcastle tests, constant tension springs were used and the frame holding them was attached to an overhead beam. The constant tension springs consisted of a line wrapped around a constant pre-tensioned drum, so that increases in line length were achieved through the paying out of more line, rather than the extension of the existing line. However, the constant tension springs were found to have significant levels of inherent stiction. An example of this is that they were supposed to be held with 10N tension, but in fact with plus or minus 1N they wouldn't move either.

The Lancaster tests saw a change to a longer spring design, to ensure the natural period of the EB Frond did not change significantly when the collector oscillated with larger amplitudes. The springs used in the restoring force system were three metres long when unextended, and the minimum number of springs was used in each case. The springs selected were as light and long as possible to reduce the stiction and detuning effects suffered with the earlier designs. To enable the inclusion of these long springs the support frame was heightened, as indicated above. This arrangement had a low spring rate so that when the collector oscillated and slightly increased the spring extension, the net force changed as little as possible, see Figure 7.



Figure 7 – Lancaster collector attachment to restoring force system

2.5 Wave Tanks

The EB Frond Phase two 1/25th scale physical testing consisted of testing in the University of Newcastle wave tank and two sets of tests performed in the Lancaster University wave tank.

2.5.1 Newcastle

The wave tank at Newcastle University is shown in Figure 8 and Figure 9. It is 36m long and has a rectangular cross section 3.6m wide with a water depth of 1.2m. A

multi-paddle wave-maker at one end generates the waves with a servo-controlled motor individually driving each paddle.

The wave-maker is fixed in the tank, and the water depth cannot be changed. The depth is greater than was used in the Phase one tests at Lancaster, which at a fixed wave period has the effect of changing the proportion of wave energy intercepted by the 1/25th scale model collector. The tank is equipped with seven wave height gauges, comprising two rows of three in front of the model and one roving gauge situated next to the device.

The tank is used primarily for towing tests and does not have wave energy absorbing beaches that are sufficiently effective for EB Frond testing. Additional beaches were hired from the Wave Group at Edinburgh University and installed at Newcastle for the duration of the tests.



Figure 8 – Newcastle University Wave Tank (showing Beaches)



Figure 9 – Example of Experimental Arrangement at Newcastle

2.5.2 Lancaster

For the later stages of the small-scale testing, the project returned to the Engineering Department of Lancaster University. This wave tank is shown in Figure 10. The facility was upgraded during 2003 with the addition of Edinburgh Designs Ltd. wave paddles and control software. Seven paddles are used to generate waves of various periods and amplitudes, which propagate along the tank towards the beaches at the far end where their energy is absorbed. The paddles can produce sinusoidal waves and controlled random sea wave spectra consisting of many superimposed sine waves. The EB Frond test frame was placed in the tank next to an underwater window. Wave gauges were arranged in an array around the test frame to record water levels fore, aft and alongside the EB Frond model.

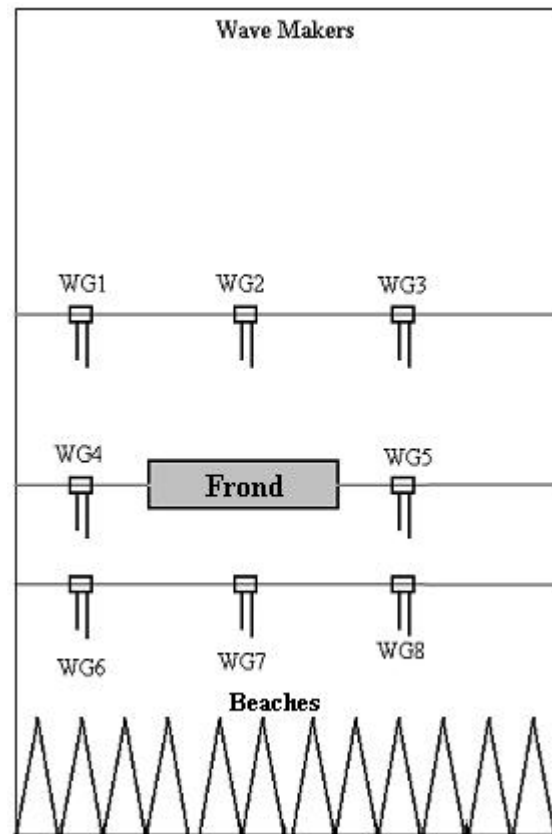


Figure 10 – Wave tank and corresponding schematic showing wave gauges (photograph courtesy Lancaster University Engineering Department)

The internal dimensions of the tank are 11.50m x 2.50m with a water depth of 0.855m. Limitations of the ability of the paddles to generate waves are shown in Figure 11. Achievable wave height is limited by the maximum travel of the paddle (for longer period waves the required travel for a given wave height is greater). For short period waves the limitation is that the waves break on the paddle when exceeding a certain height.

The efficiency of the beaches at removing energy from the waves falls as the wave period increases. Therefore longer period waves will generate some reflection through the beaches off the back wall of the tank. However, in the regime of interest, reflected waves only contain approximately 1% of the power of the generated waves. The wave generating paddles are force driven, to absorb reflected waves.

Eight wave gauges were used to measure wave heights and periods around the test area. Wave gauges are devices, which measure the water level at a certain point. The wave gauges worked by having two vertical wires dipped into the water. Electricity is conducted between the wires through the water. The higher the water levels the lower the resistance in the device. Hence through the monitoring of the effective resistance of the gauge, time histories of water levels are produced.

Data collection was provided by a digital acquisition board and dedicated computer running data acquisition software. This allowed 12 analogue voltage channels to be monitored and recorded at a sampling frequency of 30Hz. Signals were monitored from the eight wave gauges, a load cell measuring the PTO force, a load cell

measuring the restoring force and an encoder measuring the position of the EB Frond. An encoder is a device, which converts linear or rotary displacement into digital or pulse signals. Load cell and position sensor data were channelled through a programmable logic controller (PLC). Measurements of the geometric arrangement of the test rig enabled time histories of PTO and restoring torques, as well as collector angle to be built up from the raw data. These time histories were used to examine behavioural trends, including average power output.

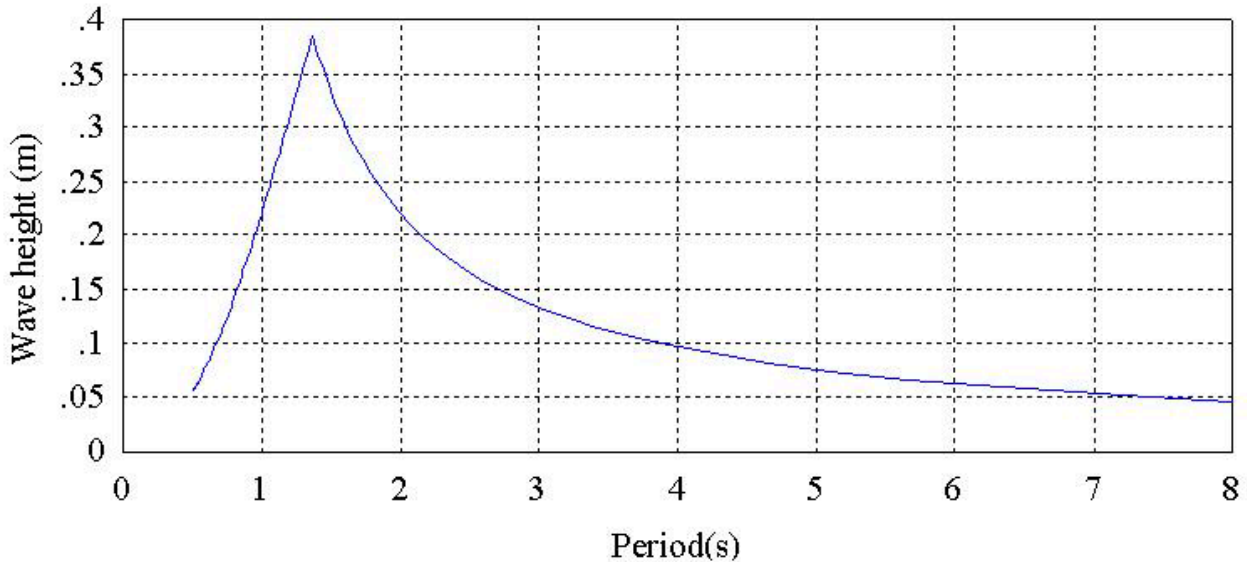


Figure 11 – Achievable wave heights and periods for wave production in the Lancaster tank

The wave gauges, position sensor and load cells were calibrated at the beginning of the experiments and checked each morning before tests began. Tank water height was also checked.

The wave tank used was calibrated so that the sinusoidal waves arriving at the test rig were of the period and amplitude requested. The Edinburgh Designs Ltd. software is said to be capable of producing complex sea-states, including Pierson-Moskowitz sea-states, via the superposition of a number of sinusoids. Such sea-states require a large range of constituent sinusoidal waves in terms of both period and amplitude, some of which may fall outside of the window of sinusoids the wave tank can reliably produce. Three Pierson-Moskowitz spectra were requested, the largest of these sea-states was at the limit of what the wave generating paddles could produce.

Before the test rig entered the wave tank the requested sea spectra were run and time histories taken of water elevation from wave gauges from the tank. This data was analysed to produce measured values for spectral peak period and significant wave height and these were compared to what is expected of the state. Results of this analysis are displayed in Table 1.

Full-scale Equivalent of Requested Significant Wave Height (m)	Requested Significant Wave Height (m)	Requested Spectral Peak Period (s)	Measured Significant Wave Height (m)	Measured Spectral Peak Period (s)
1.5	0.060	1.2246	0.0558	1.3645
2	0.080	1.4141	0.0850	1.5246
2.475	0.099	1.5740	0.0967	1.6337

Table 1 – Comparisons of requested and measured spectral parameters

No wave tank will produce perfect wave spectra, however the requested and measured spectral parameters do show reasonable correlation suggesting that the sea-states are correctly formed. The discrepancy between requested and measured parameters is smallest in the larger sea-states, which are of most interest. A significant proportion of the discrepancy between parameter values may be due to errors in experimental data capture. Lancaster University indicated that the tank was fully calibrated and could produce the required spectra. Data shown in Table 1 can be considered to be a sanity check of this claim rather than a rigorous analysis.

2.6 Experimental Procedure

2.6.1 Maximum Time-Averaged Power Output

All small-scale testing involves monitoring the change in the EB Frond maximum time-averaged power output, averaged over sufficiently long for readings to settle, with some variable, such as wave characteristics or collector design. Any particular test configuration can have a variety of power outputs depending upon the tuning of the device in terms of both its PTO and restoring force systems.

In the case of sinusoidal tests, the natural period of the EB Frond is set to the period of the waves. In the case of wave spectrum tests, the optimum natural period of the EB Frond is not so obvious and so further tests must be performed to ascertain the optimum period.

With the case of PTO tuning, it is logical that an infinitely weak PTO system will have no damping effects and extract no power, and similarly an infinitely strong PTO system will hold the device in place and also extract no power. The PTO system applies a torque, proportional to the angular velocity of the device against the direction of motion. The exact PTO setting, in $\text{NM}\cdot\text{s}\cdot\text{rad}^{-1}$, which gives the highest power output, must be experimentally determined. Through the testing of a variety of PTO settings a relationship between the maximum collector displacement and time-averaged power output can be built up. In the case of sea spectra, where the maximum collector displacement changes with each oscillation, the average modulus of the displacement (the average displacement when taking both positive and negative readings as being positive) is used instead. These relationships create third order polynomial functions. Through differentiation of these functions the maximum possible time-averaged power output can be calculated.

Having estimated the maximum power output value, by curve fitting, it is not necessary to experimentally measure this value. Once the curve is produced further results always fit well to it, so the production of such a point would provide no new information. Also the control of the PTO system is not expressed in $\text{NM}\cdot\text{s}\cdot\text{rad}^{-1}$, so it would be difficult to select the exact required PTO setting, though this will not be a problem with actual full-scale device.

In this report when power output variations are investigated in relation to a variable factor, the "maximum power" values discussed correspond to maximum time-averaged power values at the optimum PTO setting. For the sake of clarity, the majority of data points used to calculate these values are not reproduced in this report.

The tuning of the PTO system should not be confused with the tuning of the restoring force system. For optimum power output both systems must be appropriately tuned. The restoring force system is concerned with the tuning of the natural period of the device to achieve large energetic resonance oscillations the tuning of the PTO system is concerned with the most efficient power extraction from the resonance oscillations.

2.6.2 Power to Restoring Force Ratio

For many of the small-scale tests the amount of vertical restoring force required to achieve the necessary EB Frond time periods is investigated with relation to the power produced. The density of the collectors has a significant effect on the amount of restoring force required for two reasons - buoyancy provides restoring force, and collectors with more inertia require more restoring forces. To remove this variable the imposed restoring forces were adjusted to the values of restoring forces which would have been required had neutrally buoyant collectors been used.

It is believed that the cost of the restoring force system will be one of the major costs of the EB Frond system. Designs which have large power outputs and require more restoring force may produce electricity at a higher unit energy cost. Although this relationship cannot be accurately quantified at this time, the relationship between the power output, the maximum required restoring force, the unit energy cost and the cost of the restoring force system, and hence the ratio between power output and restoring force required, is of interest.

2.6.3 EB Frond Efficiencies

There is not one simple way in which the efficiency of the EB Frond at extracting energy from the waves can be expressed. As a result it is expressed in a number of formats in the results section.

- Point Absorber Efficiency - This is the efficiency of the EB Frond at extracting energy from the theoretical point absorber resource. This value is slightly limited in validity, because point absorber resources are calculated for infinite seas, whereas tests are performed in a finite wave tank. More importantly the EB Frond is not believed to be a simple point absorber.

- **Collection Width Efficiency** - This is the efficiency of the EB Frond at extracting the amount of energy that would pass through its collection width were it not there. This can exceed 100%, as the EB Frond is capable of absorbing energy from beyond its collection width.
- **Wave Tank Efficiency** - This is the efficiency of the EB Frond at extracting all the energy in the wave tank. This value can not exceed 100% regardless of the manner in which the EB Frond functions. Its use as an efficiency gauge is limited because it is more a function of the tank than the device in question, however it can serve as a warning, if values are approaching 100%, that tank energy resource limitations are becoming a significant factor.

2.7 Experiments

2.7.1 Newcastle University

The purpose of the tests in Newcastle was to ascertain how an EB Frond of a particular design would perform in a variety of sinusoidal waves, across a range of wave periods and amplitudes. Once these tests were performed, additional tests were performed with the purpose of ascertaining the effect of a slight collector thickness variation and the effect of directionality. It was found that large increases in power output could be achieved by slightly increasing the thickness of the collector. The Newcastle test schedules are shown in Table 2 and Table 3.

Cuboid Collector Width (m)	Cuboid Collector Draught (m)	Cuboid Collector Thickness (m)	Angle (degrees) *	Freeboard (m) **	No of wave height settings	No of wave period settings	Total number of test sets ***
0.630	0.305	0.051	0	-0.05	2	4	8
0.630	0.305	0.051	0	0	2	4	8
0.630	0.305	0.051	0	0.05	2	3	6
0.630	0.305	0.051	10	0	2	2	4
0.630	0.305	0.051	20	0	2	2	4
0.630	0.305	0.051	30	0	2	2	4
0.630	0.305	0.102	0	0	2	3	6

* Angle between collector thickness axis, and direction of wave propagation

** Freeboard negative values indicate that collectors are submerged

*** Each test set contained a minimum of 5 PTO setting tests

Table 2 - Newcastle Sinusoidal tests

Cuboid Collector Width (m)	Cuboid Collector Draught (m)	Cuboid Collector Thickness (m)	Angle (degrees) *	Freeboard (m) **	Sig. Wave Height (m)	Spectral Peak Period (s)	Total number of test sets ***
0.630	0.305	0.051	0	0	0.08	1.29	1

* Angle between collector thickness axis, and direction of wave propagation

** Freeboard negative values indicate that collectors are submerged

*** Each test set contained a minimum of 5 PTO setting tests

Table 3 - Newcastle ISSC Spectrum Tests

The models tested had a scale of 1:25, a collector face of 630 x 305mm and thicknesses of 51mm and 102mm. The thickness was changed by attaching rigid panels of closed-cell foam to the collector as shown in Table 11. The basic model is that tested in the Lancaster wave tank in Phase one of the project, with the pivot at the bottom of the arm.

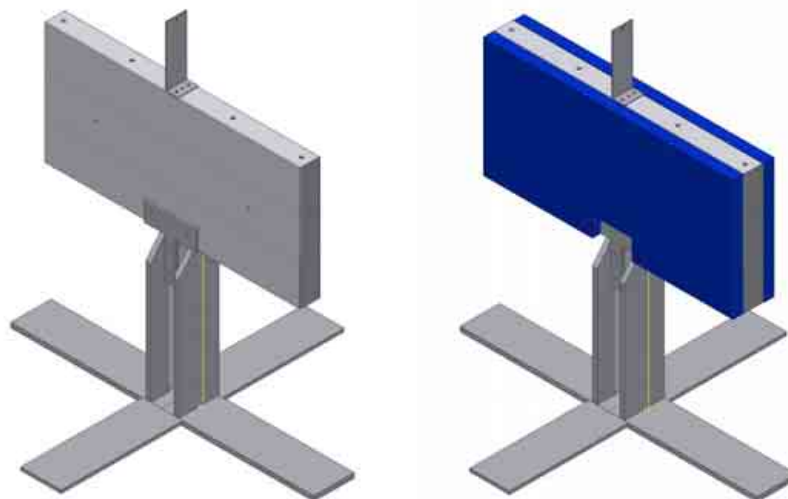


Figure 12 – 1/25th Scale Newcastle Models

The strain gauges were calibrated by progressively loading and then unloading the dynamometer with weights, and the displacement potentiometer by moving a mark on the cord against a scale, while recording the data.

As with previous tests, the natural period of each model was measured in calm water by displacing it and timing a number of oscillations. This was carried out for a number of values of restoring force. The tuned wave periods chosen for sinusoidal tests matched the natural periods within 0.025 seconds. For random waves, the peak spectral periods matched within 0.12 seconds.

For each test the PTO strength was adjusted through a number of settings so that the maximum power obtainable could be calculated. Throughout this report the term 'maximum power' refers to the average power output that is achieved when the PTO system is optimised. This technique of calculating the maximum obtainable

power output is the same as used in the previous stage, and the same as used throughout this stage in all facilities.

With hindsight, it is apparent that the Newcastle tests should be taken as indicative rather than definitive. The Newcastle wave tank was not adequately calibrated (compared with the LUED tank used subsequently) and the reflection-control beaches were of unquantified adequacy.

2.7.2 Lancaster University Visit One

Before the first set of Lancaster tests it was decided that, given the results from Newcastle, the project would benefit from reassessing the collector design. This ensured the reduction of wasted time in the performance of detailed tests on a collector design, which could later be changed or rejected, reducing the usefulness of any test results.

The first set of Lancaster tests was performed, predominantly, with only one type of sinusoidal wave, draught and orientation. The purpose of these tests was to choose the optimum collector geometry for these simple conditions. Although the investigation of the performance of each collector shape was not as rigorous as had been undertaken for the limited collector shape variables in previous stages, these tests did highlight designs which performed significantly better. The purpose of these tests was not to produce any estimations of overall power output, merely to facilitate the choice of the collector which was likely to produce the highest overall outputs. The Lancaster, visit one, test schedule is shown in Table 4.

The tests used only sinusoidal waves of periods of 1.2s, 1.6s, 2.0s and amplitude 0.025m, corresponding to 6s, 8s and 10s, 0.625m amplitude waves at full-scale.

A variety of collector shapes were tested. Each collector was tuned so that it had a natural period equal to the period of the waves. The tops of all collectors were level with the still water level. The restoring force required for tuning and the volume and inertia of the collector were used to calculate the restoring force that would be required if the collector were built at full-scale and made to be neutrally buoyant.

The merit of each collector was judged by its ability to produce power, the amount of restoring force required if it were to be built neutrally buoyant (as large restoring force generation will be expensive and cause energy losses), and its engineering feasibility. Variation of maximum power to restoring force ratio was investigated with parameter change. This is calculated by dividing the maximum power, in Watts, by the required vertically applied restoring spring force for a neutrally buoyant collector of the same dimensions and natural period, in Newtons.

Collector Name	Collector Dimension Width (m)	Collector Dimension Draught (m)	Collector Dimension Thickness (m)*	Freeboard (m) **	No of wave period settings	Total number of test sets ***
Basic	0.630	0.305	0.100	0	3	3
Extra Thick	0.630	0.305	0.400	0	1	1
Thick	0.630	0.305	0.200	0	1	1
Thin	0.630	0.305	0.050	0	1	1
Extra Thin	0.630	0.305	0.015	0	1	1
Wide	0.630	1.030	0.100	0	1	1
Narrow	0.630	0.230	0.100	0	1	1
Extra Deep	0.505	0.305	0.100	0	2	2
Deep	0.405	0.305	0.100	0	2	2
Shallow	0.205	0.305	0.100	0	2	2
Rounded	0.630	0.305	0.053	0	1	1
Half Cylindrical	0.630	0.305	0.362	0	1	1
Cylinder	0.630	0.305	0.305	0	1	1
Added Mass Interchange	0.630	0.305	0.055	0	1	1

* Thickness quoted is, in cases of non-uniform thickness collector, the largest possible value

** Freeboard negative values indicate that collectors are submerged

*** Each test set contained a minimum of 6 PTO setting tests

The angle between collector thickness axis, and direction of wave propagation, was zero in all cases

All tests were performed with 0.025m amplitude sinusoidal waves

Table 4 - Lancaster Tests (Visit one)

The efficiency of the collectors at energy extraction was also investigated. Three different efficiencies were calculated. The efficiency at capturing the theoretical power resource available to a point absorber, the efficiency at capturing the amount of power in the waves across a wave-front width equal to that of the collector width, and the efficiency at extracting the power entering the wave tank. These efficiencies are referred to as "point absorber", "collection width" and "wave tank" respectively in the results sections. The efficiencies are calculated by dividing the maximum power output by the corresponding power resource-

A number of different collector parameters were varied, to produce a number of different behavioural trends. Most of these tests used cuboid collectors. The "Basic EB Frond" collector was used in the majority of tests. This had a width of 0.630m, thickness of 0.104m and draught of 0.305m. To investigate the effect of changing these dimensions, one parameter was changed at a time, keeping the other two dimensions as in the "Basic EB Frond".









The purpose of the tests was to provide a qualitative indication as to how the properties of the collector could be adjusted to improve the EB Frond collector




design. The effect of variations in different collector parameters may have different significance in different sinusoidal waves. As time constraints meant that the number of test runs had to be kept to a minimum. All sinusoidal waves used were of 0.05m height (this scales up to 1.25m at full-scale), and most had a period of 1.6 seconds (this scales up to 8 seconds at full-scale). 8 seconds is a period to which the full-scale device could often be expected to be tuned. In some tests it could be argued that collector parameter changes may have significantly different effects in different period sinusoids, therefore some other periods of sinusoids were used.





Most tests were performed using cuboid shaped collectors. These are defined in terms of three dimensions:



- Thickness: The horizontal length of the collector, in the direction perpendicular to the axis of rotation.
- Width: The horizontal length of the collector, in the direction of the axis of rotation.
- Draught: The vertical distance from the top of the collector, to the bottom of the collector.


One of the cuboid collectors, referred to as the “Basic EB Frond” collector had a thickness of 0.100m, a width of 0.603m and a draught of 0.305m. All other cuboid collectors differed from the Basic EB Frond collector in only one of these variables.



Thickness Variation – Cuboid Collectors		This test was performed with 1.6s waves. Cuboid collectors were used		
				
Extra Thick (0.4m)	Thick (0.2m)	Basic (0.1m)	Thin (0.05m)	Extra Thin (0.015m)
				
Extra Thick	Basic	Extra Thin (with Added Mass Interchange test plates attached)		

Width variation – Cuboid Collectors	This test was performed with 1.6s waves. Cuboid collectors were used. The narrowest of the three collectors used did not produce sufficient power to drive the dynamometer, so the power trend could only be shown for the basic (0.63m) and wide (1.03m) models.		
			
Wide (1.03m)	Basic (0.63m)	Narrow (0.23mm)	

Draught Variation – Cuboid Collectors	This test was performed with both 1.6s and 2.0s waves. Two wave periods were used because the proportion of total wave power in a depth range varies with wave period. Cuboid collectors were used.			
				
Extra Deep (0.505m)	Deep (0.405m)	Basic (0.305m)	Shallow (0.205m)	

Added Mass Interchange	<p>To investigate the effect of swapping collector volume for added mass volume, a cuboid collector with thickness of 0.015m was compared to the same cuboid collector but with the addition of two plates on either side attached centrally. This added more than 50% to the volume of the collector. The additional plates were placed in positions such that the combined volume and expected added mass volume of the collector would be unchanged. No variation in restoring force was required between the two tests. This test was performed with 1.6s waves.</p>
	
Added Mass Interchange	Extra Thin

Radiussed Collector	<p>The cuboid collector (0.05m thick) performance was compared to the performance of a collector of the same width, draught and volume, but with rounded edges to reduce drag. To conserve volume, the cuboid section of the radiussed collector was slightly thicker at 0.053m. The radiussed edges were constructed from half cylinders, and the corners rounded. This test was performed with 1.6s waves.</p>	
---------------------	--	---

Half Cylindrical Collector	The performance of a half cylindrical shaped collector was compared to that of the cuboid designs. The collector was not strictly a half cylinder since it had the same width, draught and bottom thickness as the Basic EB Frond collector, but had a top thickness of 0.362m. This test was performed with 1.6s waves.	
Cylindrical Collector	The performance of a cylinder shaped collector was compared to that of the cuboid designs. This collector had the same diameter as the draught of the Basic EB Frond. This test was performed with 1.6s waves.	
Wave Period Variation	A number of 0.025m amplitude waves with different periods were used, with the EB Frond tuned to them in each case, to investigate the trends of EB Frond performance with sinusoidal wave period. This test was performed with the basic EB Frond collector.	

2.7.3 Lancaster University Visit Two

The second set of tests was conducted between 24th and 27th May 2004. After analysis of results from the first Lancaster tests, and discussions regarding the engineering feasibility of some of the shapes, it was determined to adopt the Triangular EB Frond geometry, which had the same draught, width, top and bottom thickness as the half cylindrical collector, see Figure 13. It therefore had slightly less volume than the half cylindrical collector but was nevertheless expected to behave very similarly. The triangular shape was developed with the aim of increasing simplicity while maintaining performance.

The second set of Lancaster tests investigated this new geometry in the same simple sinusoidal waves as the previous tests to check that it performed as expected, compared with the half cylindrical collector. Once the design had passed these basic sanity checks, the effect of varying its buoyancy was investigated and its optimum freeboard was ascertained in the simple sinusoidal waves.



Figure 13 – Half cylindrical Frond

In the freeboard tests rather than raise or lower the water level, which would have invalidated tank calibrations, the pivot upon which the EB Frond arm was mounted was raised and lowered. To achieve this the base was modified to include additional pivot holes. The desired range of freeboard dictated the position of the new pivot holes. At the mid position of the freeboard range the top of the collector was 0.015m clear of the still water surface, not level with it as it was in the first set of tests. For this reason a test of the half cylindrical collector was repeated at this freeboard so as not to invalidate comparisons of the two collectors.

With the chosen design and draught it was now possible to perform detailed analysis on a realistic collector design. It was decided, unlike the Newcastle tests, not to test the device in a variety of sinusoidal waves, as these do not occur at sea, but in the more realistic representation of sea-states provided by Pierson-Moskowitz spectra (see Lancaster, visit one, test schedules in Table 5 and Table 6). These have periods and wave heights that are directly related, consequently fewer tests are required to describe the EB Frond behaviour in a range of sea-states. However, the Pierson-Moskowitz sea-state tests are very time consuming and were performed for only three significant wave heights. Nevertheless from this data the performance of the chosen EB Frond design could be estimated in any Pierson-Moskowitz sea-state. The acquisition of this data enabled power output predication across a range of sea-states for a possible full-scale design. With this data it was now possible to make estimations of the likely yearly power output of a full-scale EB Frond, which had never previously been possible on the EB Frond project.

Collector Name	Collector Dimension Width (m)	Collector Dimension Draught (m)	Collector Dimension Thickness (m) *	Freeboard (m) **	No of wave period settings	Total number of test sets ***
Half Cylindrical	0.630	0.305	0.362	0.015	1	1
Triangular	0.630	0.305	0.362	0.015	1	1
Triangular Extra 9kg	0.630	0.305	0.362	0.015	1	1
Triangular Extra 18kg	0.630	0.305	0.362	0.015	1	1
Triangular	0.630	0.305	0.362	-0.315	1	1
Triangular	0.630	0.305	0.362	-0.645	1	1
Triangular	0.630	0.305	0.362	-0.985	1	1
Triangular	0.630	0.305	0.362	0.345	1	1
Triangular	0.630	0.305	0.362	0.675	1	1
Triangular	0.630	0.305	0.362	1.015	1	1

* Thickness quoted is, in cases of non-uniform thickness collector, the largest possible value

** Freeboard negative values indicate that collectors are submerged

*** Each test set contained a minimum of 6 PTO setting tests

The angle between collector thickness axis, and direction of wave propagation, was zero in all cases

All tests were performed with 0.025m amplitude sinusoidal waves

Table 5 - Lancaster Sinusoidal Tests (Visit two)



Collector Name	Freeboard (m) *	Significant Wave Height (m)	Spectral Peak Period (s)	No of EB Frond Natural Period Settings	Total number of test sets **
Triangular	0.015	0.06	1.2246	4	4
Triangular	0.015	0.08	1.4141	4	4
Triangular	0.015	0.099	1.574	4	4

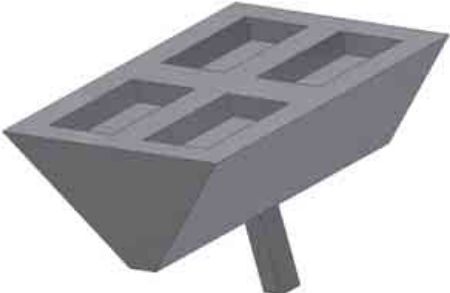
* Freeboard negative values indicate that collectors are submerged

** Each test set contained a minimum of 6 PTO setting tests

The angle between collector thickness axis, and direction of wave propagation, was zero in all cases

Table 6 – Lancaster Pierson-Moskowitz Spectral Tests (Visit two)

<p>Comparative Tests - Half Cylindrical and Triangular Collectors</p>	<p>The half cylindrical and triangular collectors were tested, at a freeboard of 0.015m, with waves of 0.025m amplitude and 1.6s period. Examination of results showed little difference between the behaviour of the two collectors. It was decided that only the more simplistic, and easier to engineer, triangular shaped collector would be used for the subsequent tests.</p>
	
<p>Half cylindrical</p>	<p>Triangular</p>

<p>Buoyancy</p> 	<p>The top plate of the triangular collector was removable, exposing pockets in the closed cell foam inside. Foam or steel blocks were used to fill the pockets and change the mass of the collector. Foam was removed from the inside of the triangular EB Frond collector, and additional masses of 9kg and 18kg were added to increase the mass of the collector, and therefore cancel the effect of some of its buoyancy. This also has the effect of increasing the inertia of the collector, so restoring forces were adjusted to keep the natural period of the EB Frond unchanged. The inertia of the collector was increased by approximately 50% and 100% with the two additions of mass.</p> <p>This test was performed with 1.6s waves 0.025m amplitude sinusoidal waves with a freeboard of 0.015m.</p> <p>No significant differences were found between the performance of the collectors in terms of maximum power outputs, or in terms of displacements and power outputs with any given PTO set-up. The triangular set up with the least mass was used in all subsequent tests, as it required less restoring force for the desired natural period tunings.</p>
---	--

Freeboard	<p>The triangular collector was tested in 1.6s, 0.025m amplitude waves with freeboards of; 0.115m, 0.081m, 0.048m, 0.015m, -0.018m, -0.051m and -0.085m (negative values are submerged)</p> <p>It was decided that the final tests would be performed with the freeboard set to 0.015m.</p>
-----------	---

Pierson-Moskowitz Seas	<p>The triangular EB Frond, with a freeboard of 0.015m, was tested in three Pierson-Moskowitz sea-states. The sea-states had significant wave heights of 0.06m, 0.08m and 0.099m, which was the largest significant wave height that could be produced in the tank. These significant waves heights correspond to 1.5m, 2.0m, and 2.5m respectively at full-scale.</p> <p>As sea-states are built up of many sinusoids, of different periods, the optimum tuning of the EB Frond's natural period is more complex than with pure sinusoids. Each sea-state was tested with a variety of EB Frond natural periods, and the maximum possible power determined in each case through PTO variation tests. The optimum natural period of the EB Frond and the optimum power output could then be determined.</p>
------------------------	---

3 TEST RESULTS

3.1 Newcastle

3.1.1 Wave Amplitude Variation

The variation in power output with sinusoidal wave amplitude for the 0.051m thick collector, with 0m freeboard for a variety of wave periods, is shown in Figure 14.

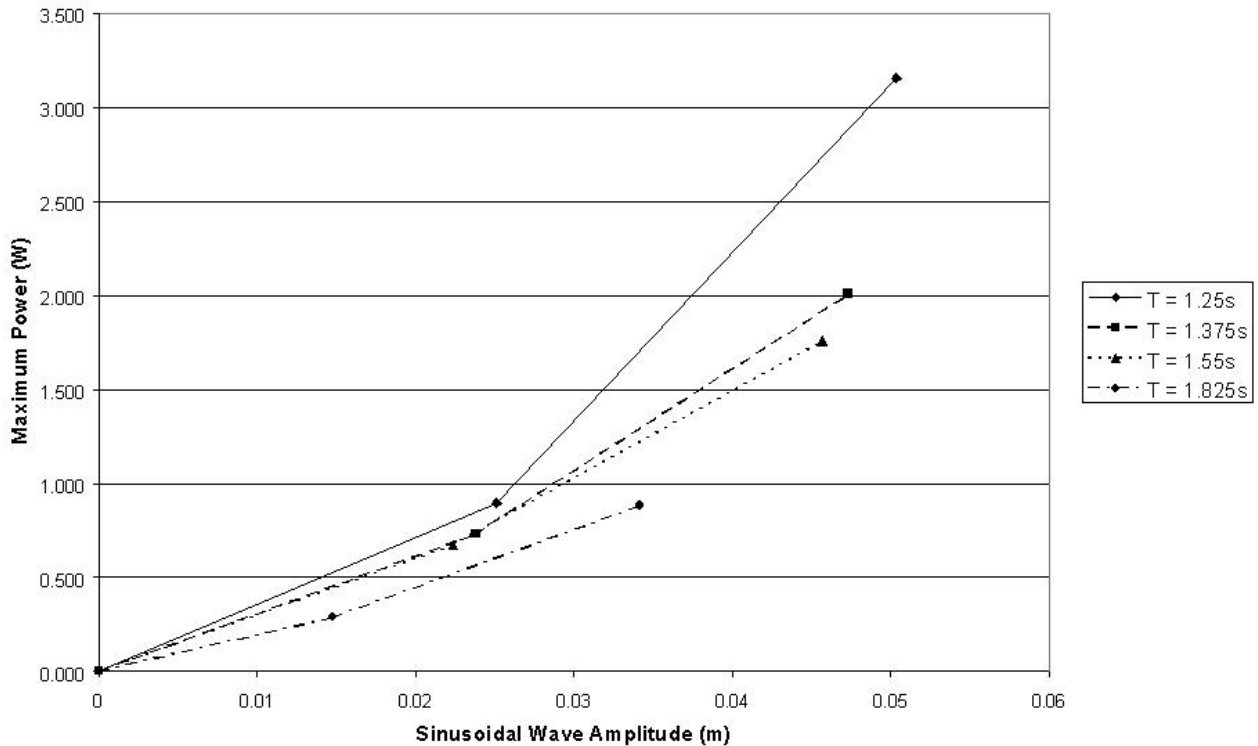


Figure 14 - Maximum power variation with wave amplitude for the 0.051m thick collector with 0m freeboard for a variety of wave periods

3.1.2 Freeboard Variation

The variation in power output with freeboard for the 0.051m thick collector, with two different sinusoidal waves is shown in Figure 15.

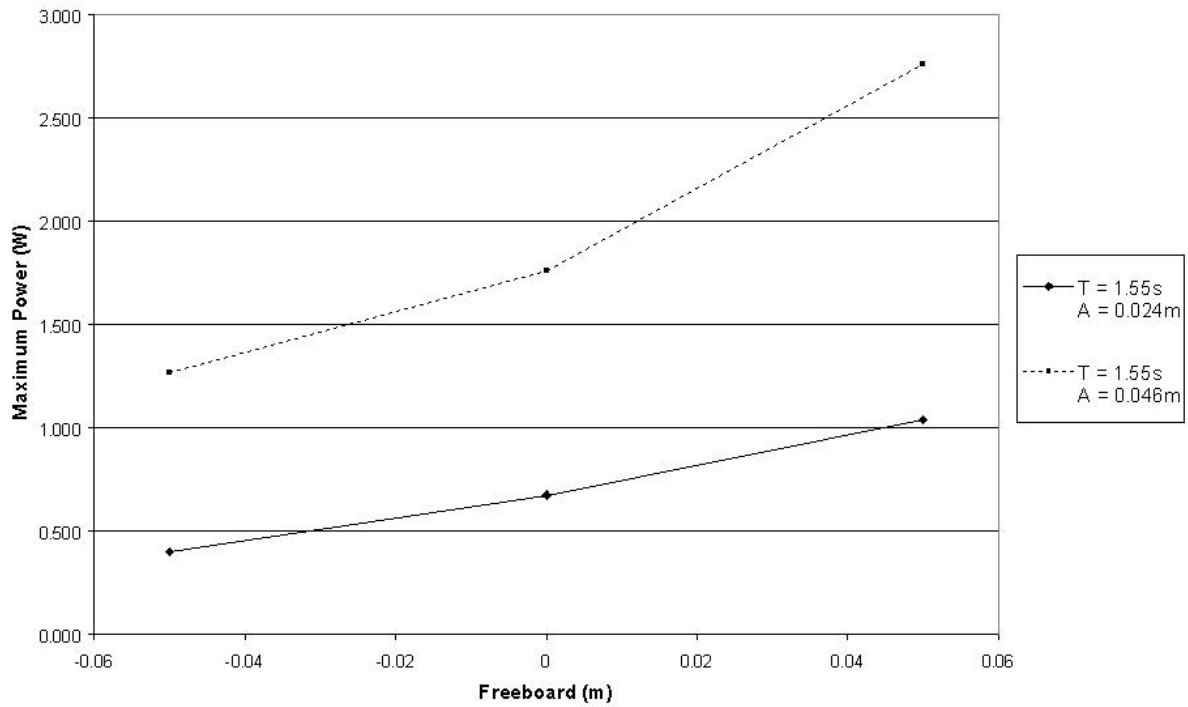


Figure 15 - Maximum power variation with freeboard for the 0.051m thick collector

3.1.3 Wave Incidence Angle Variation

The maximum power variation, for the 0.051m thick collector, with 0m freeboard, with wave incidence angle is shown in Figure 16.

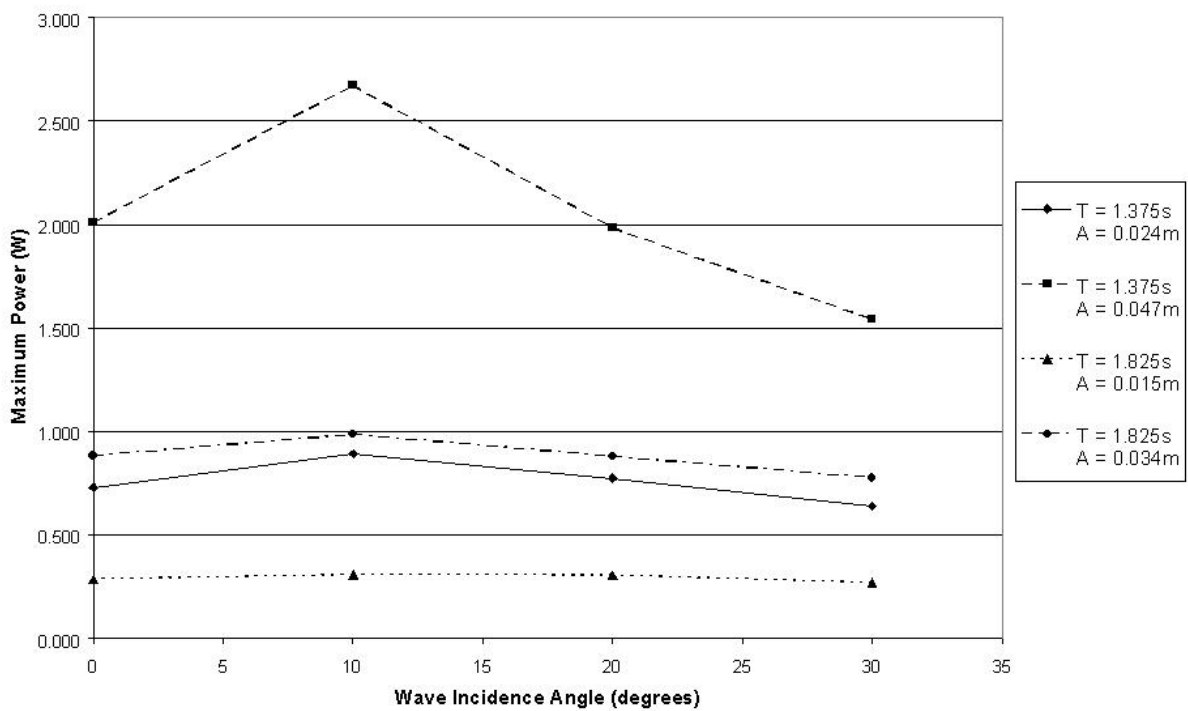


Figure 16 - Maximum power variation with wave incidence angle for the 0.051m thick collector with 0m freeboard for a variety of sinusoidal waves

3.1.4 Collector Thickness Change

The maximum power variation, with 0m freeboard, with collector thickness is shown in Figure 17.

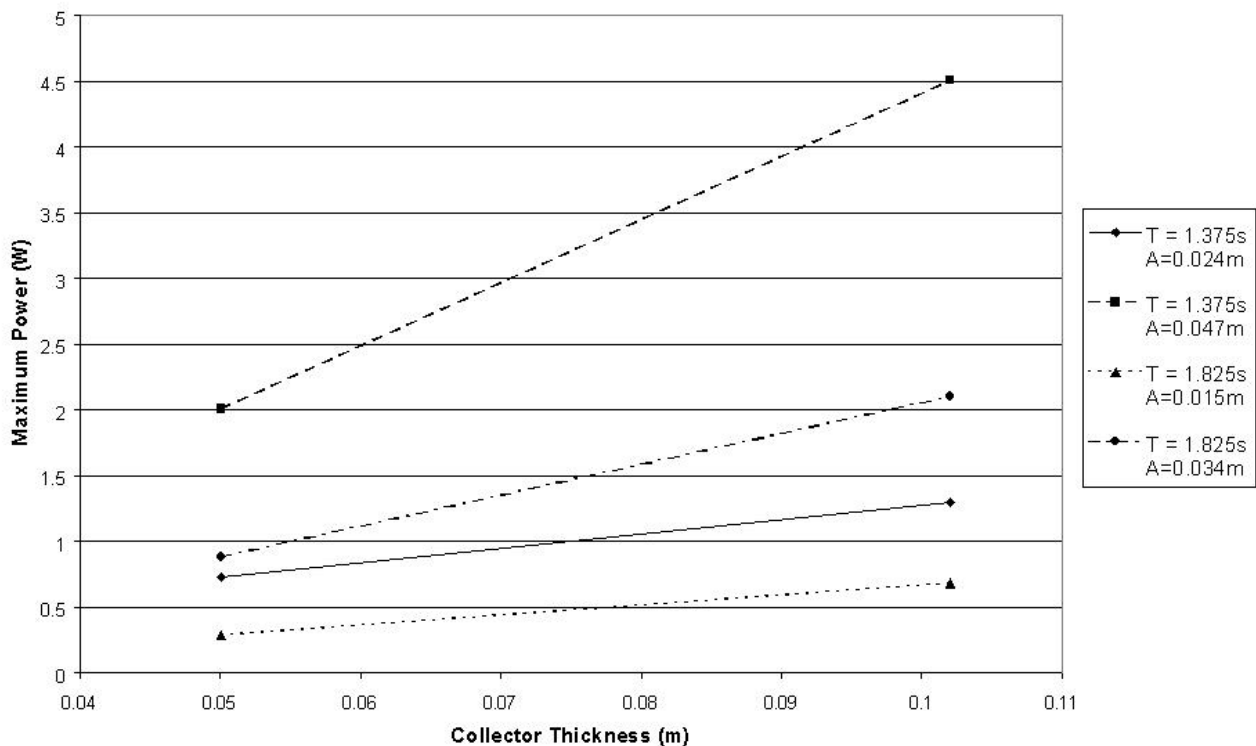


Figure 17 - Maximum power variation with collector thickness with 0m freeboard for a variety of sinusoidal waves

3.1.5 Sea Spectra

One time-averaged maximum power output value was obtained for one sea spectra. The desired sea spectrum was an ISSC spectrum, with a significant wave height of 0.08m and a peak period of 1.4s, which was the same as the natural period of the EB Frond. ISSC spectra represent fully developed sea states, but unlike some other fully developed sea-state representations any combination of significant wave height and peak period can be chosen. When the spectrum was later analysed it was found that although the significant wave height was 0.08m the peak period was 1.29s. Nevertheless the time-averaged power output achieved from the EB Frond in these conditions was 0.91W.

3.1.6 Comparison with Phase One Test Results

Results obtained in Phase one at Lancaster were compared with those in Phase two from Newcastle, as shown in Table 7.

The exact test conditions, such as the nature of the damping from the dynamometer and the constraints on motion due to the restoring force springs could not be duplicated, and changes in the tank depth could not be avoided.

The comparison in Table 4 shows power output agreement within 10% for wave periods differing by 7.5% and wave heights within 8% of each other.

Test Location	Submergence (m)	Time Period (s)	Wave Height (m)	Max Power (W)
Lancaster	0.05	1.370	0.465	0.585
Newcastle	0.05	1.275	0.503	0.536

Table 7 – Comparison of Lancaster and Newcastle Results

3.2 Lancaster First Set of Results

3.2.1 Thickness Variation

This test was performed with 1.6s waves. Cuboid collectors were used to assess the variation of power output with cuboid thickness in the thickness range of 0.015m to 0.400m. Results are shown in Figure 18, Figure 19 and Figure 20.

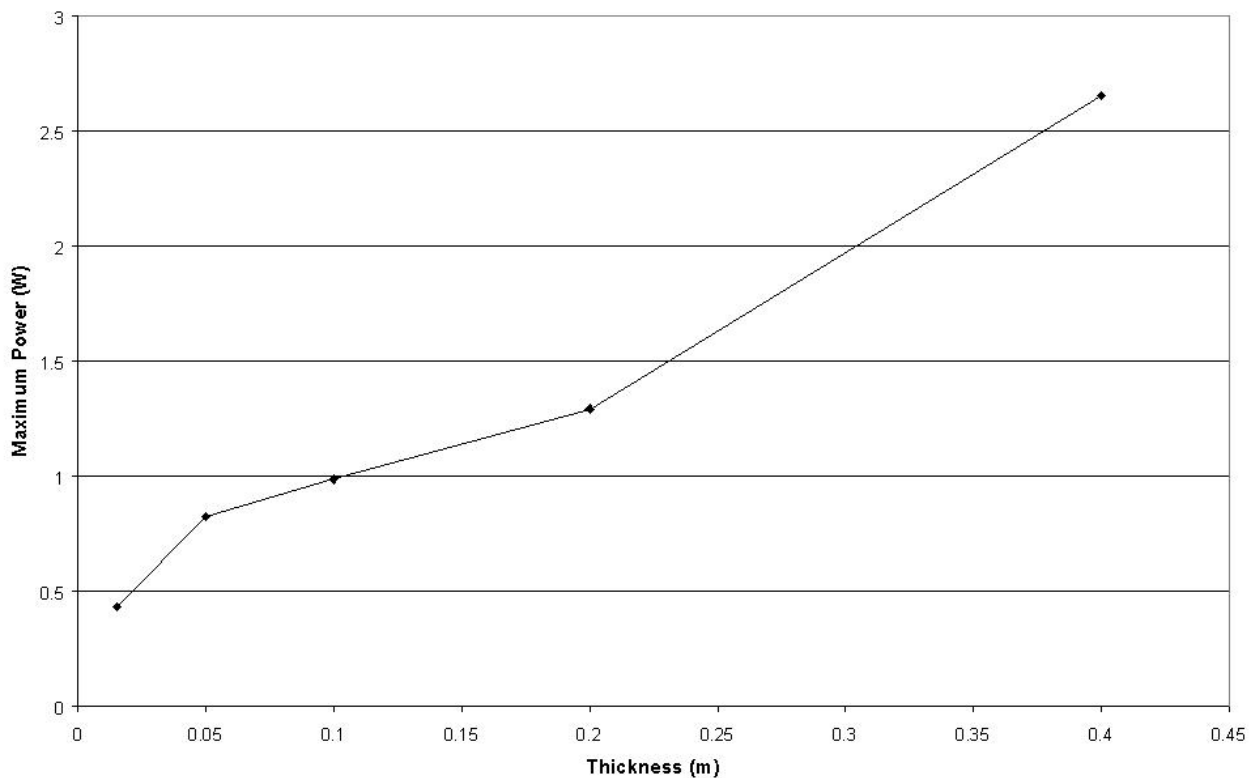


Figure 18 – Maximum power variation, in 1.6s 0.025m amplitude sinusoidal waves, with cuboid collector thickness

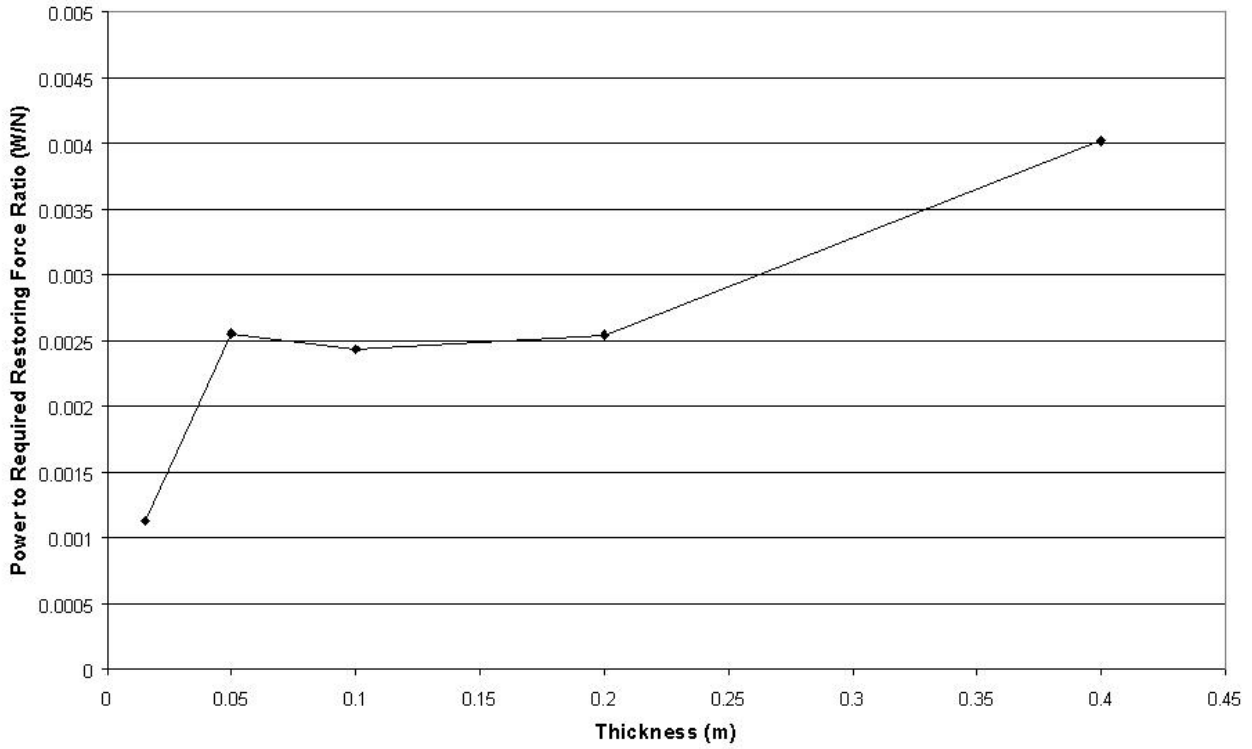


Figure 19 – Maximum power to restoring force ratio variation, in 1.6s 0.025m amplitude sinusoidal waves, with cuboid collector thickness

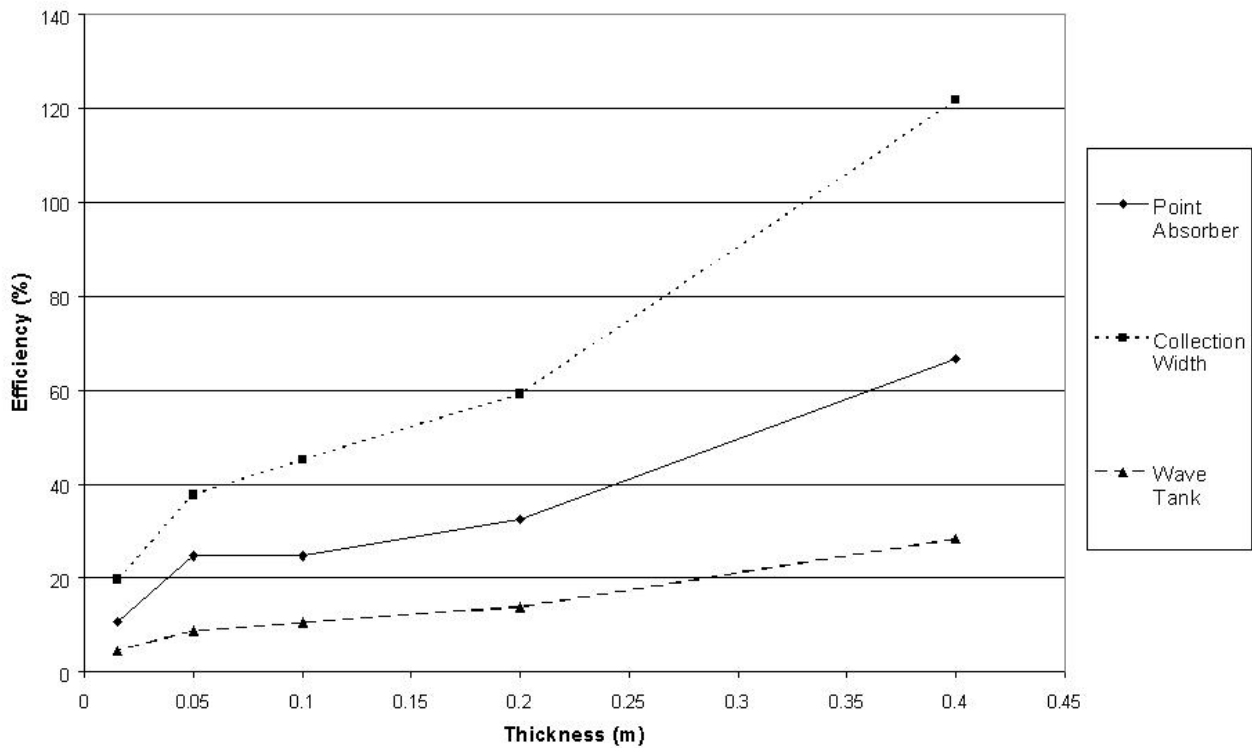


Figure 20 – Efficiency variations, in 1.6s 0.025m amplitude sinusoidal waves, with cuboid collector thickness

3.2.2 Width Variation

This test was performed with 1.6s waves. Cuboid collectors were used to assess the variation of power output with cuboid width in the width range of 0.630m to 1.030m. It was planned for another collector, with width 0.230m, to be tested, but the collector had a power output too low to quantify. Results are shown in Figure 21, Figure 22 and Figure 23.

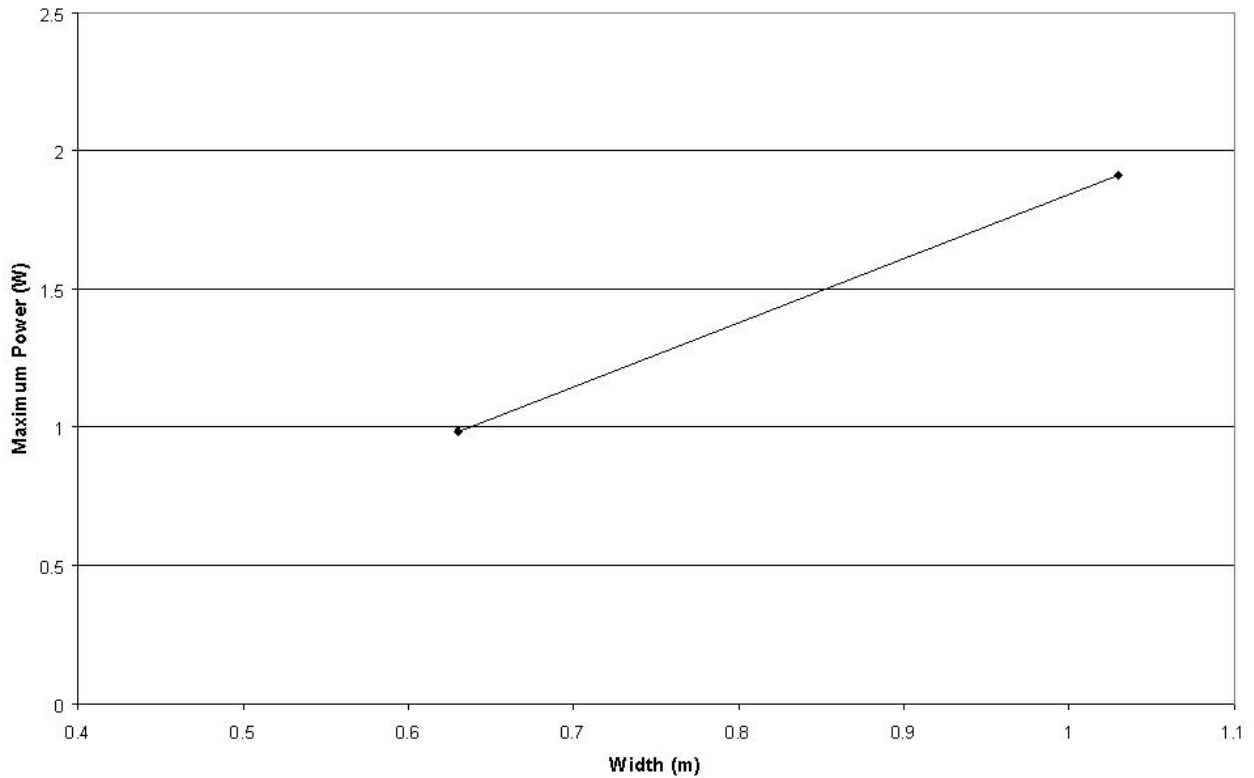


Figure 21 – Maximum power variation, in 1.6s 0.025m amplitude sinusoidal waves, with cuboid collector width

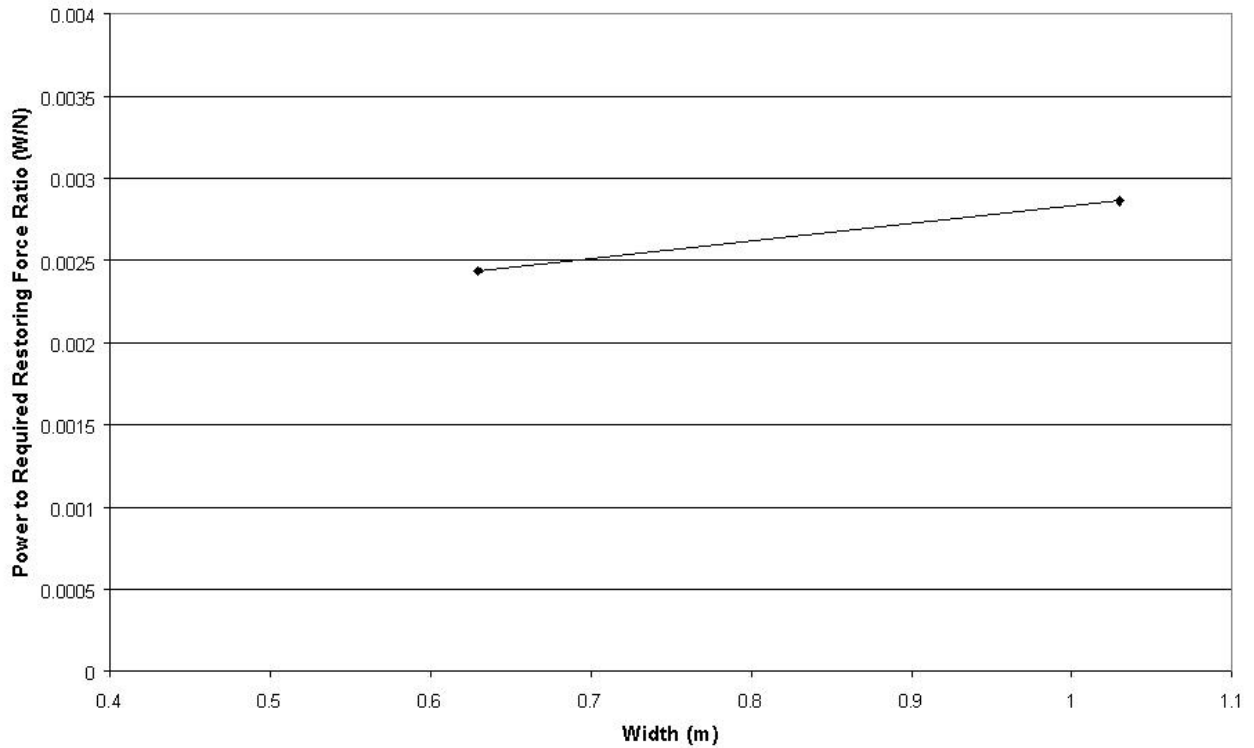


Figure 22 – Maximum power to restoring force ratio variation, in 1.6s 0.025m amplitude sinusoidal waves, with cuboid collector width

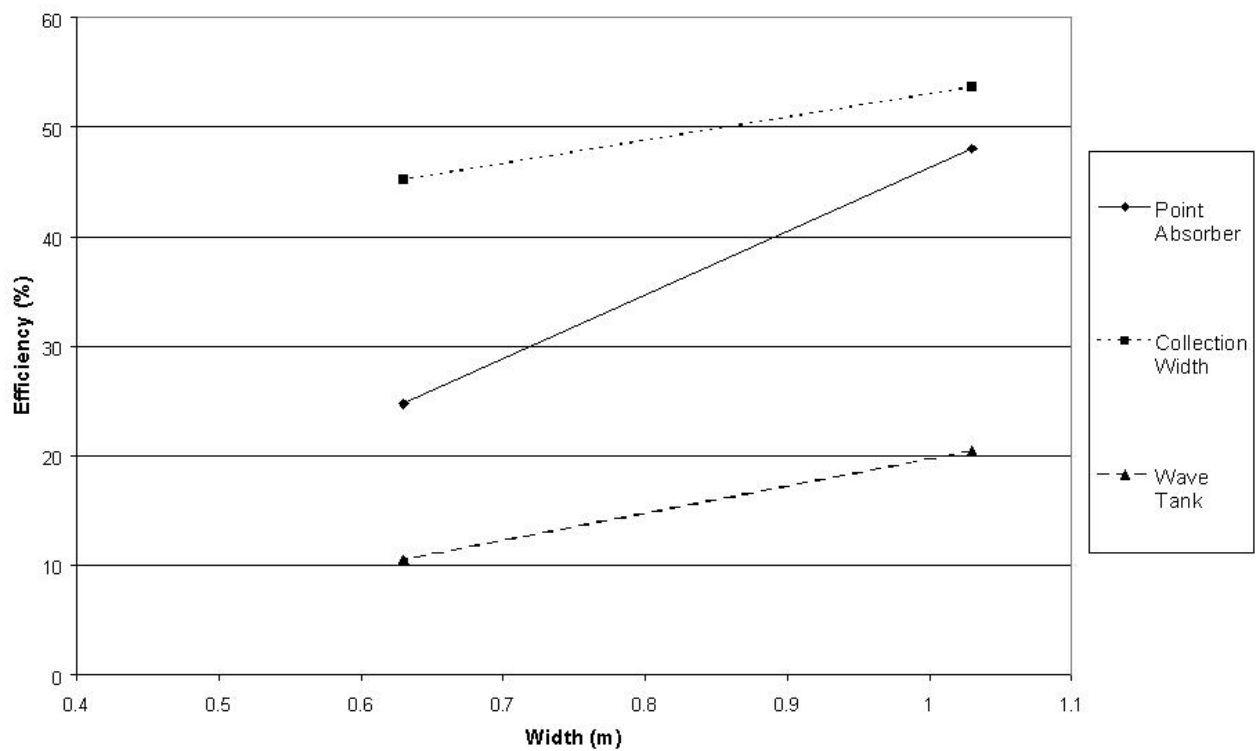


Figure 23 - Efficiency variations, in 1.6s 0.025m amplitude sinusoidal waves, with cuboid collector width

3.2.3 Draught Variation

This test was performed with both 1.6s and 2.0s waves. Cuboid collectors were used to assess the variation of power output with cuboid draught in the draught range of 0.205m to 0.505m. Results are shown in Figure 24, Figure 25, Figure 26 and Figure 27.

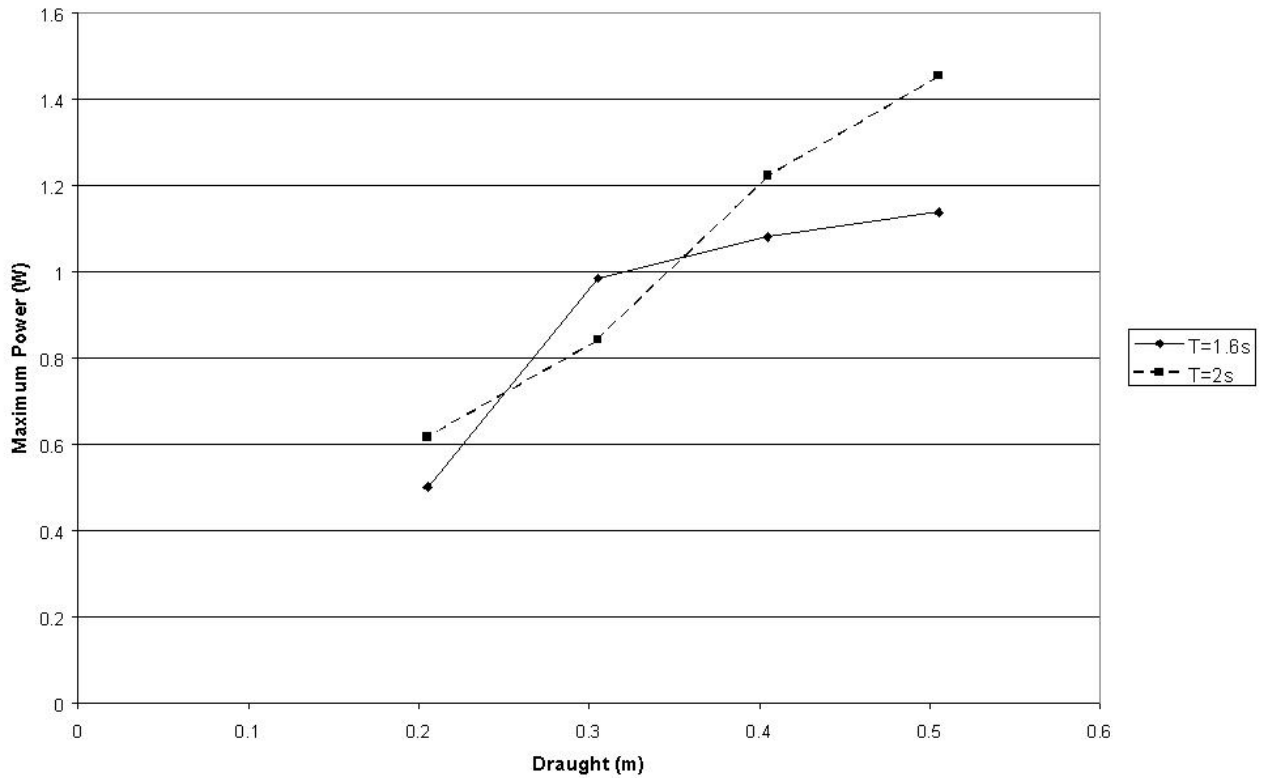


Figure 24 – Maximum power variation, in 1.6s and 2.0s 0.025m amplitude sinusoidal waves, with cuboid collector draught

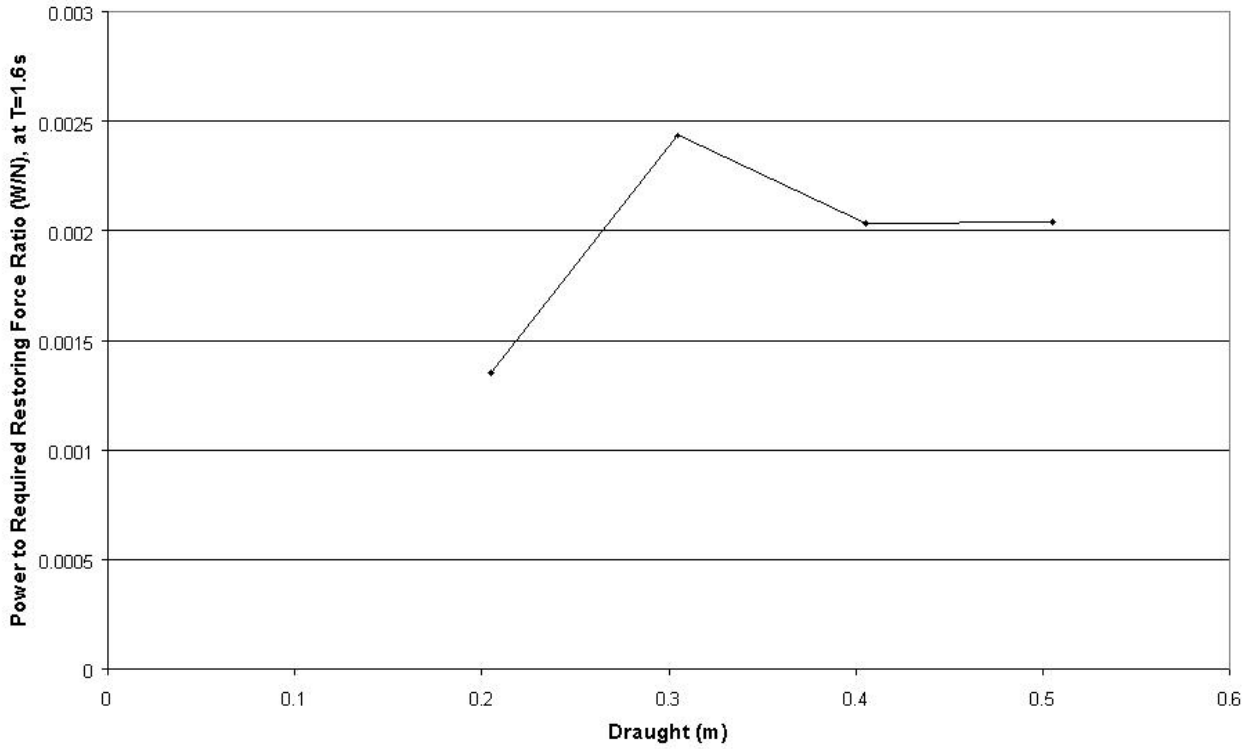


Figure 25 – Maximum power to restoring force ratio variation, in 1.6s 0.025m amplitude sinusoidal waves, with cuboid collector draught

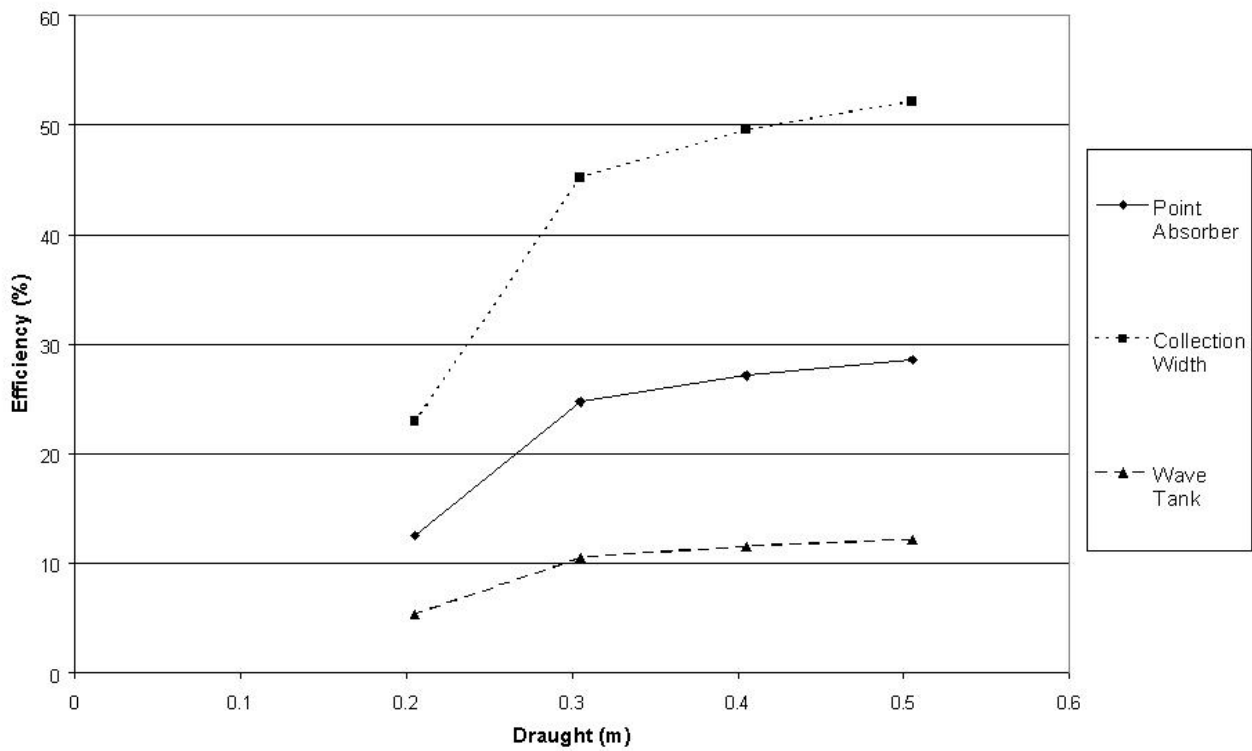


Figure 26 – Efficiency variations, in 1.6s 0.025m amplitude sinusoidal waves, with cuboid collector draught

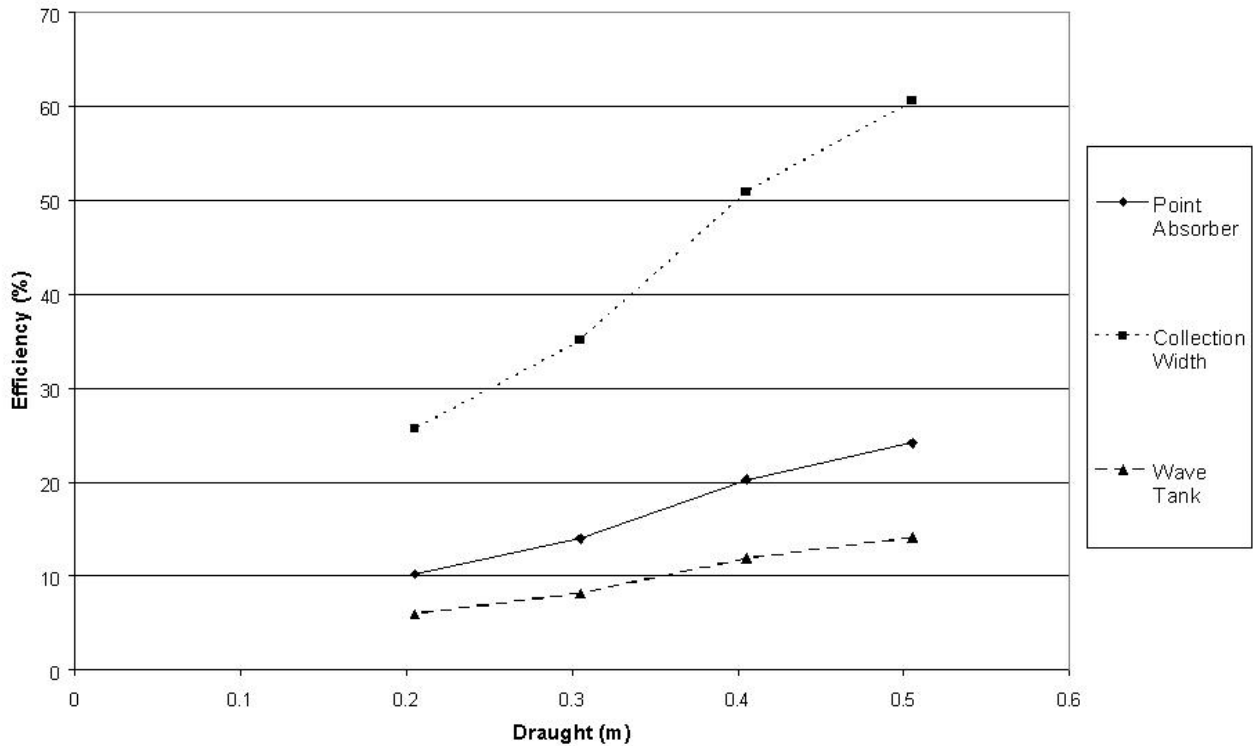


Figure 27 – Efficiency variations, in 2.0s 0.025m amplitude sinusoidal waves, with cuboid collector draught

3.2.4 Added Mass Interchange

To investigate the effect of swapping collector volume for added mass volume, a cuboid collector with thickness of 0.015m was compared to the same cuboid collector but with the addition of two plates on either side attached centrally. This added more than 50% to the volume of the collector. The additional plates were placed in positions such that the combined volume and expected added mass volume of the collector would be unchanged. No variation in restoring force was required between the two tests. This test was performed with 1.6s waves.

The collector with the additional plates produced 3.6% power more than the collector without.

3.2.5 Radiussed Collector

The cuboid collector (0.05m thick) performance was compared to the performance of a collector of the same width, draught and volume, but with rounded edges to reduce drag. To conserve volume, the cuboid section of the radiussed collector was slightly thicker at 0.053m. The radiussed edges were constructed from half cylinders, and the corners rounded. This test was performed with 1.6s waves.

The collector without radiussed edges produced 82% more power than the collector with radiussed edges.

3.2.6 Half Cylindrical Collector

The performance of a half cylindrical shaped collector was compared to that of the cuboid designs. The collector was not strictly a half cylinder since it had the same width, draught and bottom thickness as the Basic EB Frond collector, but had a top thickness of 0.362m. This test was performed with 1.6s waves.

The half cylindrical collector had a maximum power output of 2.1W. This is comparable to cuboid collectors, with thickness similar to the thickness of top of the half cylindrical collector, as shown in Figure 28 and Figure 29.

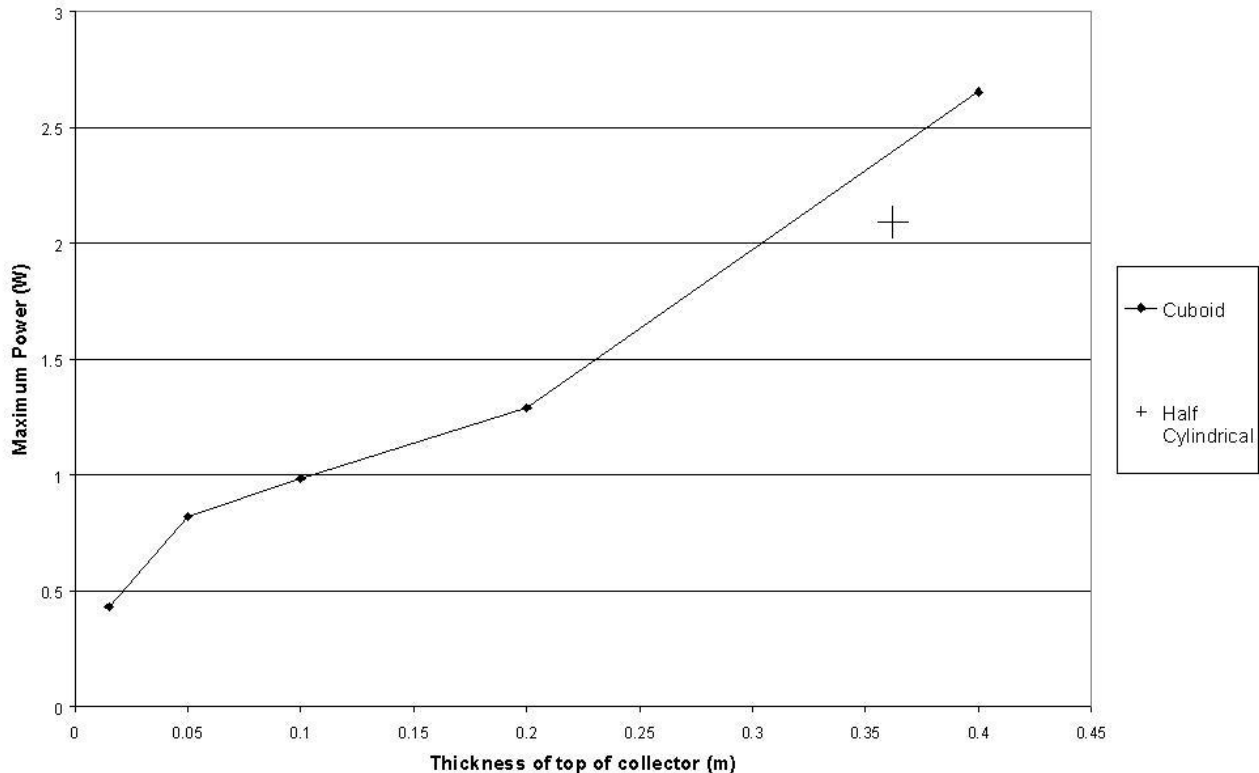


Figure 28 – Comparison of Half Cylindrical collector maximum power, with that of cuboid collectors of varying thickness, in 1.6s 0.025m amplitude sinusoidal waves

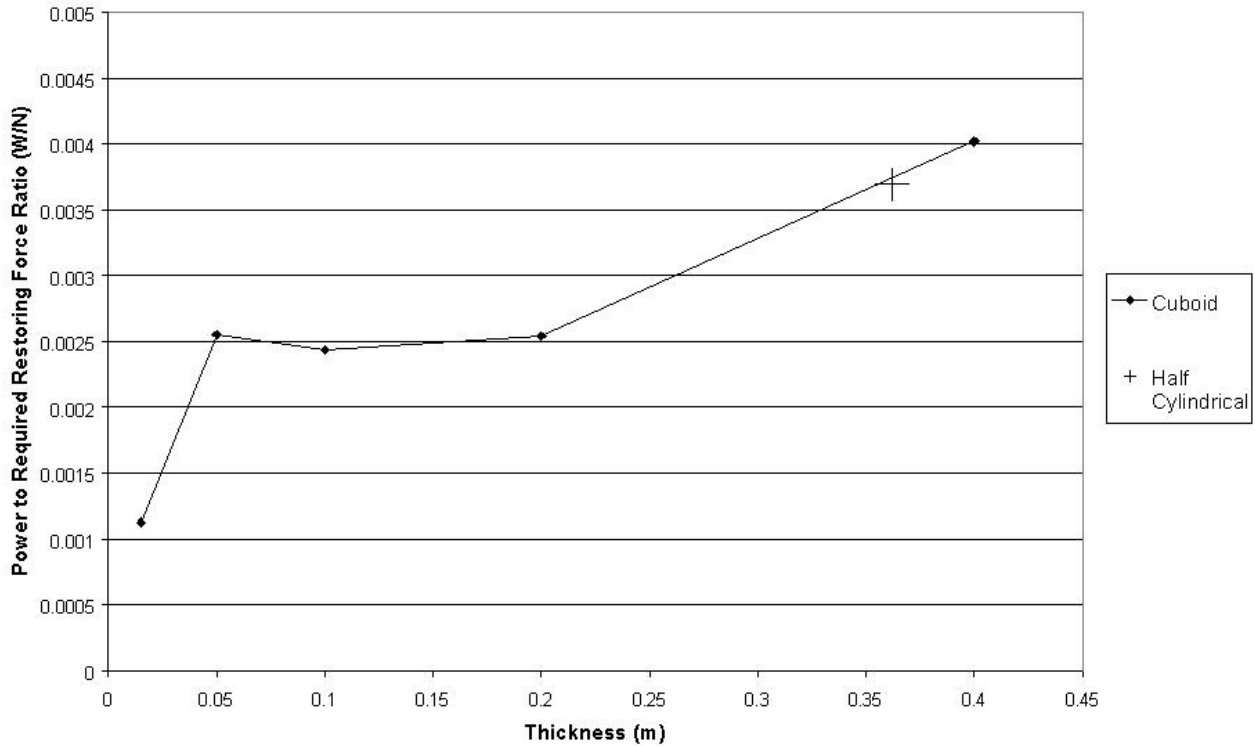


Figure 29 – Comparison of Half Cylindrical collector maximum power to restoring force ratio variation, with that of cuboid collectors of varying thickness, in 1.6s 0.025m amplitude sinusoidal waves

3.2.7 Cylindrical Collector

The performance of a cylindrical collector was compared to that of the cuboid designs. This collector had the same diameter as the draught of the Basic EB Frond. This test was performed with 1.6s waves. The cylindrical collector produced 2% less power than the basic EB Frond.

3.2.8 Wave Period Variation

A number of 0.05m height waves with different periods were used, with the EB Frond tuned to them in each case, to investigate the trends of EB Frond performance with sinusoidal wave period. This test was performed with the basic EB Frond collector. Results from this test are shown in Figure 30 and Figure 31.

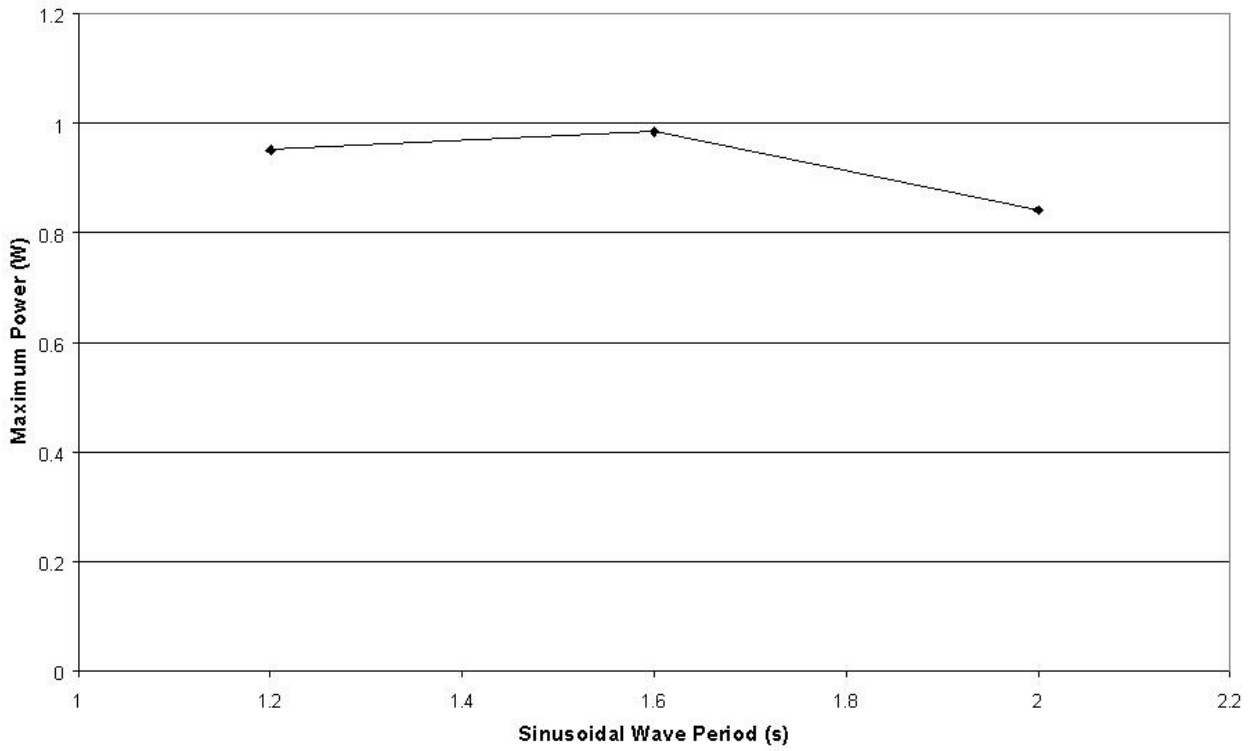


Figure 30 - Maximum power variation with wave period, in 0.025m amplitude sinusoidal waves, for the basic EB Frond

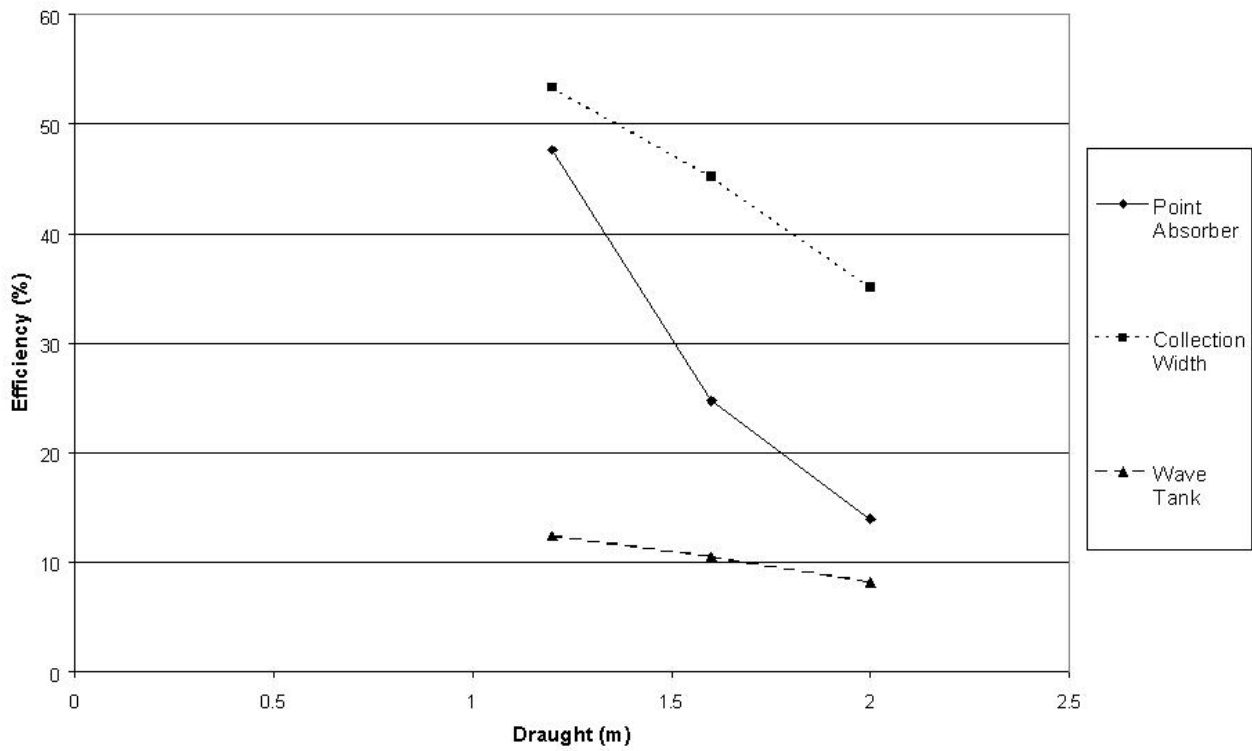


Figure 31 - Efficiency variations with wave period, in 0.025m amplitude sinusoidal waves, for the basic EB Frond

3.2.9 Summary

The maximum power produced by all collectors tested, in the first set of phase two Lancaster tests, is shown in Figure 32 and the ratios of power to restoring force in Figure 33.

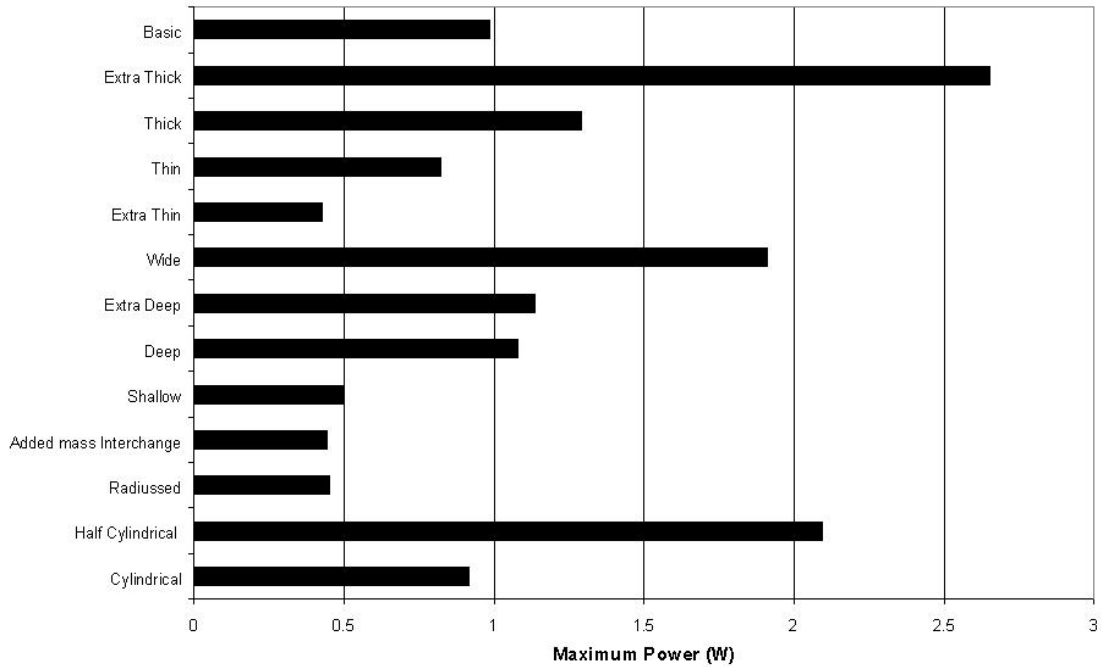


Figure 32 – Summary of maximum power, in 1.6s 0.025m amplitude sinusoidal waves, for all collectors tested in the first set of tests

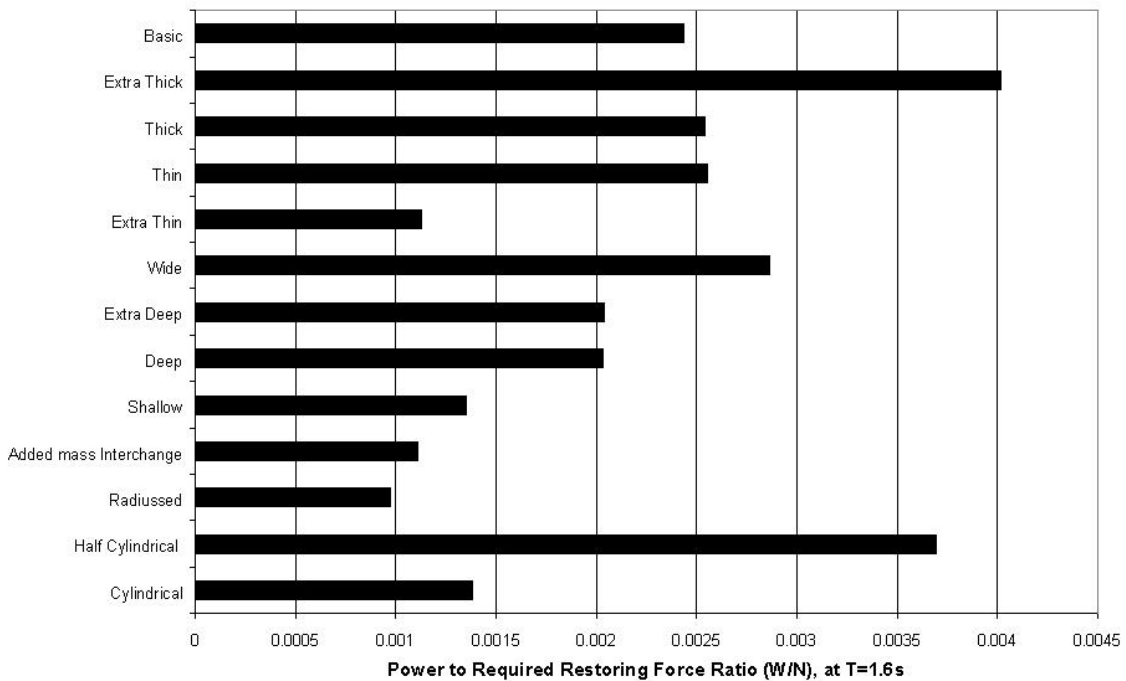


Figure 33 - Summary of maximum power to restoring force ratio, in 1.6s 0.025m amplitude sinusoidal waves, for all collectors tested in the first set of tests

3.3 Lancaster Second Set of Results

3.3.1 Comparison of Half Cylindrical and Triangular Collectors

The triangular and half cylindrical collectors were tested, at a freeboard of 0.015m, with sinusoidal waves of 1.6s period. Results are shown in Figure 34 and Figure 35.

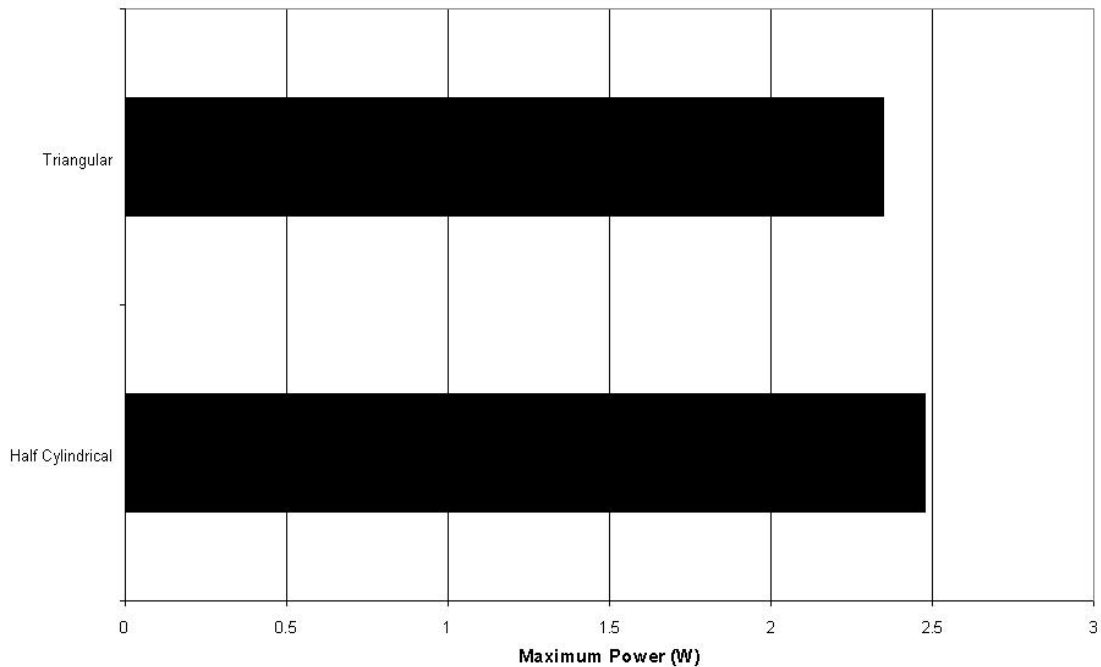


Figure 34 - Comparison of maximum PTO between the triangular collector and the half cylindrical collector, in 1.6s 0.025m amplitude sinusoidal waves

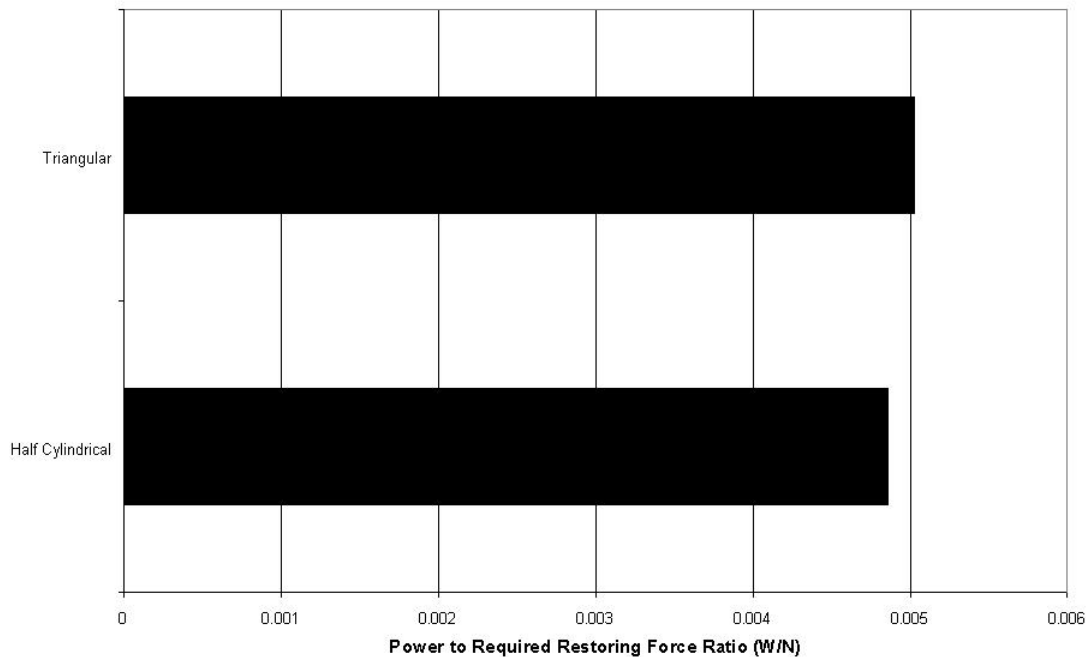


Figure 35 – Comparison of maximum power to restoring force ratio between the triangular collector and the half cylindrical collector, in 1.6s 0.025m amplitude sinusoidal waves

3.3.2 Buoyancy

Foam was removed from the inside of the triangular EB Frond collector, and additional masses of 9kg and 18kg were added to increase the mass of the collector, and therefore cancel the effect of some of its buoyancy. This also has the effect of increasing the inertia of the collector, so restoring forces were adjusted to keep the natural period of the EB Frond unchanged. The inertia of the collector was increased by approximately 50% and 100% with the two additions of mass.

This test was performed with 1.6s sinusoidal waves with a freeboard of 0.015m. Results of the individual time averaged power data points for a variety of PTO settings are shown in Figure 36 and Figure 37.

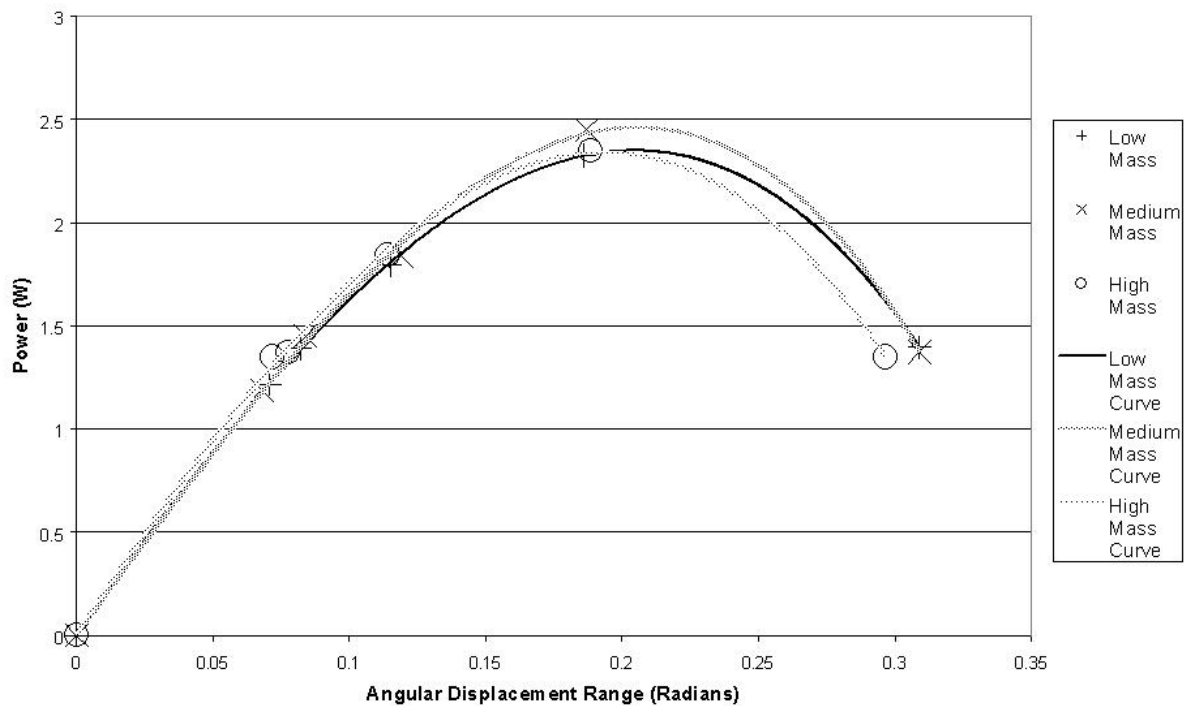


Figure 36 – PTO, angular displacement range relationships for triangular collectors, of different masses, in 1.6s 0.025m amplitude waves

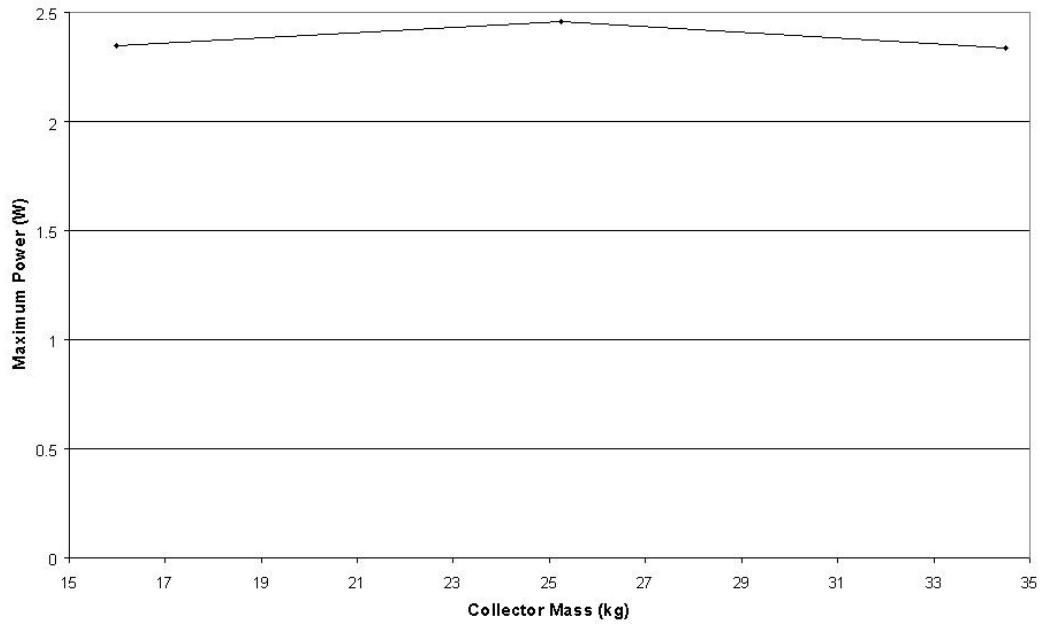


Figure 37 – Maximum power variation, in 1.6s 0.025m amplitude sinusoidal waves, with triangular collector mass

3.3.3 Freeboard

The triangular collector was tested in 1.6s waves with freeboards of; 0.115m, 0.081m, 0.048m, 0.015m, -0.018m, -0.051m and -0.085m. Results are shown in Figure 38 and Figure 39.

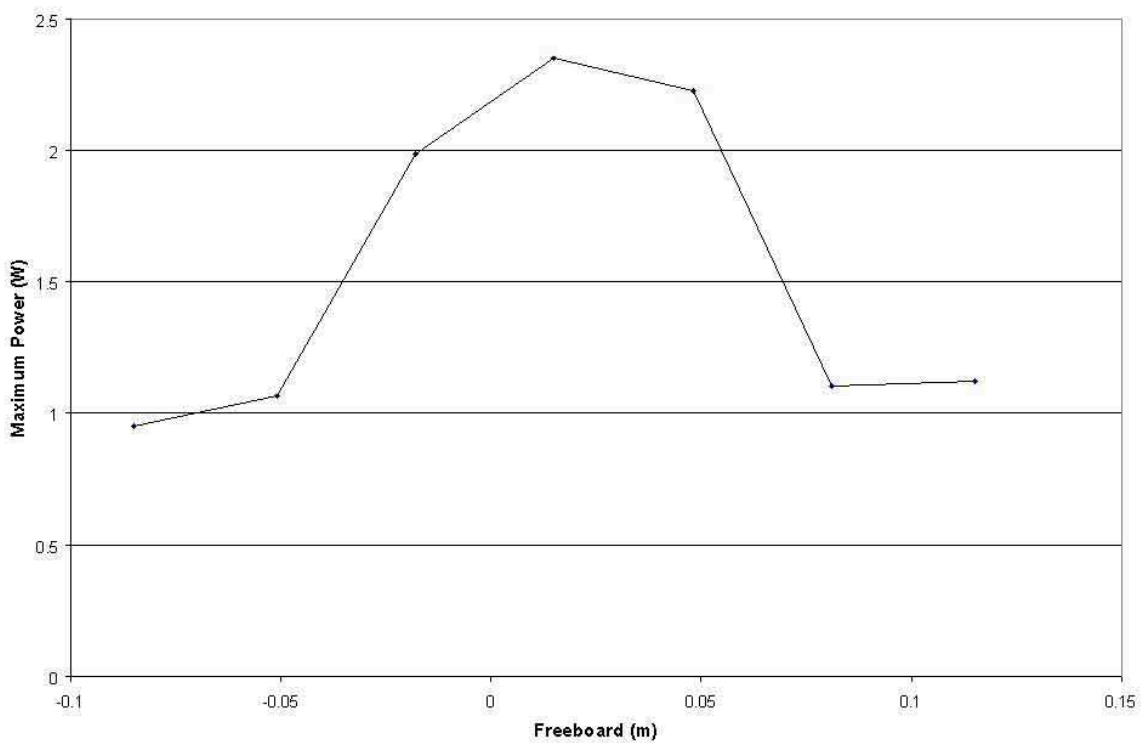


Figure 38 – Maximum power variation, in 1.6s 0.025m amplitude sinusoidal waves, with triangular collector freeboard

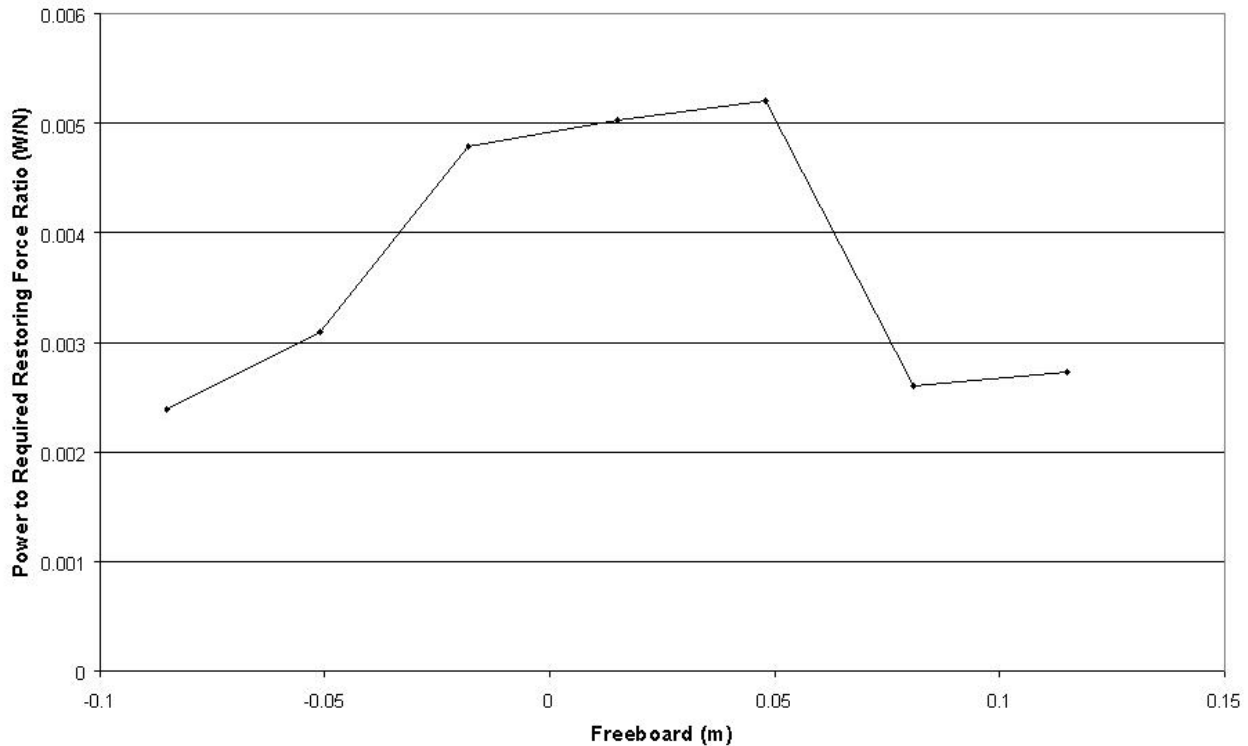


Figure 39 – Maximum power to restoring force ratio variation, in 1.6s 0.025m amplitude sinusoidal waves, with triangular collector freeboard

3.3.4 Pierson-Moskowitz Seas

The triangular EB Frond, with a freeboard of 0.015m, was tested in three Pierson-Moskowitz sea-states. Pierson-Moskowitz spectra represent fully developed sea states, with the peak period and wave heights being calculable from one another. As sea-states are built up of many sinusoids, of different periods, the optimum tuning of the EB Frond's natural period is more complex than with pure sinusoids. Each sea-state was tested with a variety of EB Frond natural periods, and the maximum possible power determined in each case through PTO variation tests. The optimum natural periods of the EB Frond and the optimum power outputs were then be determined, this is shown in Figure 40. Figure 41 shows the variation in optimum power output with significant wave height in Pierson-Moskowitz sea-states.

The Lancaster wave tank is not capable of producing Pierson-Moskowitz sea-states with a significant wave height of greater than 0.099m due to the limited travel of the wave making paddles. The ability of the paddles to accurately produce sea-states decreases with decreasing significant wave height, as any inaccuracy in the amplitudes of the sinusoids generated becomes proportionally larger. After calibration of the tank and analysis of the states generated it was decided that Pierson-Moskowitz sea-states, with significant wave heights in the range of 0.06m to 0.099m could be used with confidence.

Power to restoring force ratios and efficiencies for the Pierson-Moskowitz results are shown in Figure 42 and Figure 43.

Figure 44 shows these the power output results scaled up to full-scale predictions. Extrapolating from experimental results in a 3m Pierson-Moskowitz sea a power capture of 263kW is expected. Such an EB Frond in such a sea with such a power capture would be 28% efficient at extracting power from the theoretical power resource available to a point absorber. This efficiency falls with increasing wave height. For the smallest sea-states tested, which scaled up to a 1.5m significant wave height Pierson-Moskowitz sea-state, the EB Frond was 56% efficient at extracting power from the theoretical power resource available to a point absorber.

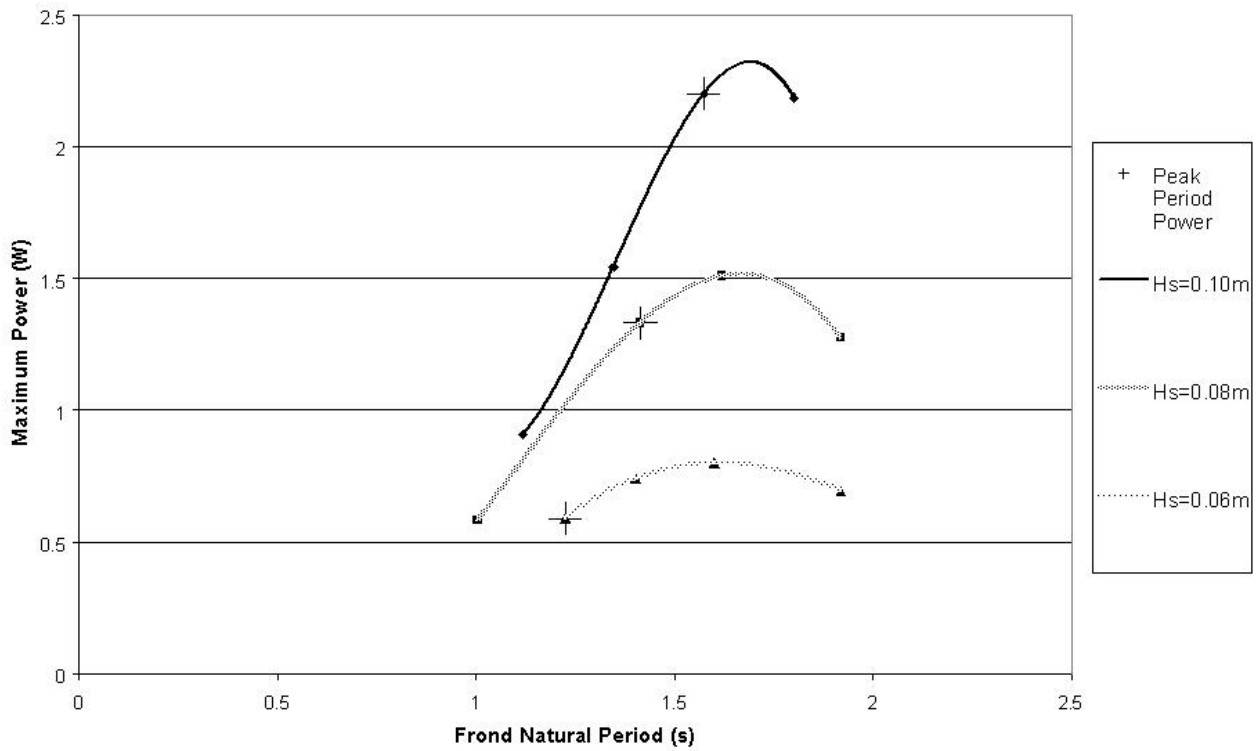


Figure 40 – Maximum power variation, in Pierson-Moskowitz sea-states, with triangular collector natural period

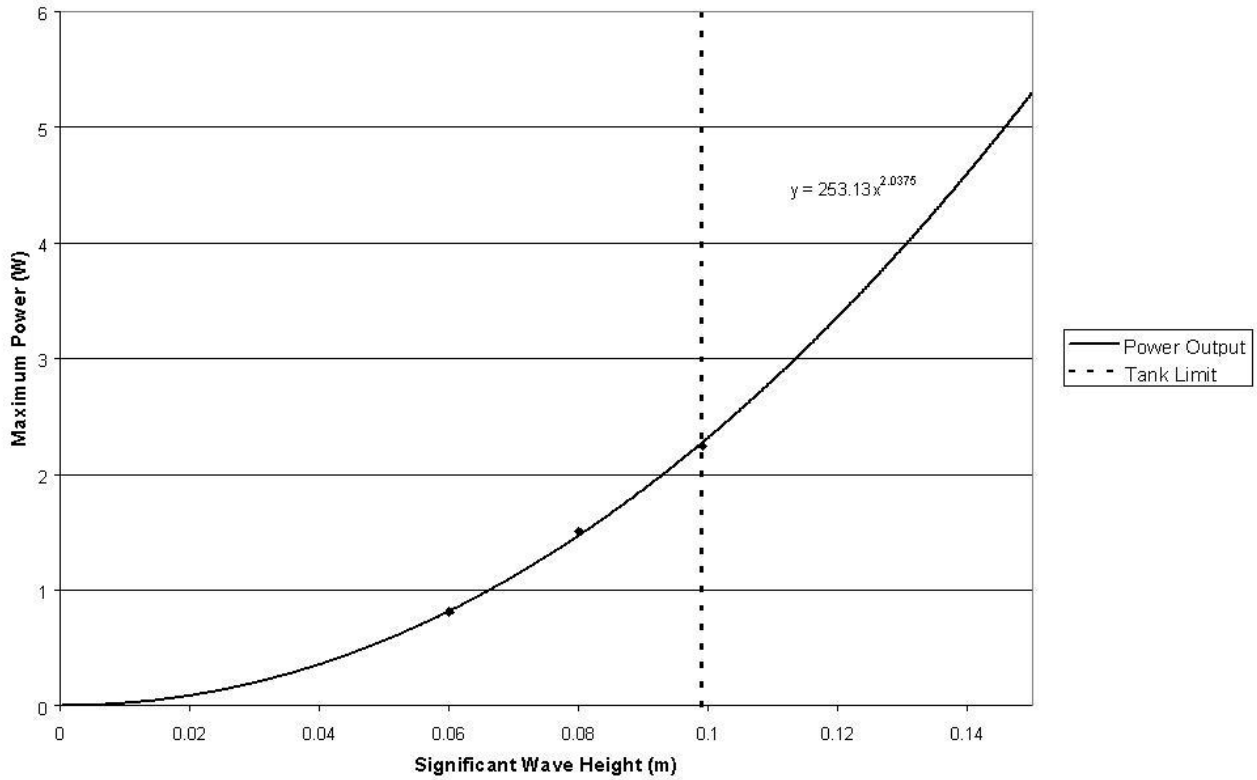


Figure 41 - Maximum power variation, in Pierson-Moskowitz sea-states, with significant wave height

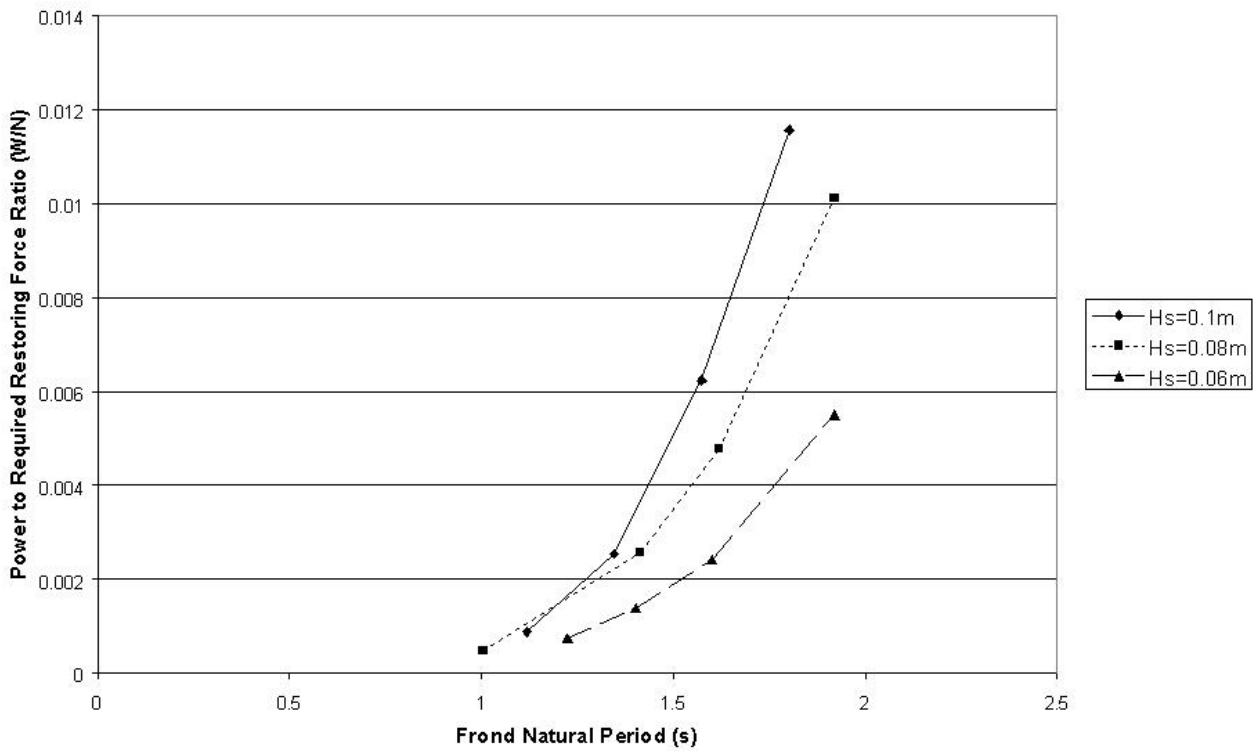


Figure 42 – Maximum power to restoring force ratio variation, in Pierson-Moskowitz sea-states, with triangular collector natural period

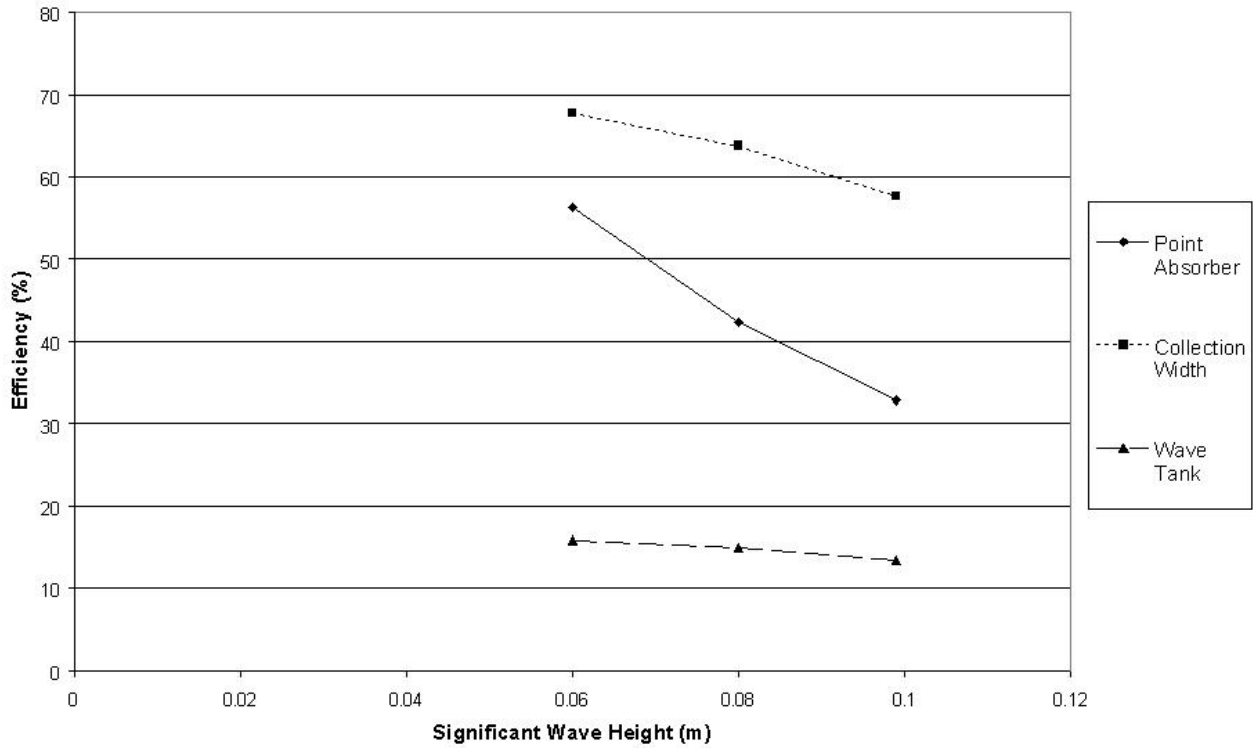


Figure 43 - Efficiency variations, in Pierson-Moskowitz sea-states, with triangular collector natural period

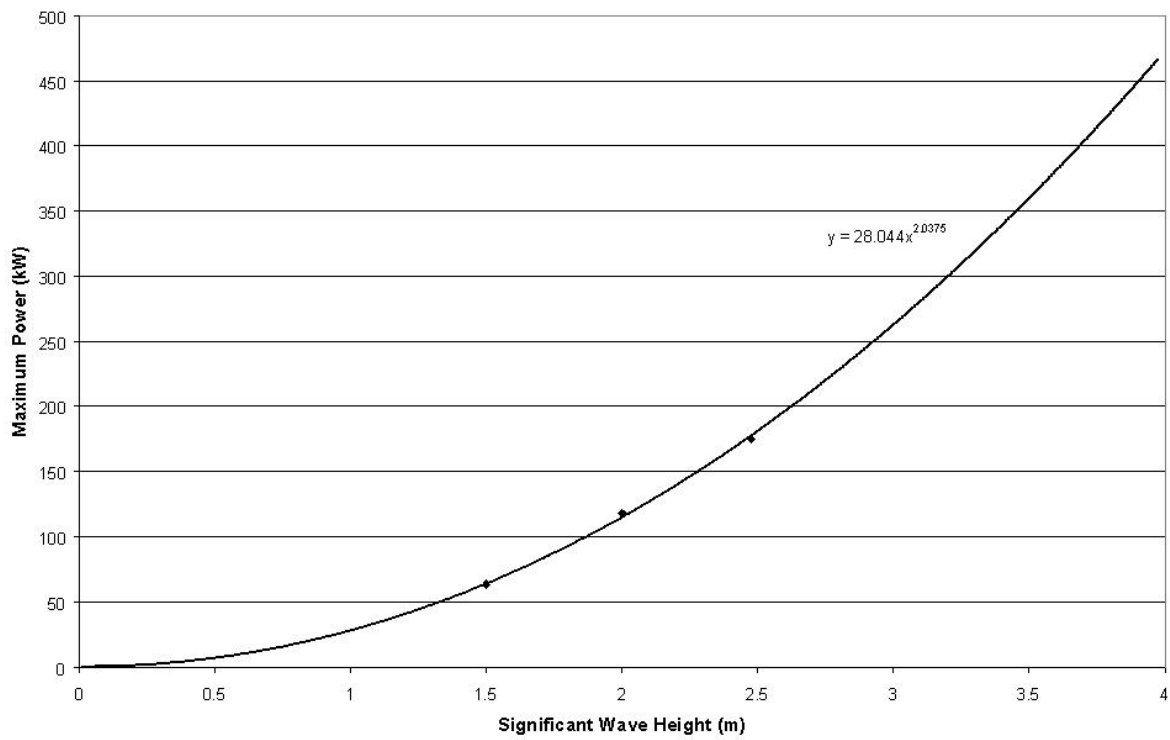


Figure 44 – Full-scale predictions of maximum power variation, in Pierson-Moskowitz sea-states, with significant wave height

4 MATHEMATICAL MODELLING

4.1 Philosophy and Objectives of Modelling

The purpose of the mathematical model was to produce power predictions and trends for EB Frond designs which could be used to effectively steer the more time consuming and expensive physical model testing. The mathematical model eliminated the need to physically test inappropriate designs, and predicted more efficient designs, the power outputs of which were later checked and verified with physical modelling. As with any development project, the EB Frond project has evolved through a series of design changes, which have often been the result of lessons learned from the mathematical modelling process. The move to a flat plate collector from a tubular design, the increased thickness of the collector, and the final triangular shape were all design improvements predicted by the mathematical model and later confirmed by physical testing.

The mathematical model is also used for more detailed power predictions of model designs, which have been physically verified, in a range of sea conditions which time constraints would not permit the physical testing of.

4.2 Choice of Model

Point absorbers have, traditionally, been modelled using linear theory. However, EB elected to review the validity of this theory for EB Frond and consider the use of an alternative time domain model.

The linear model can be used to predict EB Frond performance. It is often assumed with linear theory that radiation damping coefficients and driving torque amplitude are dependent upon one another. As a result of this dependency the linear model predicts that collector size and shape will have no effect on the power output of the EB Frond. Experimental findings disprove this concept, and that in fact collector size and shape have an extremely significant effect on power output.

However, the linear model can be used with separately calculated radiation damping coefficients and driving torque amplitudes. In this case the linear model can predict some power output variation with collector size and shape. Even with this modification, results from the linear model still show disappointing correlation with experimentally determined results. There are many non-linear effects at work in the behaviour of the EB Frond, which cannot be included in the linear approach. As a result the linear model is only used as a first approximation tool. More detailed analysis is performed using the time domain and physical models.

The linear model and time domain model were both used to model eight tests for one of the collectors tested, in sinusoidal waves, in the Newcastle tank tests. For the tests performed the linear model produces maximum time-averaged power estimations which, at best differ from the physical results by 176%, and at worst by 1556%. For the same tests the time domain model maximum power predictions differed from physical results by 7% at best and 61% at worst. All the linear model power predictions were over estimations; time domain model result discrepancies were both over and under estimations.

The linear model power predictions were produced between the Lancaster and Newcastle testing phases. It should be noted that the testing facilities at Newcastle were inferior to those used later at Lancaster and as a result the results from Newcastle are treated with more caution. However, the additional error in the Newcastle test results are assumed negligible when compared to power discrepancies of the order produced by the linear model. It was therefore felt that there was no need to repeat a mathematical model comparison with the new and more accurate Lancaster physical results.

4.3 Workings of Model

4.3.1 Introduction

The collector of the EB Frond wave power device is subjected to a variety of forces from the waves, gravity, buoyancy and mechanically applied forces. To obtain the most power from the waves the characteristics of the device must be optimised, and to assist in this a time-domain mathematical model has been constructed using Matlab's Simulink. This can, at a point in time, calculate all forces acting on the collector, and then calculate a new position, velocity and acceleration at the next instant in time. By continuing this process through many small time intervals a history of device motions can be built up. The waves can be turned off and the natural time period can be observed, or additional damping can be added to extract power, and this can be quantified and used to optimise PTO systems.

4.3.2 Overview

A simplified representation of the top level of the mathematical model is displayed in (fig 32) so that the manner in which the program executes can be seen. Each block in the diagram represents a subroutine. The lines into and out of the subroutines represent their inputs and outputs respectively.

Many pieces of information are calculated before the model starts, such as device and sea-state properties. These are not included in the above diagram as they are not key to the understanding of the time domain processes at work. The factors could be calculated externally and input into the model. They are not, as it is more efficient to have the model perform these calculations.

4.3.3 Time Domain Calculations

4.3.3.1 Torque / Inertia

This is the application of Newton's second law. With the total torque and inertia, including added mass inertia, known, the angular acceleration (θ'') of the arm can be calculated.

4.3.3.2 Theta' and Theta

By integration, with respect to time, the angular acceleration of the arm can be converted to angular velocity (θ') and angular velocity converted to angle (θ).

4.3.3.3 PTO Torque

The PTO force is calculated by multiplying the angular velocity by a constant, input by the user, and is applied in a direction such to oppose the motion of the arm, see Figure 45.

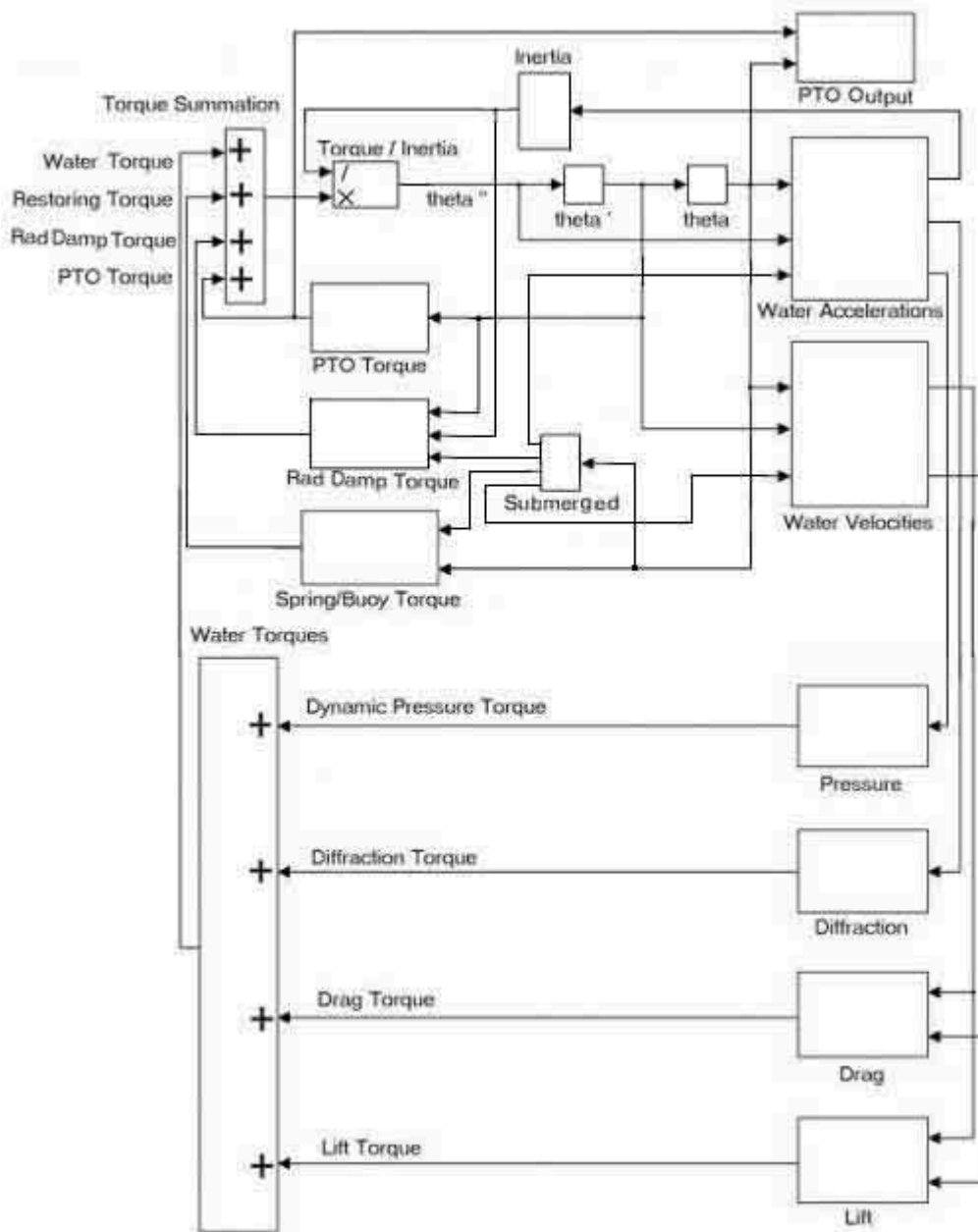


Figure 45 - Mathematical Model Top-Level

There is a certain amount of friction in the PTO system, which must be overcome, even at low speeds. Such a torque could, in an iterative process, actually drive the collector back and forth, as without time steps being infinitesimal, the final force in the time step before the collector stops could actually give it motion in the opposite direction. To avoid this problem a similar function is used for this friction as for the main PTO torque, producing very high sinusoids with angular velocity which are capped to approximate a step function.

It is ensured that the PTO torque cannot act to change the direction of motion of the collector, but only to stop it. The time step before the collector is due to change direction, the PTO torque is deactivated for one time step. This is to ensure that the PTO system cannot actually put energy into the system.

4.3.3.4 PTO Output

From the rule that the torque multiplied by angle moved is equal to the work done by the torque, the work done by the PTO system in each time step can be calculated. The time-averaged power over a long period, or the instantaneous power can be displayed.

In similar fashion it is possible to output similar results for all other sources of power loss in the EB Frond system, such as radiation damping, hydrodynamic damping, or spring losses.

4.3.3.5 Submerged

To calculate whether or not each of the collector mass and added mass finite elements are currently submerged the EB Frond angle is required to calculate the height and horizontal displacement of each element. From the wave-state and time the water levels at these horizontal displacements are calculated and compared to the heights of the elements.

4.3.3.6 Spring / Buoyancy Torque

From the mass distribution and density it is a simple matter to calculate the torques on the EB Frond due to gravity and buoyancy at any arm angle. The gravity and buoyancy torques are calculated for a number of collector finite elements and the arm, these are summed to produce a net torque. In the case of buoyancy torques, buoyancy effects are deactivated for all finite elements, which are not currently submerged.

In general buoyancy will not be sufficient and additional restoring forces will be required to achieve natural periods in the required range of wave periods. In the full-scale machine these may be applied by a hydraulic system, forcing the collector back into a vertical position. In the small-scale tests, springs attached to the top of the collector are used.

The spring system of the small-scale model is replicated in the mathematical model. The spring length, spring constant, spring friction, attachment points, the spring force and angle of it can be calculated for each collector angle. The magnitude of the spring force varies slightly with angle, greater angles lead to greater spring extensions and therefore shorter time periods. Also the line of action does not remain vertical, so the overall effect is not the same as that of buoyancy. These effects can be replicated in the mathematical model, or deactivated for a more simplistic solution. The restoring force system can be adjusted to mimic a hydraulic restoring force system that may be used in the full-scale machine. Figure 46 shows the direction of the torques in question.

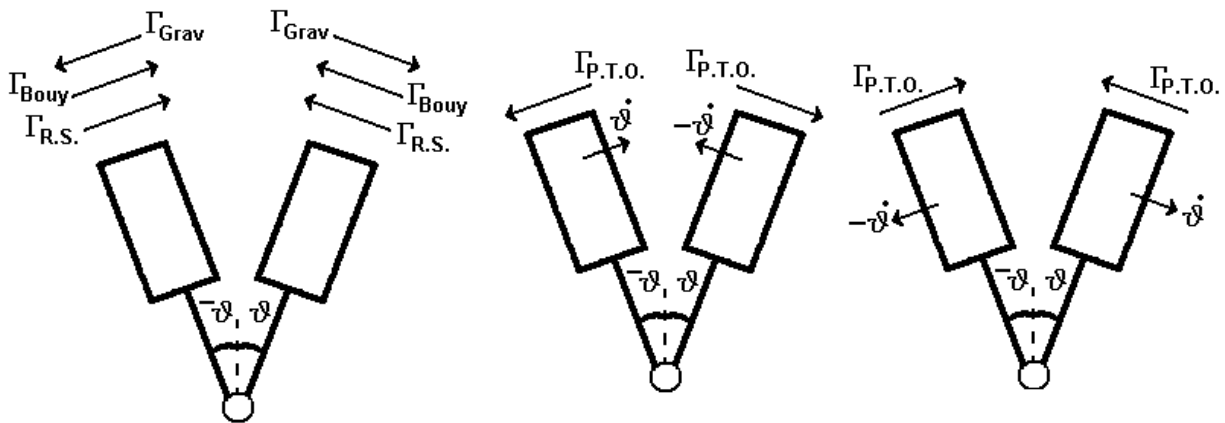


Figure 46– Directions torques arising from non-water forces.

4.3.3.7 Radiation Damping Torque

The radiation damping torque is calculated in the same manner as the PTO torque, with the exceptions that the damping coefficient used is time variable and the relative velocity between the collector and the water is used instead of the velocity of the collector.

Derivation of damping coefficients depends on, amongst other things, the amount of added mass present, the collector's level of submergence in the water and its vertical position relative to the seabed. As all of the above vary with time, it is logical to assume that the radiation damping coefficient is also time variable. At all time steps the radiation damping coefficient is derived. The radiation damping coefficient is also calculated for the collector in a central, vertical, position in still water. At each time step the current derived radiation damping coefficient is used in conjunction with the still water derived damping coefficient to produce a ratio. If an experimentally measured radiation damping coefficient is in use, this ratio is used to adjust the experimentally measured damping coefficient accordingly. Both the originally derived damping coefficients and the experimentally measured ones are calculated from simple still water oscillations, and so should be subject to the same relative effects.

The time domain model can generate damping coefficients which show good agreement with other mathematically determined damping coefficients from established software packages, such as Wamit. However, mathematically derived radiation damping coefficients have been widely found to be under estimations, especially in resonance cases, when compared to physically measured ones. Where possible, experimentally measured damping coefficients are used in favour of derived ones.

The radiation damping coefficient of a specific collector can be measured from the observation of its free decay in still water. The collector is displaced and its induced oscillation allowed to decay. In the time domain model relative velocities between the collector and the water are used in conjunction with the still water measured radiation damping coefficients. For this reason it is important that when measuring free decays the water is as still as possible so that collector speed, and collector speed relative to the water, are approximately the same.

The average relative velocity across the face of the collector is used as the relative velocity for the damping torque.

4.3.3.8 Water Accelerations

The tangential acceleration component of the water about the arm pivot is calculated at all submerged finite element points relating to the dynamic pressure and diffraction forces, see Figure 47. These values vary in time and space, as the waves are constantly changing and the EB Frond is constantly in motion.

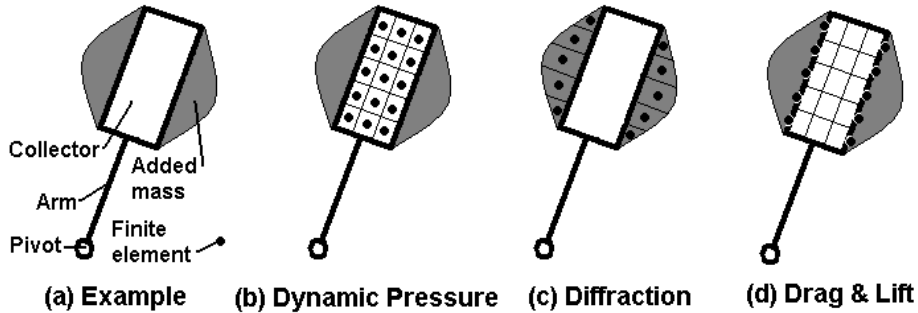


Figure 47 - Division of EB Frond system into sections, and positions of the finite elements for different water forces

For the diffraction force it is the relative tangential angular accelerations between the water and the collector's added mass that are of interest. However subtracting the collector's tangential acceleration from the water's tangential acceleration would create an algebraic loop in the program. To avoid this problem non-relative tangential angular accelerations are used at the points of interest. Using the non-relative acceleration values does not introduce an error, because it is accounted for by the increasing of the EB Frond inertia to include that of the added mass.

The water accelerations are calculated for all of the sinusoid wave components in use and these values are summed at all points of interest.

The amount of added mass related to the collector is dependent upon the angle of the relative acceleration between the water and the added mass. To calculate this angle the relative components of the water's acceleration are required.

There is no acceleration of the collector radially, so the radial relative acceleration of the water is the same as the non-relative acceleration. To calculate the tangential relative acceleration, the EB Frond's tangential acceleration is required. Using this would create an algebraic loop in the program. To avoid this problem the EB Frond's tangential acceleration from the previous time step is used. As the time steps are small and the acceleration only slowly varying the error is small. The water acceleration components are calculated for all of the sinusoid wave components in use and these values are summed at all the points of interest. From the two total relative acceleration components, an angle of attack is calculated for each point of interest.

4.3.3.9 Water Velocities

The tangential and radial components of the water velocity about the EB Frond pivot are calculated at all the submerged finite element points of interest (those relating to lift and drag forces, see Figure 47). These values vary in time with space.

The water velocities as a result of a tidal stream, if one is present, are calculated at all the same finite elements.

The water velocities are calculated for all of the sinusoid wave components in use and the tidal stream, and these values are summed at all the points of interest.

The angular velocity of the arm is used to convert the tangential velocity component values into relative tangential velocity values; the radial components are unaffected. The resultant relative velocity of the water and its angle of attack relative to the face of the collector are then calculated for all finite element points.

4.3.3.10 Inertia

The inertia of the EB Frond system is constantly changing, as added mass is gained and lost. The quantity of added mass associated with the collector is dependent upon the angle of attack of the water acceleration, relative to the acceleration of the collector. If an added mass element is not submerged it is assigned zero added mass.

4.3.3.11 Dynamic Pressure Torque

The dynamic pressure force is calculated for each finite element by multiplying the water acceleration by the mass of water the element has displaced. Each of the forces on the elements of the collector is converted to a torque, and these torques then summed.

4.3.3.12 Diffraction Torque

For each element, the diffraction force is calculated by multiplying the water's acceleration by the amount of added mass of the element. The added mass of each element is dependent upon the angle of attack of the relative acceleration and the maximum amount of added mass. Each of the forces on the elements is converted to a torque and these torques are then summed.

4.3.3.13 Drag Torque

There are relationships for different shapes stored in the program, which can be used to convert angles of attack into drag coefficients. The angle of attack at each collector element is used to generate appropriate drag coefficients. The drag force, using the relative water velocities and element area, is then calculated for each element.

If forces acting on the elements on the right-hand side of the collector act to the right, or vice versa, they are replaced by zero. This is because for the water to be able to cause these torques it would have to have had its position within the collector structure during the previous time step, which it could not have done.

Each of the forces on the elements is converted to a torque and these torques are then summed.

4.3.3.14 Lift Torque

The Lift torque is calculated in exactly the same manner as the drag torque, with the lift coefficients in place of drag coefficients.

4.3.3.15 Water Torques

All four water torques are summated to produce one net torque caused by the waves.

4.3.3.16 Torque Summation

The four torque groups are now summed: the wave torque, the restoring torque, the PTO torque and the radiation damping torque, to produce one net torque which will determine the next instantaneous arm angular acceleration. The program can then repeat all of the above steps with different results as the waves will have changed slightly with time and position, and the arm will have a slightly different angle, angular velocity and angular acceleration.

4.3.4 Non-Time Domain Calculations

4.3.4.1 Mass Inertia

The inertia of the EB Frond mass is not variable. The inertia of the collector and arm are calculated separately and summed. The arm is a simple thin rod and its inertia can be calculated by a simple relation. As collectors of a variety of different shapes are used the inertia of the collector about the pivot is calculated by finite element analysis.

4.3.4.2 Maximum Added Mass

The program has relations for simple shapes between their dimensions and the amount of added mass they have, assuming that they are deep underwater and that they are not close to any other structures.

If an underwater object is close to the free surface of the water, there will be an effect on the added mass of the object. This effect may be dependent upon the frequency of oscillation of the object. Physical results have indicated no significant variation in added mass with frequency, therefore the low frequency assumption is made, and added mass variations, in the frequency range of interest, with frequency are ignored.

The only available literature on added mass surface effects gives added mass increase ratios for cylinders near the water surface. The added mass increase factor is determined from the radius cylinder, and the distance from the centre of the cylinder to the still water surface. This relationship was generalised to all collector shapes used, with half the collector draught being used in place of the cylinder radius.

It is necessary to calculate the inertia of the EB Frond system, and calculate added mass related torques on various finite elements of the EB Frond collector. As a result it is necessary to understand not only the amount of added mass present, but also the distribution of said added mass about the collector, so that added mass quantities can be assigned to individual finite elements. Different relations are used for different collector shapes to appropriately distribute the calculated amount of added mass about the added mass finite elements.

Despite the use of many approximations to estimate added mass quantity and distribution, the calculated values have been verified with physical results. It is also possible to directly input maximum added mass quantities, for each finite element, without deriving them. This may be appropriate for some of the less regular shaped collectors, which may be tested in the future.

4.3.4.3 Wave Spectra Components

The model currently produces two types of wave spectra, Classical Pierson–Moskowitz spectra and Modified Pierson–Moskowitz (ISSC) spectra. Classical Pierson–Moskowitz spectra have a given peak period with a given significant wave height, whereas the ISSC spectra can have any peak period with any significant wave height.

The program uses 20 sinusoidal wave components to represent a spectrum. So that only a few components do not represent the most significant part of the spectrum, with the others having little or no effect, the condition is imposed that all sinusoidal waves will be of equal amplitude and therefore comparable significance. Sinusoidal waves at the frequency extremes therefore represent much larger frequency ranges, than those in the middle.

4.3.4.4 Wave Numbers

For each wave component used it is necessary to know its wave number. The wave spectrum equations express the wave components in terms of time periods, not wave numbers. Although the two are related a wave number can not be directly calculated from a time period.

The program uses an initial guess at the wave number and an iterative process to calculate the wave numbers from the time periods.

4.3.4.5 Radiation Damping Coefficient

The linear radiation damping coefficient is derived using the Haskind relations. The radiation damping coefficient is dependent upon the frequency of oscillation of the collector. In wave spectra the collector will undergo a number of different frequency oscillations, in this case the radiation damping coefficient corresponding to the natural frequency of the collector is used, as oscillations at this frequency can be expected to be largest and most significant, due to resonance effects. In pure sinusoidal waves the radiation damping coefficient corresponding to the frequency of the waves is used, as this is the frequency at which the collector will oscillate.

4.4 General Testing Process

4.4.1 Natural Period Tests

As with the physical testing, before the mathematical model is run with waves, free oscillations are observed to correctly tune the device. This is achieved by applying different amounts of vertical restoring force to the collector, displacing the arm and, on its release, the periods of the subsequent oscillations are recorded. By building up a relationship between applied restoring force and observed period it is possible to calculate the restoring force necessary to tune the device to any required period. The restoring force to natural period relationships are not an exact match in the physical and mathematical tests, therefore slightly different amounts of restoring force are applied in the two cases. However, the natural period tuning of the two models should be comparable. Physical tests have shown that the behaviour of the EB Frond is dependent upon the natural period of the device, not the amount of restoring force applied, therefore errors introduced from tuning discrepancies are assumed to be negligible.

4.4.2 Radiation Damping Coefficient Tests

The radiation damping coefficient of a specific collector is measured from the observation of its free decay in still water. For analysis of the decays the peak angles and the time at which they occur are of interest. The modulus of peak angles is plotted against time and exponential decay curves calculated. Mostly submerged and near surface collectors produce significant waves during their free oscillations. In such cases, only the very initial part of the decay can be considered to be a true still water decay. Therefore only the decay curve of the initial decay is used in the calculation of the radiation damping coefficient.

The exponent of the exponential decay function fitting the experimental data is used to calculate the radiation damping coefficient.

Radiation damping coefficients are measured for each collector, and position in the water, across a range of oscillation frequencies. Radiation damping coefficient relationships with oscillation frequency are built up for each collector and set-up, so that coefficients can be extrapolated for any oscillation frequency of interest.

4.4.3 Maximum Power Output Tests

The maximum power output of a given collector, with a given natural period and in a given sea-state, is calculated in the same way for both the time domain and physical models. The time domain model is run with a given sea-state, and PTO setting. The motion is allowed to settle and the average power output and displacement range are measured. By performing a number of similar tests with a variety of PTO strengths a relationship between displacement range and average power output can be produced. This relationship can be used to calculate the maximum possible obtainable average power in that particular state with that particular collector and natural period. Figure 48 shows an example of a displacement range versus average power curve produced from both the physical and time domain mathematical models. The two curves Figure 48 show good agreement, although the individual points on the two curves are not comparable, as the PTO strength was not adjusted in the same increments in both of the two testing procedures.

Third order polynomial curves are fitted to the displacement range versus average power curves, and these are differentiated to calculate the maximum possible time-averaged power value. Only four data points are required to generate a third order polynomial function. With the mathematical model, as repeatability of individual tests is perfect, only four data points are used.

It has been checked that the functions produced by the mathematical model are third order polynomials. Displacement range versus average power curves have been generated with many more data points. All data points were accurately positioned on a third order polynomial curve, indicating that there is no need to generate more than four points.

With the physical model, third order polynomial curves are generated from six points. The addition of the two extra points is to cancel any possible random effects present in any of the individual readings. The fact that physical data points fit well

to third order polynomials is an indication of the repeatability of the physical tests, because after the first four points the relationship is roughly known, the fact that the next two points agree with the relationship increases confidence in results.

The maximum power output in random seas is calculated in similar fashion. Power outputs must be averaged over a much longer time, as the effect of fluctuations in the wave train must be allowed to cancel out. As the collector does not settle into a regular motion, power output is plotted against the time-averaged modulus of the displacement (the average displacement when taking both positive and negative readings as being positive).

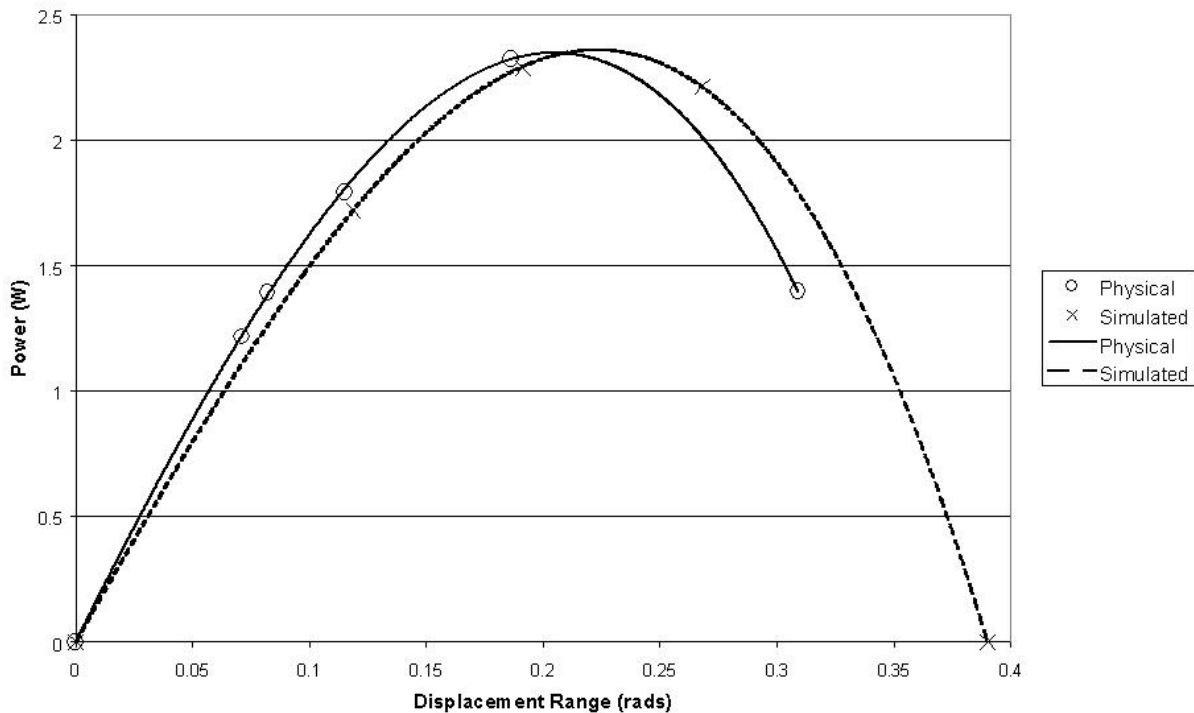


Figure 48 – Power Displacement curve for Triangular collector, of natural period 1.6s, protruding 15mm in 1.6s 0.025m amplitude sinusoidal waves

4.4.4 Water Torque Amplitude Tests

In the physical tests the EB Frond is held vertically, unable to move about its pivot. The waves are activated and the torque exerted on the collector by the waves about the pivot is recorded. Linear theory suggests that when the input waves are sinusoidal this torque should be sinusoidal with time. This is not strictly true, but as the EB Frond is stationary many of the non-linear effects are either decreased or not present, and so the wave torque can be seen to be approximately sinusoidal in time.

The amplitude of this torque is dependent predominantly on the amount and distribution of added mass about the collector and the collector volume. Therefore good agreement between the amplitude of this torque determined from both the physical and time domain models used indicates good validity of the mathematical model used.

4.5 Validation Process

The process of validation of the mathematical model was agreed as embodying the following stages:

- Verification of the physics in the mathematical model, and correction if necessary.
- Development of a programme of physical scale model testing.
- Comparison of the results of the physical and mathematical models.

The mathematical model would be considered validated if the comparison showed agreement within reasonable engineering tolerances.

Professor Bradshaw, of Lancaster University and Professor Incecik of the University of Newcastle upon Tyne were commissioned to investigate the EB mathematical modelling process and report on its suitability. The conclusions reached by the two experts indicated no need for EB to change its mathematical modelling approach, based on a time domain model.

As part of the verification process, EB commissioned the development of a linear model (working in the frequency domain) from the University of Lancaster. Comparison of the results of the two mathematical models showed that EB's time domain model was superior in almost all respects.

5 ANALYSIS AND INTERPRETATION

5.1 Newcastle

5.1.1 Wave Amplitude Variation

The power in the waves, and the theoretical point absorber power resource, rises with the square of the wave amplitude. Linear theorists have predicted no change in efficiency with wave amplitude. For all wave periods tested a power output increase was seen with increasing wave amplitude, however not as much as predicted by linear theory. This test showed that the EB Frond is more efficient at capturing wave energy at lower wave amplitudes (Figure 14).

5.1.2 Freeboard Variation

A power output rise was seen as the EB Frond was slightly raised out of the water, and a power decrease was seen as it was slightly lowered (Figure 15). The beneficial effect of raising the EB Frond was noted, but for the remaining tests at Newcastle a freeboard of zero was used. The purpose of this test was to investigate possible power output variations across a tidal range.

5.1.3 Wave Incidence Angle Variation

It was found that the power output of the EB Frond increased as the angle of incidence was increased from 0° to 10°, and then decreased with further incidence angle increases, returning approximately to its 0° value at approximately 20°, see Figure 16. The purpose of this test was to investigate the possible effects on power generation of the wave angle of incidence varying. Since, in real seas, the angle of incidence is expected to vary by more than 10°, the idea of orientating the EB Frond at an angle to the predominant wave direction was discounted. It is anticipated that the EB Frond will be orientated to face the predominant wave direction, and variations in incidence angles of approximately ± 20 degrees will lead to performance improvements.

It should be noted that these results might be very specific to the collector. For example, collectors which are symmetric about the arm axis could be expected to suffer only performance decreases with incidence angle, as the forces acting would not change with angle but they would produce smaller torques. This test highlights the fact that the shape can be improved.

5.1.4 Collector Thickness Change

With all wave tests a significant increase in EB Frond power output was seen with the move to the thicker collector, see Figure 17. The possibility of moving to thicker collectors was noted and investigated further in the Lancaster tests.

5.1.5 Sea Spectra

The results give a scaled up power of 71kW in a 2m significant wave height sea spectrum. This value was not as high as required, but was high enough to be encouraging at such an early point in the EB Frond design.

It should be noted that, due to the fact that the optimum natural period of the EB Frond in this spectrum was not ascertained, the power output could only be expected to rise with further tuning.

Due to problems with the calibration of the wave tank, there are doubts as to whether the spectrum used was a true ISSC spectrum. Results from this test should, therefore, be treated with some caution. More rigorous sea spectra testing was performed in later stages at Lancaster with more evolved EB Frond designs.

5.2 Implemented Improvements in Experimental Operation

With hindsight, the Newcastle results are believed to have had certain limitations. Improvements were made in apparatus and experimental technique before the Lancaster tests. Some of the limitations of the tests have already been discussed, but the key differences between testing at the two sites are outlined below.

5.2.1 PTO System

It is believed that the electric motor used as part of the PTO system at Newcastle put some energy into the system. A new motor and control system was used in Lancaster, eliminating the possibility of reoccurrence of this effect.

The attachment from the collector to the PTO system was, at Newcastle, via a cord, which was free to extend, compress and slip. In the Lancaster testing, the PTO system was upgraded and the attachment to the collector was via an inextensible rod.

5.2.2 Restoring Force System

At Newcastle constant tension springs were used. These were found to have significant levels of inherent stiction. The effect of this stiction was the removal of energy from the EB Frond system in a manner unrepresentative of the full-scale device. In the Lancaster testing the restoring force was applied via the use of long light springs with negligible inherent stiction.

5.2.3 Wave Tank

The Newcastle tank was not accurately calibrated. The desired and requested wave amplitudes corresponded only loosely to what was physically generated. Although many of the tests performed at Newcastle required equal amplitude sinusoids in all test cases, the fact that this was not achieved significantly constrains the value of the results.

An attempt to generate ISSC spectra using the Newcastle wave tank was made. The spectra produced had neither the desired significant wave heights nor peak periods. As spectra consist of many superimposed sinusoids, and the Newcastle wave tanks sinusoids were not calibrated, it is unlikely that the spectra produced were accurate representations.

The beaching effects at Newcastle were of uncertain adequacy. The tank was not originally equipped with beaches, therefore beaches were rented and installed in the tank, but their effectiveness was never accurately quantified.

The Lancaster wave tank was calibrated for all frequencies, before testing began. The ability of the tank to produce accurate wave spectra and the efficiency of the beaches was also checked and found to be acceptable.

5.2.4 EB Frond Natural Period

At Newcastle the oscillations used to calibrate the EB Frond tuning system were timed manually with a stopwatch, resulting in the potential for relatively large errors in the tuning of the natural period of the EB Frond being introduced. For the later tests at Lancaster, this error was mitigated through the use of a PLC-based control and monitoring system.

The restoring force system could only be set to certain discrete values, at Newcastle, as could the period of the waves produced by the wave-makers. Natural period and wave period settings that were similar were chosen. With the subsequent Lancaster tests the natural period and wave period could be set to any desired value.

5.2.5 Calculation of Maximum Possible Power

Maximum possible average power values were obtained from the physical results by matching a third order polynomial curve to the power and displacement points from each PTO setting test in a test set. Only four points are required to produce such a polynomial, but more points improve accuracy. In Newcastle five points were used. All tests in a set were completed before the data was analysed. As a result, it was sometimes found that many of the points were clustered in one region of the polynomial, almost functioning as a single point. In such cases the accuracy of the polynomial generated is questionable, leading to some results being entirely disregarded on such grounds. During the Lancaster testing the number of data points used was increased to a minimum of six. Data analysis software was written, in advance of the tests, which enabled real time analysis of results on site such that the points on the polynomial curve could be viewed as the tests were completed, and decisions based on them as to what PTO settings to test next. This ensured that data points were collected across the entire range of interest.

5.2.6 Summary of Limitations

The reliability of the raw data gained from the Newcastle tests is less than that of the data obtained from the Lancaster tests due to limitations of the EB Frond apparatus, monitoring equipment and tank. The value of this data is also reduced because limited data points, similar data points and changing extraneous variables mean that conclusions drawn from its analysis must be treated with some caution. The Newcastle tests were valuable in shaping the direction of the subsequent stages of the project. However, with the subsequent acquisition of more accurate and useful data on more evolved EB Frond designs, it should not be taken as a prime source of EB Frond data.

5.3 Lancaster First set of results

5.3.1 Thickness Variation

It was seen that the power output rose significantly as the cuboid thickness was increased. In the thickness range tested the thickness was increased by a factor of 27, and the power output of the EB Frond was observed to rise by a factor of over 6 (see Figure 18, Figure 19 and Figure 20).

The power to restoring force ratio was also seen to increase significantly over the thickness range investigated, indicating that the restoring force system costs were not likely to limit the move, in this range, to thicker collectors.

It is believed that the increase in power output associated with thickness increase is due to an increase in both collector volume and the amount of added mass attributed to it. The two most significant, and driving, torques acting on the collector from the water are the dynamic pressure torque and the diffraction pressure torque, which are proportional to the collector volume and added mass quantity, respectively. Hence thicker collectors should receive a larger driving torque from the waves.

It is also noticeable that the thicker collectors had an observable effect on the water surface, producing a barrier to the flow of water. The increased thickness means that it is more difficult for water to spill over the top of the collector, and that the collector when the collector is displaced, although its centre line is moved down, one of its sides maybe moved upwards, maintaining partial protrusion from the water of the collector, thereby maintaining a barrier to the flow of water. This allowed a slight head difference to build up across the two sides of the collector, which would lead to a slight increase in wave forces. It is believed that this effect may have contributed to the observed increased efficiency of power capture.

The above arguments for increased power output with increased collector size, and added mass quantity, are valid not only for collectors used in thickness variation tests, but also for all collectors used.

5.3.2 Width Variation

It was seen that the power output was almost doubled as the cuboid width increased from 0.630m to 1.030m, see Figure 21, Figure 22 and Figure 23. The reasons for this power increase are the same as the reasons for the power increase with increasing thickness, although with the possible exception of the "barrier effect" described above.

The power to restoring force ratio was seen to increase slightly over the width range investigated.

5.3.3 Draught Variation

Two wave periods were used because the proportion of total wave power in a depth range varies with wave period.

It was seen that the power output rose significantly as the cuboid draught was increased, in both 1.6 and 2 second waves. The reasons for this are again increased volume and added mass quantity. It should be noted that with the 1.6s waves only a slight power increase is observed as the collector draught is increased from 0.305m to 0.505m, whereas in 2s waves large power output increases are still measured across this draught increase range. This is because longer period waves contain a larger proportion of their power deeper in the water. In the case of the of 1.6 second waves the larger draught extensions are extending the collector into a region where there is little power.

It was seen that with 1.6s waves the power to restoring force ratio was highest with a draught of 0.305m. This implies that the current choice of draught for the collector is reasonable. However, this may change if the freeboard of the collector is significantly adjusted (Figure 24, Figure 25, Figure 26 and Figure 27).

5.3.4 Added Mass Interchange

The observed variation in performance was judged to be insignificant. No significant benefit was observed in the interchange of small amounts of added mass for volume.

5.3.5 Radiussed Collector

The poor performance of the radiussed collector was attributed to a reduction in its added mass, reducing the driving wave torque, and an increased radiation damping effect due to the water's ability to flow with ease over and around the collector's radiussed edges as it oscillated generating significant surface wave effects.

5.3.6 Half Cylindrical Collector

The half cylindrical collector has the majority of its volume in the higher proportion of the wave where a larger proportion of the wave energy is, and where larger driving forces can be generated. The thicker cuboid collectors seem to incur only small power benefits from having large amounts of volume lower in the water. Due to its smaller volume, and therefore lower required collector inertia, and lower potential forces on it from large storm waves (which have large amounts of power lower in the water), the half cylindrical collector would appear to be more practical than a cuboid collector built to produce the same power output (see Figure 28 and Figure 29).

5.3.7 Cylindrical Collector

The cylindrical collector produced comparable power outputs to the basic EB Frond, which is a much smaller and simpler to engineer collector shape. As a result interest in a cylindrical collector was discontinued. The reason for its poor performance is attributed to increased radiation damping effects for the same reasons as with the radiussed collector.

5.3.8 Wave Period Variation

No significant variation in power output was noticed across the time period range investigated, despite changes in power resources, with the basic EB Frond collector (Figure 30 and Figure 31).

5.3.9 Summary

At the end of the first set of tests it was decided that the half cylindrical collector shape was the most promising. Although the extra thick collector produced more power, both its buoyancy and the restoring force it requires were considered too large. Thickness, width and draught tests indicated that these dimensions were of the correct order in the half cylinder shape (Figure 32 and Figure 33).

5.4 Lancaster Second Set of Results

5.4.1 Comparison of Half Cylindrical and Triangular Collectors

The two shapes are very similar in size, shape and added mass distribution; it was therefore expected, and predicted by the mathematical model, that power outputs would not vary much between the two devices.

The half cylindrical collector had a volume which was 26% larger than that of the triangular collector but produced only 5% more power. Despite a slight power decrease in the move to the triangular collector a slight rise in power to restoring force ratio was also observed. It was decided that only the more simplistic and easier to engineer triangular shaped collector would be used for the subsequent tests. See Figure 34 and Figure 35.

5.4.2 Buoyancy

No significant differences were found between the performance of the collectors in terms of maximum power outputs, or in terms of displacements and power outputs with any given PTO set-up. This lack of difference with collector inertia is predicted both by linear models and the time domain mathematical model used. The triangular set-up with the least mass was used in all subsequent tests, as it required less restoring force for the desired natural period tunings (Figure 36 and Figure 37).

5.4.3 Freeboard

The results of this test are as expected. As the collector is submerged, its added mass will decrease (since surface effects act to increase added mass), and it is moved into a less energetic region of water, and therefore suffers a decrease in power output. As the collector is raised out of the water it loses added mass, and some of its volume cannot receive forces from the waves. See Figure 38 and Figure 39. The nature of power output variation with freeboard is likely to vary with both wave period and amplitude. Shorter period waves have a smaller proportion of their power deeper in the water, meaning that a sharper fall in power output with submersion could be expected. Smaller amplitude waves extended a smaller distance above the still water level, so a sharper fall in power output with protrusion

could be expected. This test highlights the significant effect freeboard can have on power output.

It was decided that the final tests would be performed with the freeboard set to 0.015m.

5.4.4 Pierson-Moskowitz Seas

To achieve estimations for the performance of the triangular EB Frond in real seas it was decided to simulate Pierson-Moskowitz seas in the wave tank. See Figure 40, Figure 41, Figure 42 and Figure 43. For Pierson-Moskowitz seas, peak period and significant wave height are defined in terms of one another. This arises from the assumption that the sea-state is fully evolved. Pierson-Moskowitz sea-states were selected since their usage over other sea-states reduces the number of variables, meaning that less testing is required to build a power relationship.

It should be noted from Figure 40 that the EB Frond natural period tuning required for maximum power capture in each of the sea-states tested is approximately the same, even though the peak period of the tested spectra vary significantly. The result of this is that if wave states change during EB Frond operation, no significant power losses will be incurred due to inefficiencies arising from incorrect EB Frond period tuning. In shorter period sea-states the required natural period is significantly longer than the peak spectral period, meaning that the shortest natural EB Frond periods may never be required. The requirement for the EB Frond to be tuned to very short natural periods will increase the costs of the tuning system. These results are therefore encouraging, as they suggest that tuning to very short natural periods should never be required.

It is not surprising that shorter peak period spectra require proportionately longer EB Frond natural periods. Sea spectra contain many wave components grouped around their peak period. Radiation damping effects increase with decreasing wave period, the rate of this radiation damping effect increase is more significant in the short wave period regime (see Figure 59 in section 5.7.3.2). Therefore in spectra with shorter peak periods there will be a more significant efficiency variation across the range of frequencies in the spectrum. In the regime of very short peak period spectra this effect will cause tuning to almost ignore the shortest period range of the spectrum, and therefore significantly skew the required EB Frond period in the direction of longer period tuning.

5.5 Full-Scale Power predictions

The scaled up Pierson-Moskowitz tests results predict a power capture of approximately 263kW in a 3m significant wave height Pierson-Moskowitz sea, see Figure 44.

A 3m significant wave height Pierson-Moskowitz sea has a theoretical point absorber power resource of 935kW, meaning that the EB Frond should have a point absorber efficiency of 28% in this sea-state. The EB Frond has much higher predicted point absorber efficiencies in smaller sea-states, for example 56% in a 1.5m significant wave height sea-state.

The current EB Frond design has reasonably high point absorber efficiencies. Point absorber proponents would argue that in sinusoidal waves, in theory, the maximum point absorber resource could be harvested; although in practice losses would be incurred. They would also predict a decrease in efficiency in mixed seas, since the point absorber must be tuned to the waves for maximum power extraction and it cannot be simultaneously tuned to all frequencies in a wave spectrum. Bearing this in mind the point absorber efficiencies witnessed seem encouraging at this stage of the EB Frond development.

It could also be argued that there is no reason why it should not be possible to achieve a power output of greater than that of a perfect point absorber. The EB Frond design has changed from its initial small collector concept and no longer resembles a "point" absorber. Nevertheless point absorber efficiency values are still a valuable analysis tool, as they offer comparisons with initial performance targets and those of other devices.

To date, the EB Frond project has, at all stages, seen large improvements in power output and overall performance. There is no reason not to believe that further improvements will be made in subsequent phases and that the already promising results will be significantly bettered.

The triangular collector concept has shown promising results. It is clear from experiments that the larger collectors perform well, and the triangular collector has its volume advantageously arranged. The majority of the volume is positioned in the most energetic section of the wave. The shape could be further optimised with more rigorous testing, if desired.

The draught of the collector was shown to be of the right order in the cuboid collector 1/25th scale tests in 1.6s, 0.025m amplitude sinusoidal waves. However, this optimum should vary with wave period. This optimisation was also performed with a freeboard of 0mm and never performed with triangular collectors. It was later decided that a freeboard of 15mm was preferred. A detailed reappraisal of the draught of the collector, at this new freeboard, would be expected to lead to a further performance improvement.

Freeboard optimisation is likely to be highly dependent on draught, and wave height, since larger waves pass over the collector and potential energy capture is not achieved. It could of course be argued that in larger waves this power loss is unimportant as the power is capped anyway. The key lies in where the power capping line is finally drawn, and how much power the current design is capturing. This is a way in which the power output in a 3m significant wave height could be improved upon. A lot of the larger, more energetic, waves in the scaled down testing of this state did pass over the top of the collector.

The whole argument of these optimisations is also site specific. Different sites statistical probability of particular wave spectra vary enormously. As a result these optimisations must take this into account for optimum efficiency.

These areas have not been investigated in detail but provide a means by which, time and budget permitting, the average power output could be improved before full-scale production.

5.6 Testing Limitations Specific to the Lancaster Results

The majority of the sinusoidal wave tests were performed with 1.6s period, 0.025m amplitude waves, and with a variety of collectors, which varied in thickness, width, or some other variable. To reduce the number of tests necessary to explore variations with all dimensions of interest, results from the basic EB Frond (cuboid collector of thickness 0.100m, width 0.630m and draught 0.305m) tests were used in all cases. The basic EB Frond was the first to be physically tested at Lancaster and, as such, was studied when the efficient operation of the equipment was least well understood. The power displacement curve (see fig 35 for an example of a power displacement curve) was the least smooth and conclusive of all the physical tests performed at Lancaster. This is not to say that the results from the basic EB Frond tests are incorrect, more that the certainty in them, and their accuracy, is lower than with other test results. This is highlighted by the fact that agreement between mathematical and physical models for these points is among the worst of all tests performed. In hindsight, the basic EB Frond tests should have been performed later or repeated as the results of them are used in a number of parameter investigations it would be desirable if they were among the most accurate.

5.7 Mathematical and Physical Model Comparisons

5.7.1 Newcastle

Testing was performed in the Newcastle University wave tank between the 3rd and 12th of September 2003. Testing was performed on cuboid collectors with a range of wave periods and amplitudes.

Time histories of collector angle during still water decays were not logged during the Newcastle testing, therefore mathematically derived radiation damping coefficients were used.

The maximum power predictions, from power displacement relationships are shown in Table 8. Results show reasonable agreement between the two models.

Wave Period (s)	Wave Amplitude (m)	Physical Model Maximum Power (W)	Time Domain Model Maximum Power (W)	Physical Model Max Power to Time Domain Max Power Ratio
1.25	0.025	0.90	0.73	1.23
1.25	0.050	3.16	2.81	1.12
1.375	0.024	0.73	0.68	1.07
1.375	0.047	2.01	2.36	0.85
1.55	0.022	0.67	0.66	1.02
1.55	0.046	1.76	2.36	0.75
1.825	0.015	0.29	0.34	0.85
1.825	0.034	0.88	1.42	0.62

Table 8 – Maximum power prediction summary from physical and time domain model tests for Newcastle tank tests

5.7.2 Lancaster First Set of Results

The first set of Phase two Lancaster tests, performed between 19th and 23rd April 2004, was concerned primarily with the selection of a collector shape. Testing was performed on a number of cuboid collectors. The tests performed physically on the cuboid collectors have also been performed using the mathematical model with physically measured radiation damping coefficients.

A number of different collector parameters were varied, to produce a number of different behavioural trends. The "Basic EB Frond" collector was used in the majority of tests. This had a width of 0.630m, thickness of 0.100m and draught of 0.305m. To investigate the effect of changing these dimensions, one parameter was varied at a time, keeping the other two dimensions the same as with the "Basic EB Frond".

5.7.2.1 Thickness Variation

Figure 49 shows the variation in power output with thickness predicted by the physical and time domain models. Both models show a trend of increasing power output with thickness. At low thickness the agreement between models is reasonable, however at greater thickness the time domain model fails to predict the large power outputs achieved with the physical model.

It can be seen from Figure 50 that the time domain model fails to predict the large water torques for the thicker collectors, which are observed using the physical model. As a result of the underestimation of the torques on the thicker cuboid collectors their power output is also underestimated. In the time domain model the cuboid faces have added mass distributions about them which are calculated from flat plate added mass distribution tables. These results indicate that for the thicker cuboid collectors this approach is less valid.

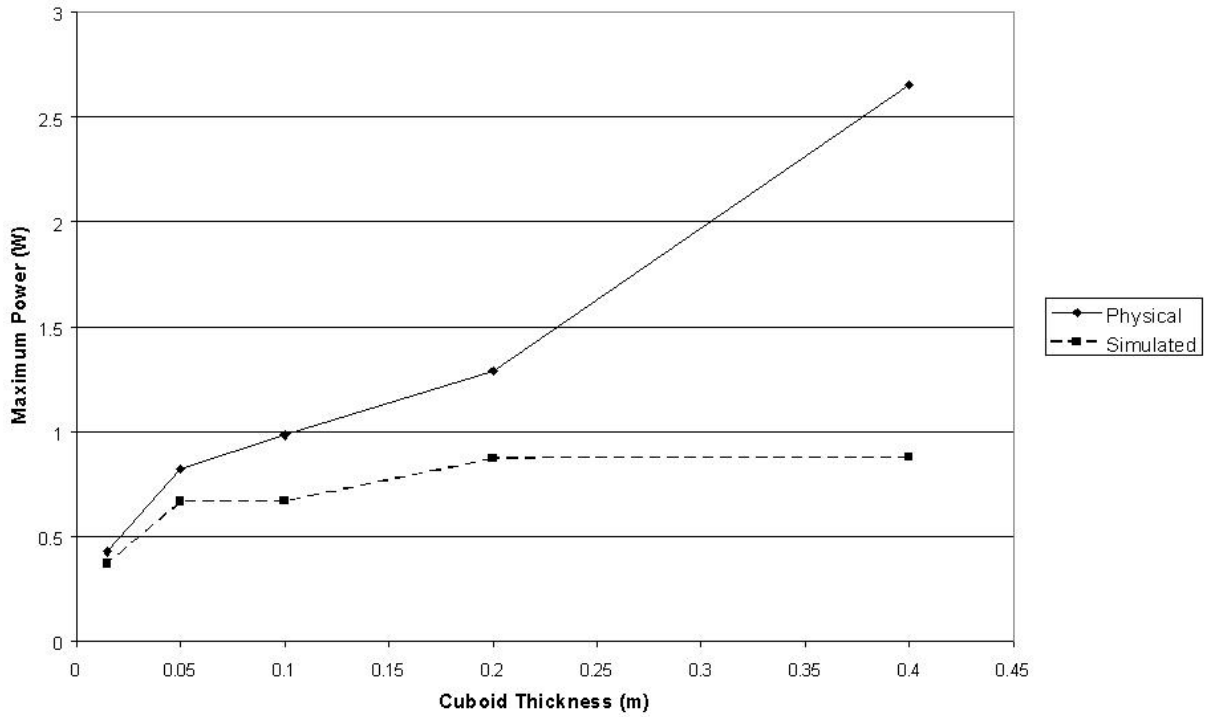


Figure 49 – Maximum power variation, in 1.6s 0.025m amplitude sinusoidal waves, with cuboid collector thickness

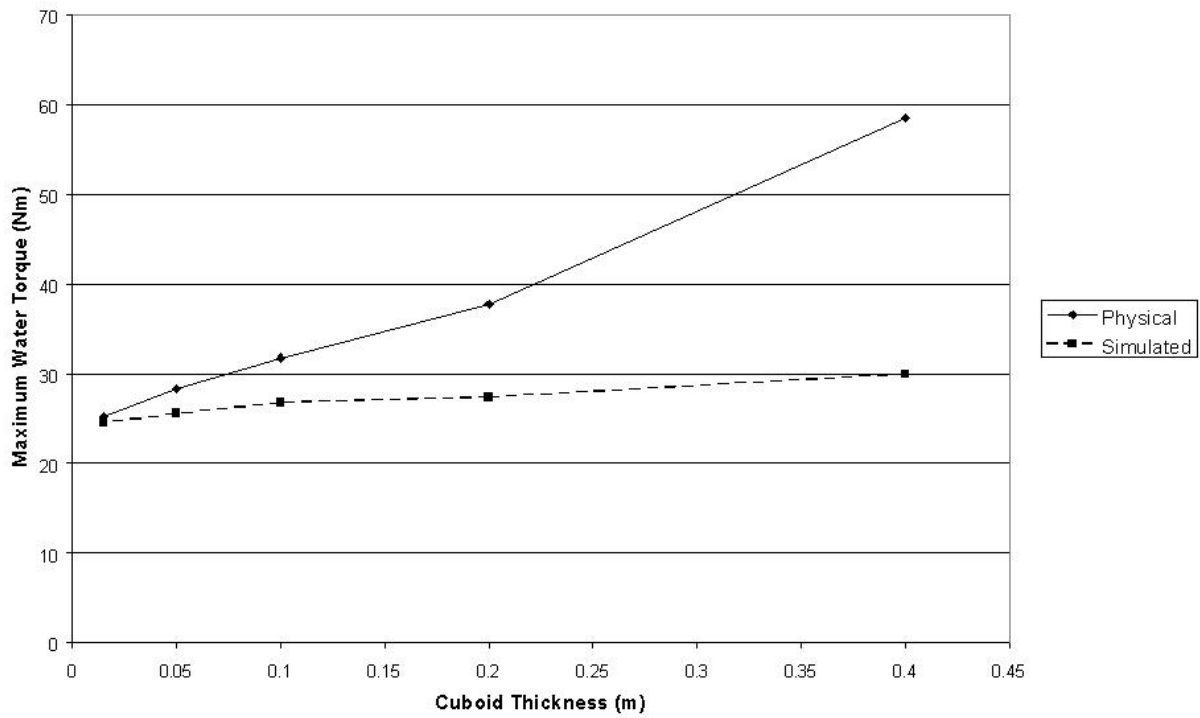


Figure 50 - Maximum water torque, in 1.6s 0.025m amplitude sinusoidal waves, with cuboid collector thickness

Discrepancies between physically and time domain modelled results are not solely due to discrepancies in wave torque amplitude, although it is a key factor and one that can be easily quantified. The cause of much of the difference will be due to the cumulative effect of a number of smaller discrepancies. The time domain model assumes that the water surface and motions are unaffected by the presence of the EB Frond, which allows much quicker run-times than computational fluid dynamic programs and the like, which would not necessarily include this assumption. This assumption becomes less valid with larger collectors, which do significantly affect the water. Hence the time domain model suffers a decrease in validity with larger collectors.

The arguments for discrepancies between physically and time domain modelled results are valid not only for the tests performed on cuboid thickness variation, but for all tests discussed in this section.

5.7.2.2 Width Variation

Figure 51 shows the variation in power output with width predicted by the physical and time domain models. Although a discrepancy exists between individual power predictions, the results show a similar trend of increasing power with cuboid thickness, suggesting that the mathematical models of the collectors used are valid.

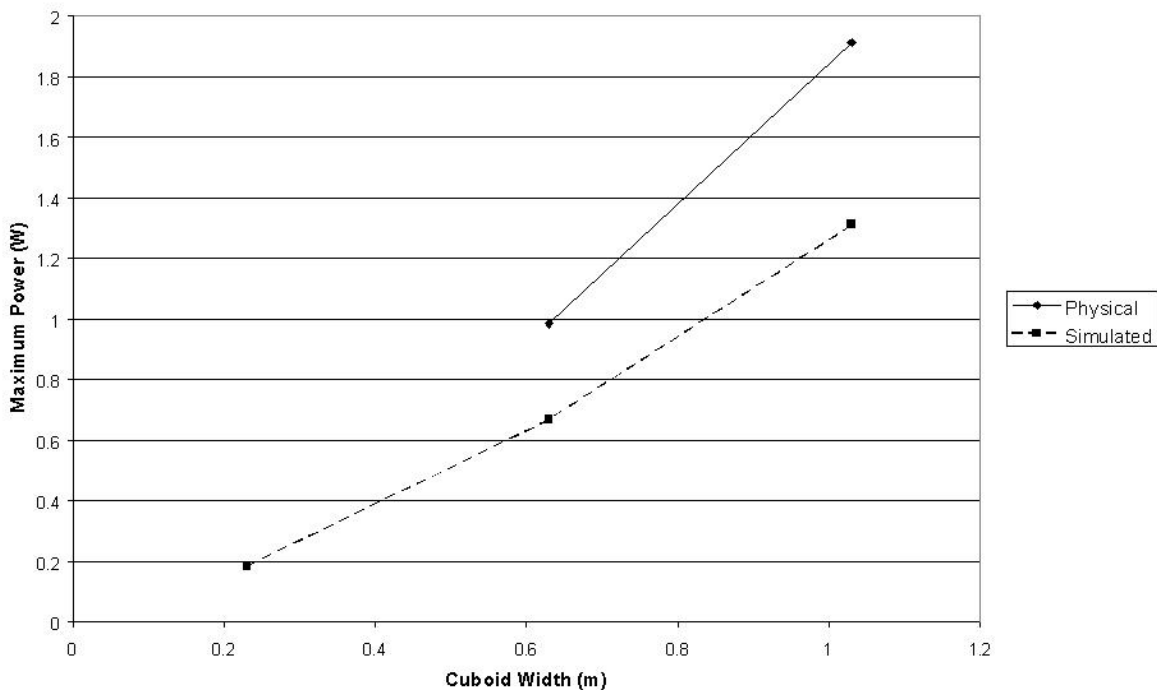


Figure 51 – Maximum power variation, in 1.6s 0.025m amplitude sinusoidal waves, with cuboid collector width

5.7.2.3 Draught Variation

Figure 52 and Figure 53 show the variation in power output with draught predicted by the physical and time domain models. The results show a similar trend of increasing power with draught in both wave cases.

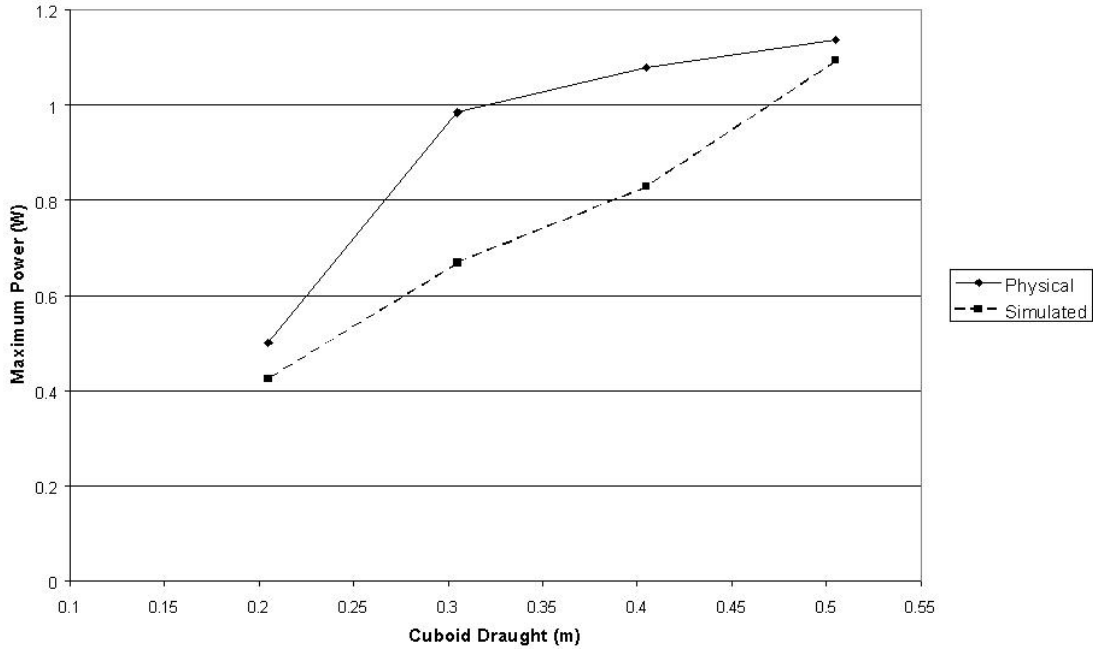


Figure 52 – Maximum power variation, in 1.6s 0.025m amplitude sinusoidal waves, with cuboid collector draught

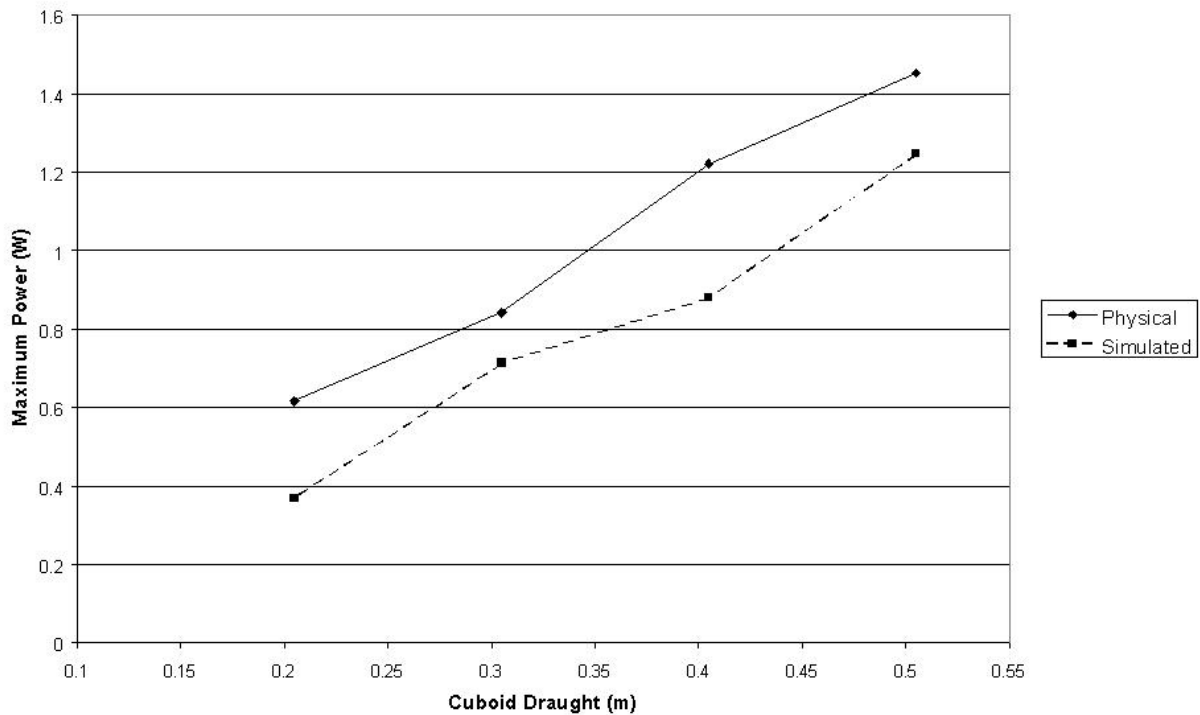


Figure 53 – Maximum power variation, in 2.0s 0.025m amplitude sinusoidal waves, with cuboid collector draught

5.7.2.4 Wave Period Variation

Figure 54 shows the variation in power output with wave period for the basic EB Frond cuboid collector predicted by the physical and time domain models. In each case the natural period of the EB Frond is tuned to be the same as that of the wave period. Both models predict no significant power variation in the wave period range of interest, which scales up to a 6 to 10 second range at full-scale. The radiation damping coefficient used in the model halves and the power in the waves rises by 35% as the wave period is raised from 1.2 to 2 seconds. Despite these differences in power resource and EB Frond properties across the time period range investigated the predicted trends in power output do not differ significantly between the two models indicating a multi-frequency validity of the time domain model.

The discrepancy between individual power predictions is significant but within expected margins. The largest discrepancy is at 1.6 seconds. This data point has been seen already and is discussed in section 5.6.

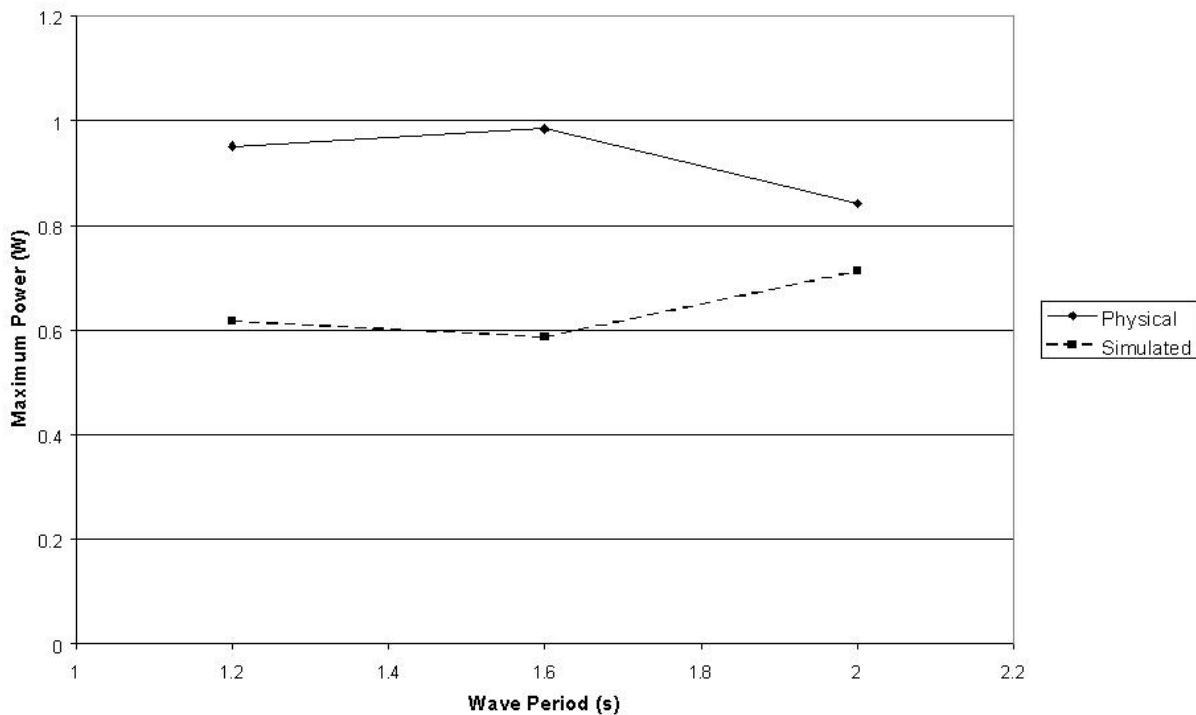


Figure 54 - Maximum power variation for the basic EB Frond collector, in 0.025m amplitude sinusoidal waves, with incoming wave period

5.7.3 Lancaster Second Set of Results

The second set of Phase two Lancaster tests, performed between 24th and 27th May 2004, was concerned primarily with monitoring the effect of freeboard changes on the triangular collector, and assessing the performance of the triangular collector in Pierson-Moskowitz sea-states. The decision for the move towards a triangular shaped collector is discussed in section 5.4.1.

5.7.3.1 Freeboard Variation

Figure 55 shows the variation in power output with the freeboard of the triangular collector predicted by the physical and time domain models. Both models show the same trend of highest power output at a freeboard of approximately 15mm. Agreement between power prediction in most cases is reasonable, suggesting that the mathematical model of the triangular collector is valid. The agreement between certain data points is disappointing, but the overall trend is encouraging. This again highlights that the usefulness of the mathematical model is more in its ability to predict overall trends than accurate power predictions, for very specific cases.

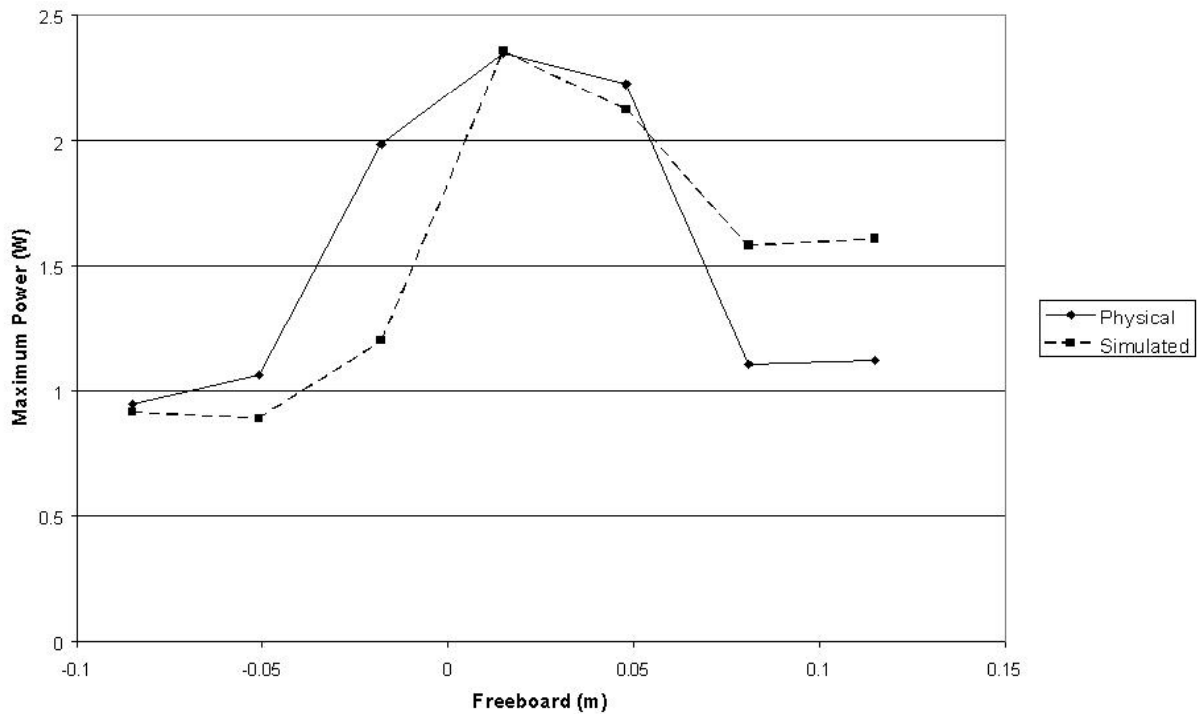


Figure 55 – Maximum power variation, in 1.6s 0.025m amplitude sinusoidal waves, with triangular collector freeboard

5.7.3.2 Pierson-Moskowitz Sea-states

The EB Frond with the triangular collector, protruding 15mm, was tested in Pierson-Moskowitz sea-states with the EB Frond tuned to different natural periods. Maximum power output was calculated in each case. Some of the tests performed at Lancaster have been repeated using the time domain model and comparisons of predicted power outputs from the two models are displayed Figure 56, Figure 57 and Figure 58.

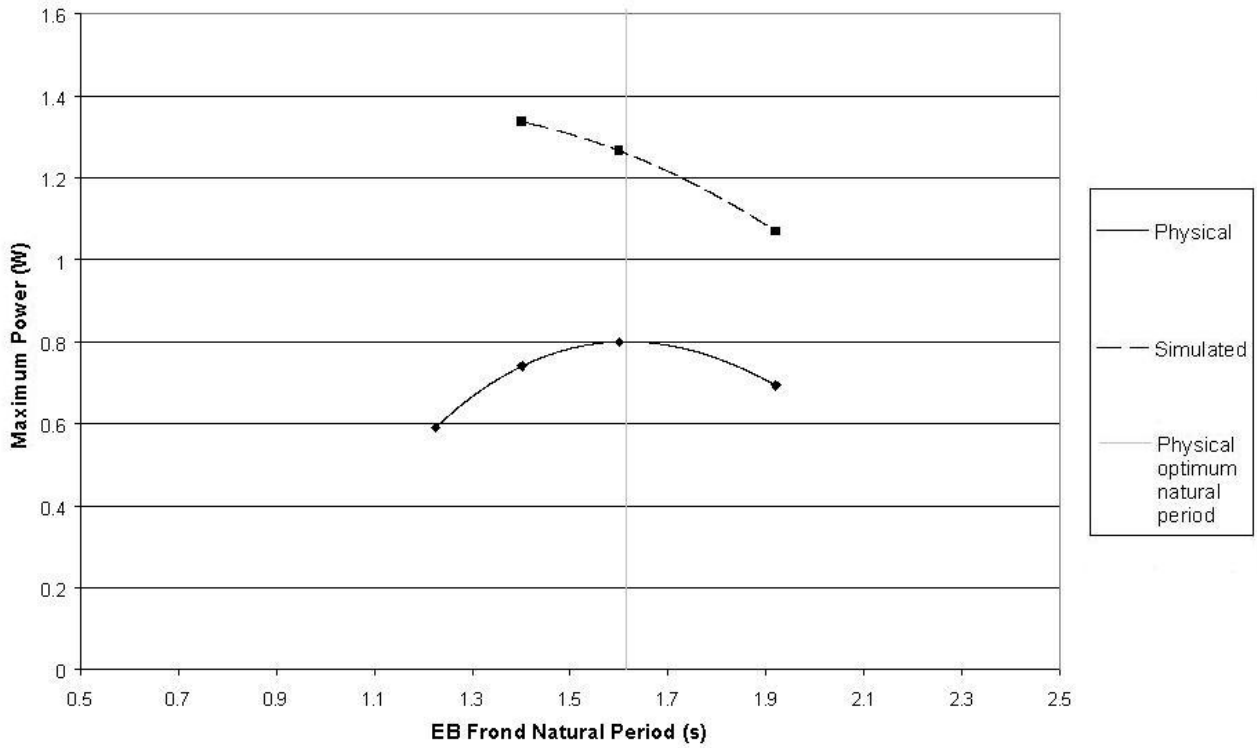


Figure 56 - Maximum power predictions from physical and time domain model tests for 0.06m significant wave height Pierson-Moskowitz sea-state tests

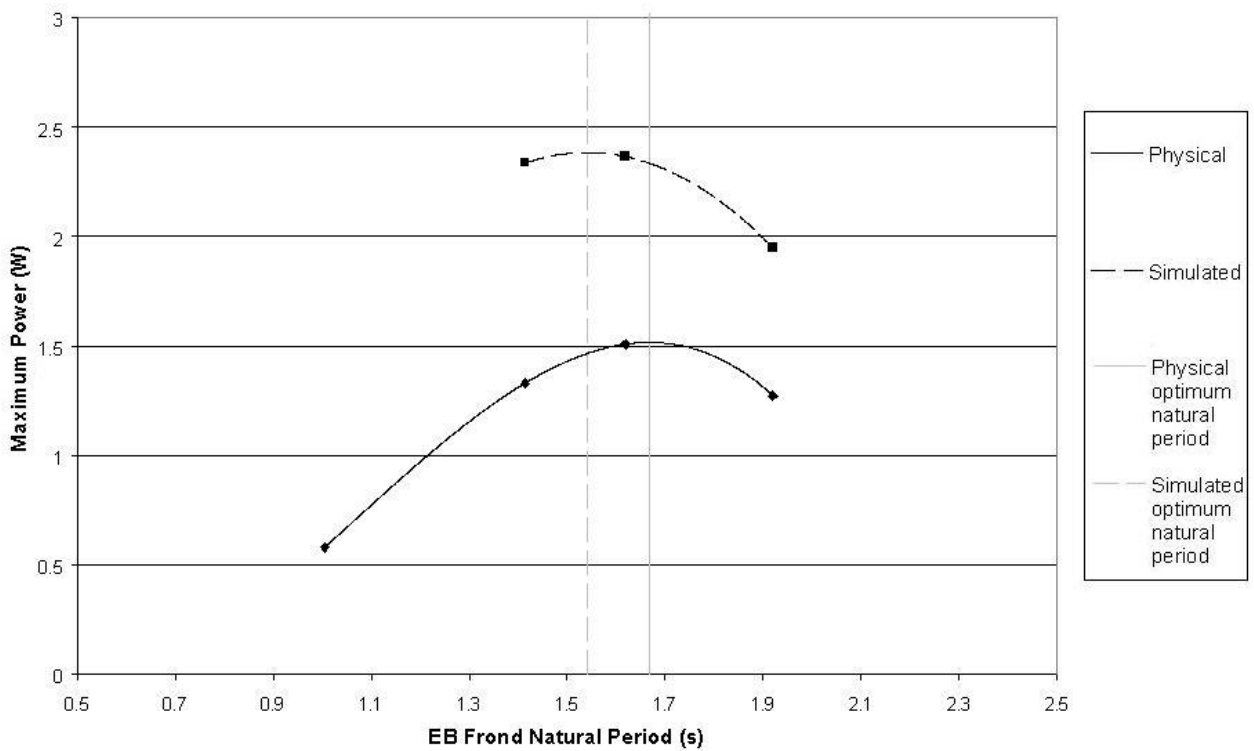


Figure 57 - Maximum power predictions from physical and time domain model tests for 0.08m significant wave height Pierson-Moskowitz sea-state tests

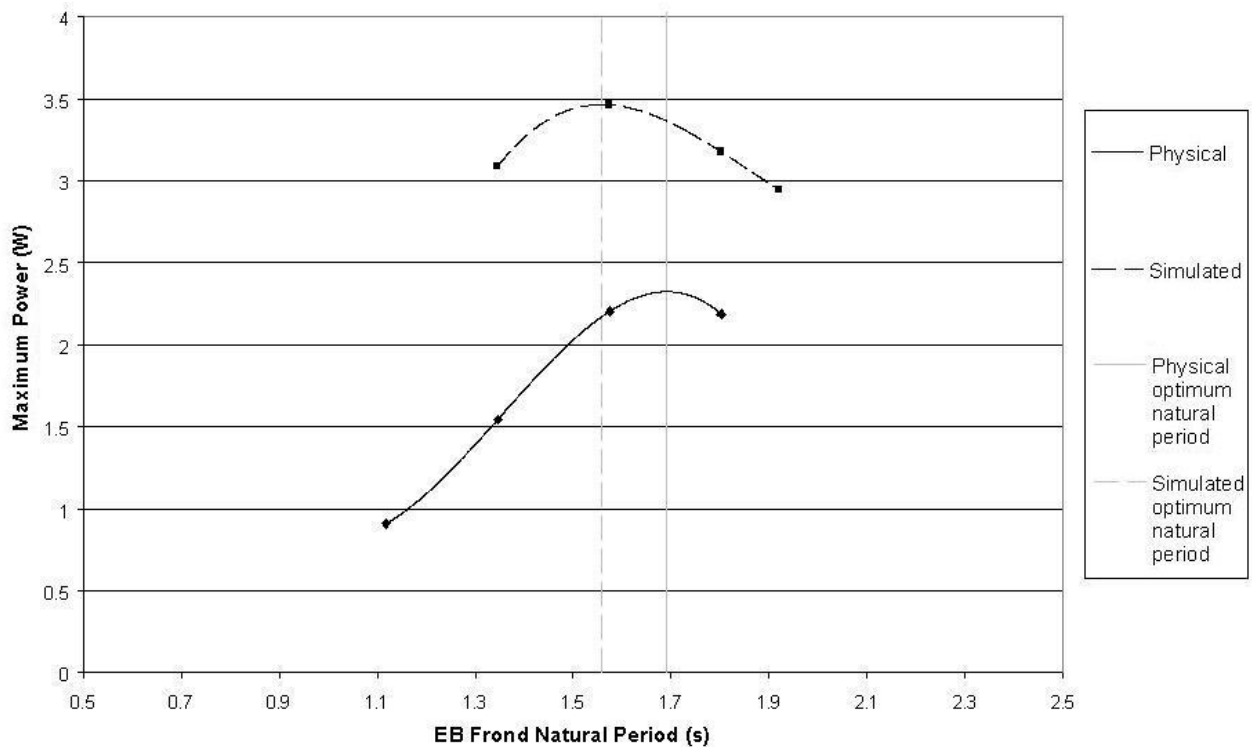


Figure 58 - Maximum power predictions from physical and time domain model tests for 0.099m significant wave height Pierson-Moskowitz sea-state tests

The agreement between power predictions produced by the physical and time domain model for the triangular collector is weaker with the Pierson-Moskowitz sea-states than it was with the sinusoidal waves. However, results are of the same order of magnitude, and agreement is still relatively strong when compared to power predictions produced from other mathematical models for similar wave power devices, see Section 4.2, in more simplistic sinusoidal waves. In the examples of the two larger sea-states the agreement between EB Frond optimum natural period is within 8%. The EB Frond optimum natural periods, determined from results, are indicated on the above graphs by the vertical lines.

It is to be expected that agreement between power predictions will be stronger in sinusoidal waves than in complex sea-states. In sinusoidal sea-states motions settle down into regular behaviour, whereas in complex sea-states they do not and the variation in forces and added mass distributions will be much more complicated and difficult to replicate mathematically.

The strength of the radiation damping of the EB Frond oscillations is dependent upon the period of the oscillations, Figure 59 shows an example of this variation. In complex seas states the EB Frond will perform oscillations with a range of different periods. The largest and most powerful of these oscillations can be assumed to occur around its own natural period, as a result of resonance, and so the damping coefficient corresponding to this period is the most logical choice. However some of the oscillations will occur at different periods, at which the choice of damping coefficient is less valid, albeit if these oscillations are smaller, less energetic and

rarer. In sinusoidal waves the EB Frond will always oscillate with the same period, and so a source of error is introduced into the time domain model which was not present in the earlier sinusoidal tests. This error introduced in non-sinusoidal waves is likely to be more significant in spectra which have lower average and peak periods (in the above cases, these are the smaller significant wave height spectra) because the radiation damping coefficient varies more dramatically with period, in the low period regime. The effect of this can be seen in Figure 60, where in the low peak period regime of spectra (around 1.23s peak period) the mathematical model loses validity and predicts inaccurate optimum natural periods.

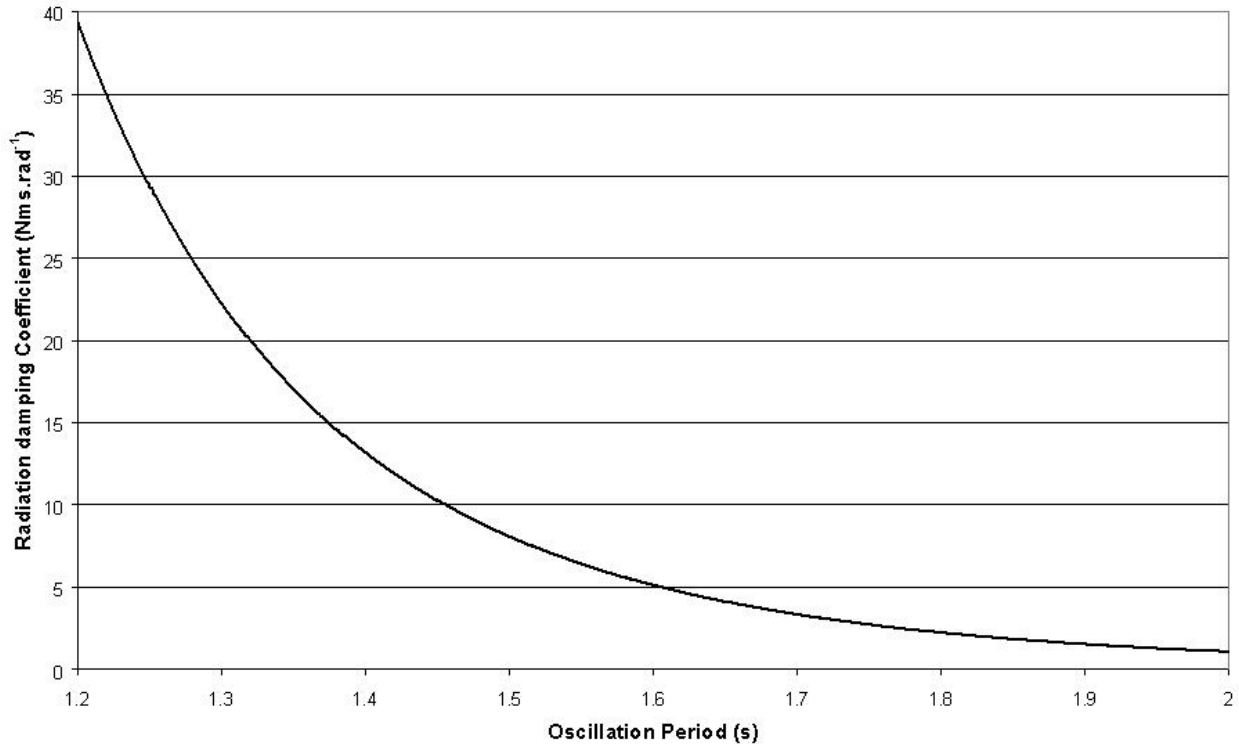


Figure 59 - Radiation damping coefficient variation with oscillation period for the 0.05m thick cuboid collector, calculated by Wamit.

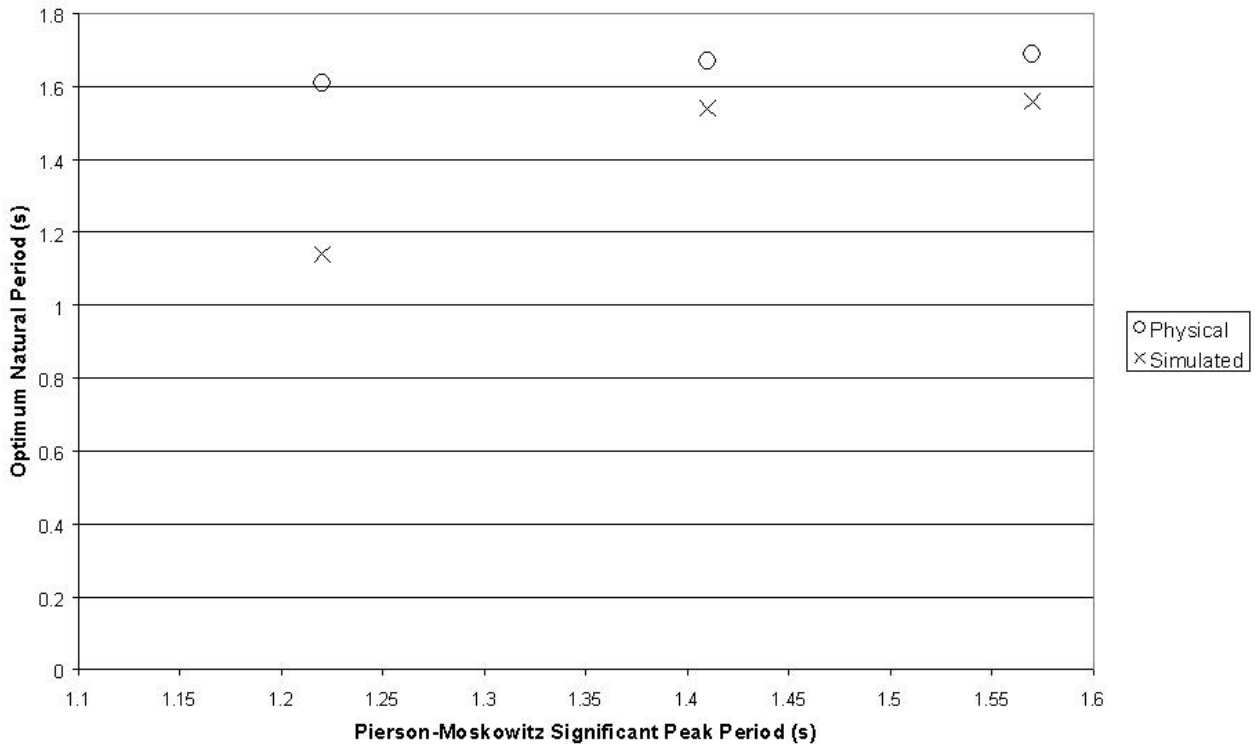


Figure 60 – Optimum EB Frond natural period predictions from physical and time domain model tests for Pierson-Moskowitz sea-states

5.7.4 Conclusions and Limitations

The time domain model has shown agreement with physical testing in terms of the trends it predicts. Most of the individual power predictions also show relatively good agreement, with the possible exception of the thickest cuboid collector, and the Pierson-Moskowitz sea-state tests where agreement is slightly reduced. The time domain model’s greatest use is for predicting qualitative trends in power output, rather than low tolerance quantitative specific power predictions.

Agreement with all sinusoidal tests can be considered to be strong when compared to the agreement that could be expected between physical models and other known types of mathematical model.

Agreement is weaker in complex sea-states, though not so much so as to invalidate the model.

The time domain model is the most accurate mathematical tool available for predicting the behaviour of the EB Frond, and can produce trends and power predictions, which bear good resemblance to physical observations. The time domain model is a valuable tool and should be used to guide the physical testing program.

The usefulness of the ability of the mathematical model to predict trends should not be underestimated. In guiding and validating the physical modelling, it enables a more rapid prototyping of potential designs, and higher confidence in test results. In addition, trends from the mathematical model could be used in conjunction with

physically obtained results to predict the variations in EB Frond performance in slightly different conditions to those physically tested. The ability of the mathematical model to match physical result in terms of required natural periods (see section 5.7.3.2) is useful in the costing estimations of the production of the full-scale device. It is expected that the tuning system will be one of the most expensive components of the full-scale device. The cost of this system will be highly dependent on the required natural periods.

Despite its impressive results compared to other modelling techniques, the time domain model should not be used as a standalone research tool. Specific power predictions should always be verified with physical testing before being used in any economic model.

5.8 Possibility of Achieving Maximum Theorised Point Absorber Power Output

The theoretical maximum power capture of a pitching point absorber is not necessarily unobtainable. In some cases the EB Frond obtained power outputs of greater than 65% of the theoretical maximum. However none of the small, point-like, collector designs achieved power captures of the orders of magnitude of the theoretical maximum. Results have suggested that the EB Frond can achieve power outputs comparable to those theorised for perfect pitching point absorbers, but only by moving to designs which take it away from the original point absorber concept. As the EB Frond is not a true point absorber there is no need to assume that the upper limit to its power output is the same as for a perfect point absorber. In fact it is conceivable that it might, with further refinements, produce more power than a theoretical perfect pitching point absorber.

5.9 Repeatability and Level of Confidence in Results

The triangular collector at a freeboard of 0.015m was tested in 1.6s period, 0.025m amplitude sinusoidal waves with a variation in collector masses. In each case the tuning system was adjusted to maintain the natural period of the collector at 1.6s. The original purpose of this experiment was to show, in agreement with theory, that the maximum power output was dependent on the natural period of the collector, regardless of its inertia, see section 5.4.2. The results of all corresponding data points produced were very similar, and it can be assumed that the variation in results is due only to the slight differences in the accuracy of the tuning, the mechanical set-up as a whole and the accuracy in the taking of readings. Three maximum power output results obtained were 2.33W, 2.35W and 2.46W. The mean of these values is 2.38W and all three reading fall within $\pm 4\%$ of this value. Although this variation may be slightly different in different mechanical set-ups and with different waves, results indicate that there is not a significant improvement in result accuracy to be obtained through the repeating of tests, with the one exception of the basic EB Frond tests, see section 5.6. It should also be noted that it is not specific maximum power results that are of interest, but their relationship with some other variable. In these cases numerous readings are taken, and the effects of random, rather than systematic errors, can be expected to cancel out to, to a large extent, across the relationship range.

Repeating of results cannot however highlight the possible existence of systematic errors, which may be affecting all readings. It is believed that the possibility of the tests results being contaminated by systematic error was greatly reduced in the Lancaster testing phase, as the apparatus used was more rigorously calibrated and checked. As the results of major concern were obtained at Lancaster, potential sources of systematic error are discussed, with reference to Lancaster, below.

- Tank Reflections

Relationships between the wavelengths of waves used and the dimensions of wave tanks can mean that, at certain frequencies, certain areas of the tank experience constructive or destructive interference effects. Unlike facilities used before, the Edinburgh Designs wave-makers were calibrated with specific reference to the point at which the EB Frond test rig was placed, so that the waves arriving there were of the correct size. This does not mean that there is absolutely no systematic error present as a result of reflections, as there are differences in the particle motions in standing and travelling waves. Beaches were placed at the far end of the wave tank, to dissipate wave energy and limit wave reflections and the formation of standing waves.

- Finite Tank Width

The EB Frond captures power not only from the waves passing across its width, but from all the waves in the tank. Theoretical power predictions for point absorbers are based on the assumption of an infinitely wide sea. As the wave tank is of finite width, and the power resource therefore reduced, it is therefore believed that the EB Frond suffers a performance drop as a result of the finite tank width. The EB Frond is most effective at removing energy from the waves across its width; it is believed that the power output is not significantly reduced by the use of a tank of finite width. Nonetheless this systematic error does exist, and cannot be accurately quantified. In the open sea the removal of this effect will lead to a power output increase, and so this error will not lead to the false conclusion that the EB Frond is economically viable.

It is not possible to accurately quantify the effect of the above possible sources of systematic error. Tank width and reflection ratios have been measured, and deemed acceptable, but it is not possible to predict exactly what their effect is on the EB Frond system as a whole. The results from the physical and mathematical model show agreement and the maximum discrepancy in the simpler cases (flush collectors in sinusoidal waves, excluding the thickest cuboidal collector) for the maximum power output maximum is 32%. It is likely that the physical model is the more accurate of the two, due to inherent complexities involved in mathematically modelling the system, and that actual errors in the physical model power predictions are much lower than 32%. Despite this the fact that the two models show similar trends and power output predictions goes some way to instilling confidence in the physical model.

6 SURVIVABILITY

As stated in the Phase one report, there are two outline storm survival strategies under consideration:

- collector free to swing
- collector fixed down.

The particular concerns for the free-swinging approach is the risk of impact with the seabed or end stops at extreme motions. For the fixed down strategy, the concern is that the hydrodynamic lift and drag forces on the collector will be sufficient to destabilise the machine.

This section of the report focuses on determining if the EB Frond is strong enough to survive in its intended environment. It starts with a general discussion of the EB Frond as it stands and the associated green (non-breaking) wave loadings on the structure. Wave data is taken from site RP30S, a site from EMEC in Orkney, where wave heights and periods have been measured over a period of 14 years. Section 6.2 discusses possible breaking and freak waves, followed by a discussion of survival strategies.

6.1 Introduction

As with most other offshore structures, EB Frond is fixed in-situ and must be able to survive all probable weather and environmental conditions for the duration of its operating life. This section summarises the extreme environmental conditions in which EB Frond is placed and reviews possible survival methods. The design of the EB Frond will be based on four main factors:

- During regular operation the structure is strong enough to ensure all components are well below their acceptable stress levels and cyclic fatigue limits.
- Survival of the structure during storms.
- Impact resistance from foreign objects.
- Ability to withstand installation, recovery and associated transport.

The full-scale EB Frond concept, as illustrated in Figure 61, consists of three main structural components:

- The collector head which is located close to, or slightly protruding from, the sea surface. It has an inverted triangular shape to optimise power capture close to the surface.
- The collector arm. This transfers power from the collector head to the fixed base.
- The base. This is fixed to the seabed through piling, anchoring or a gravity foundation. It provides the necessary reaction against which power can be captured.

Possible failure methods for each component are discussed below, in relation to the operating phase of the EB Frond and the loading factors.

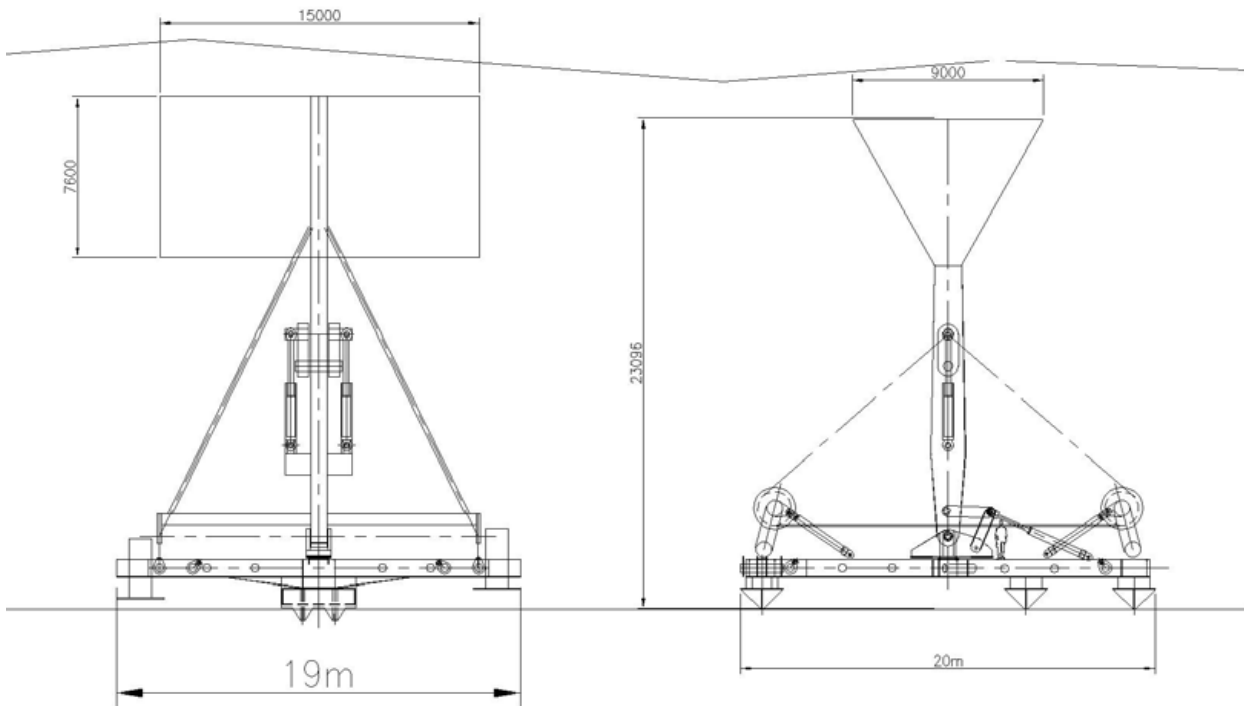


Figure 61 – EB Frond general arrangement

6.1.1 Collector Head

The collector head sits in the most energetic part of the water column and can be stressed in a variety of different ways. Assuming it is during a period of normal operation it has several main forces acting upon it:

- The Froude-Krylov force, which consists of dynamic pressure and diffraction forces, is the driving force on the collector head. This force will manifest itself as a pressure difference across the vertical faces of the collector head.
- A drag force is apparent as the collector head oscillates. This is less than the Froude-Krylov force, occurs with a phase difference of 90° to it and hence is not discussed further.
- The collector head will have a significant weight and must be capable of supporting itself during installation and operation.

At present the device has no yaw facility enabling it to face the predominant wave direction and hence the forces may occur from any direction, causing a torque over the structure. In addition water velocities and accelerations decay exponentially with depth and hence vertical loading on the structure is depth dependent.

Preliminary design assumes the collector head will be constructed in a similar way to the bow of a ship, with steel plate on the outside and associated internal strengtheners and load bearing structures. Due to its large cross section its second moment of area is correspondingly large and hence it is well suited to withstanding large forces. Table 9 details the stress due to bending moments at the centre of the collector due to anticipated wave loads from Pierson-Moskowitz sea-states.

Approximate Sea-state	Significant wave height (m)	Bending Moment (MNm)	Stress due to Bending Moment (MPa)	Shear Stress (MPa)	Principal Stress (MPa)
5	3.2	11	48	67	95
6	4.8	14	58	82	116
7	7.8	19	81	111	156
8	12.7	24	99	139	197

Table 9 – Stress on Collector Head

Although the calculation and failure condition set are simplistic, it is considered that careful design of stiffeners and load beams within the collector head will allow it to be designed to withstand the dominant Froude-Krylov force. Thus the next stage of the survival analysis (Section 6.2 onwards) concentrates on larger forces resulting from freak and breaking waves.

6.1.2 Collector Arm

The collector arm is a simple structure pivoted around the base by the action of waves on the collector head. During normal operation it has three main causes of stress.

- Reaction of the restoring force, PTO and base as the collector head is driven by the waves.
- Torque from off-centre loading of the collector head. Although this case has not been studied in detail, a variation of the design with two collector arms spaced towards each end of the collector would have significantly greater torsional stiffness.
- Heave forces on the collector will translate to direct tension and compression in the collector arm. The added mass of the collector in a vertical plane is reduced, and in turn this reduces the vertical loads on the collector arm by a factor of approximately 1.4. The load is also spread over the whole arm cross-section instead of only the members parallel to the applied horizontal force. Hence the stresses associated with vertical loads will be significantly smaller than associated with horizontal loads. Horizontal and vertical Froude-Krylov forces are related to water particle acceleration and their respective maximums occur with a 90° phase difference. The vertical load from a green wave loading on the collector arm can therefore be neglected from a survival point of view.

Wave data from RP30S shows that the majority of waves approach within an angle of around 30°, hence off-axis loading is limited. As the arm is mounted on a pin joint from one end, bending moment stresses are only experienced through the reaction

of the PTO and restoring force mechanisms. All other forces acting on the collector head are therefore transferred to the base via shear in the arm. For larger waves the shear load due to the wave force is shown in Table 10.

Approximate Sea-state	Significant wave height (m)	Shear Load (MN)	Shear Stress (MPa)
5	3.2	6.1	76
6	4.8	7.4	93
7	7.8	10.0	125
8	12.7	12.6	158

Table 10 – Shear Stress on Collector Arm

The results show that the forces present are acceptable and the design remains feasible if the collector head is allowed to oscillate in large seas. Whilst fixing of the collector head to the sea floor during large seas removes it from the highly energetic water surface, this may increase the loading, especially through bending moments, on the arm unless it is restrained close to the collector head.

6.1.3 Base

The base acts as the reaction point against which power is produced. It can be fixed to the seabed by piles, anchors or gravity base. Whichever system is used, it must not move in any weather condition. As the base is static for the purposes of survivability it has been assumed that it can be built strong enough to withstand any loads that are transferred to it through the collector arm.

6.1.4 Summary

The full-scale EB Frond is thus able to withstand forces present in standard green waves. In addition the loads associated with these waves are small enough that no avoidance action on the structure will be required. Previous modelling of the EB Frond in large Pierson-Moskowitz and JONSWAP sea-states demonstrates that a flat plate collector head doesn't contact the seabed during its motion. The behaviour of the latest triangular collector head design under these conditions should be reviewed in any future development phases.

6.2 Breaking and Freak Waves

Survivability of the EB Frond is thus concentrated into the areas of freak and breaking waves. The following sections are an explanation of the scenario of freak and breaking waves with respect to the EB Frond.

6.2.1 Breaking Waves

Research has been published on breaking waves, the conditions required to make them break and breaking types in regular sinusoidal 2D seas. Variables such as wave height, water depth, crest steepness, trough steepness and wave peak angle can be used to assess breaking criteria, with most theoretical analysis methods resulting in general agreement. For example, in a typical operating depth of 25m a wave of height 15m can be said to be on the verge of breaking. Assuming the freak wave

criteria (discussed in Section 6.3), this could occur in a sea of 6m significant wave height. Data from site RP30S shows the maximum expected significant wave height to be 13m over the course of 15 years. Thus breaking wave criteria must be assessed for EB Frond survivability.

Research into 3D real sea spectra indicates that 2D regular sea theory does not translate well into the more confused seas, with breaking occurring in a more random fashion and generally at lower levels than predicted by 2D theory. Breaking in a 3D sea spectrum can be roughly correlated to the concentration of wave energy at the point of interest, sometimes referred to as energy flux.

Forces and pressures associated with breaking waves are hard to quantify due to the large number of variables required to describe these waves and the structure. In addition, simplistic modelling of the EB Frond and impacting water assume both to be incompressible and hence loads tend to infinity. Using methodology developed for the assessment of water jet impact pressures on angled plates, and assuming a plunging breaker impacted the top of the EB Frond at an angle of 30° and velocity of 18m sec^{-1} , the pressure generated would be around 1MPa . By comparison, this figure is the same as the maximum impact load used in special or extreme conditions for ship bow sections, whilst breakwaters typically experience an impact pressure of 400kPa . As the EB Frond is partially submerged, and plunging breakers tend to impact the water's surface above the mean sea level, these forces are thought to be an overestimate of the likely maximum and hence a survival load of 500kN per metre crest width has been assumed.

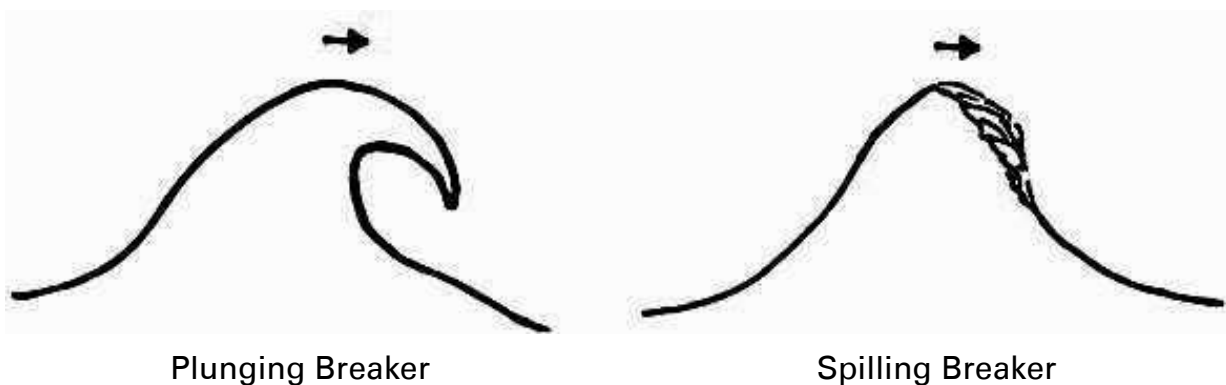


Figure 62 - Diagrams of two breaking wave types

The types of breaking that will occur in a water depth of 25m are either plunging or spilling breakers (see Figure 62). The difference between the two are that breaking occurs from the spilling breakers crest whereas a plunging breaker forms a spout which impacts on the front face of the wave. Breaking type is highly dependent on local environmental conditions. The plunging breaker would be the more serious of the two if it were to impact directly on the collector head, although it is also the less probable. Both breaker types, once broken, will consist of a large amount of water moving at the wave's velocity. This has the potential to provide large impact loads on the exposed surface of the collector head. Section 6.2.3 discusses factors that may influence breaking waves in the region of the EB Frond.

6.2.2 Freak Waves

Freak or rogue waves are generally classed as having a height of over 2.5 times the significant wave height and have a probability of occurrence of 0.07% over a 3 hour time period. Although the exact nature and formation of freak waves is not fully understood, they are known to occur as an interaction between two wave groups of differing travelling velocity and occur in naturally developed sea spectra. A result of this is that freak waves do not travel long distances.

As freak waves are a rare occurrence they are only recently becoming acknowledged in the ocean wave community and knowledge of their exact properties is limited. Although it would seem intuitive that freak waves are steeper than normal and hence break, there is strong evidence to suggest that the majority do not break. As freak waves are a rare occurrence and at present considered to be mostly non-breaking, the greatest danger to EB Frond integrity is taken to be breaking waves. Hence survivability in the next project phase will concentrate on the higher forces and impacts associated with breaking waves.

Waves from differing directions can also interact to form larger than expected waves. Although they may appear steeper than normal, addition of the velocity vectors present shows that again they are unlikely to break.

6.2.3 Wave Structure Interaction

From physical scale testing of the EB Frond it has been noted that there is a significant disturbance of the water surface, flow paths and waves as they pass over and around the EB Frond in non-breaking seas. EB Frond oscillates with a phase lag from the waves and hence there is a noticeable water flow around it, which may cause refraction or premature breaking of waves. Although EB Frond is small compared to the wavelength, it may act as a localised obstruction or shelf to waves and hence cause waves to steepen and break in its local vicinity. This may be considered a survival risk. Refraction of waves as they pass over the collector may lessen the likelihood of a direct wave impact over the full collector length.

At present no tests representing storm or breaking wave conditions have been undertaken, thus the exact nature of the wave-EB Frond interaction is not understood. Although unlikely, this possibility of waves impacting on the EB Frond must at present be considered. Work to confirm structure and breaking wave interaction is planned for the next project phase. Ideally it will consist of further physical tests in tandem with computer simulations.

6.2.4 Tidal Effects

EB Frond will be installed in tidally affected areas. This is a site-specific effect although, in general in UK waters, areas of reasonable wave energy are not the areas with the highest tidal ranges. At present it has, therefore, been assumed that, during low tides, this would leave up to 1m of the collector head protruding from the water. This may make it more susceptible to breaking waves at a time when the probability of waves breaking is increased.

6.3 Possible Damage and Failure Scenarios

Large or freak waves have the potential to impart large quantities of energy into the EB Frond via the collector head. The existing PTO system concept is not able to deal with this and thus the collector head would swing through a large angle. This has the potential for the collector head to be driven hard against the seabed or end stop, resulting in damage to the device. The Phase one analysis by Orcina into non-breaking storm waves showed that, with the modelled design of a lower volume collector head, the collector head never made contact with the seabed. For the next phase of the project it is planned to repeat the tests with the new triangular collector shape.

Breaking waves consist of large amounts of water moving with a defined constant velocity. At low tide the top of the EB Frond will be exposed to this, with the resultant potential for damage. The large number of uncertainties around the structure make calculations on the waves breaking structure hard to perform and hence further physical or computational fluid modelling of the device is required. This is planned for the next project stage.

The worst breaking wave case would be a plunging breaker impacting onto EB Frond. The high pressures involved during impact could potentially cause localised damage of the collector head or larger scale damage by yielding or failing structural members. Before the EB Frond is designed a detailed analysis of the probability of plunging breakers impacting on the EB Frond needs to be considered.

Breaking waves with their high impact forces may only require strengthening of the structure in appropriate areas, or if the forces are too high avoidance mechanisms to prevent or lessen the impact. An overview of preliminary concepts is presented in Section 6.4.

6.4 Survival Strategies

As indicated in Section 6.3, Phase one of the EB Frond project looked into survival strategies under storm wave conditions. Orcina ran simulations on the movement and loads associated with a smaller volume collector head under storm waves with two survival strategies. When the collector head was restrained close to the seabed large lift and drag forces were experienced, see Section 6.4.2, resulting in this strategy not being ideal. The alternative strategy was to allow the collector head to swing freely. A concern expressed regarding this approach was that large waves could drive the collector head into the seabed. However, the Orcina modelling data from the earlier design concept illustrated that, with a flat plate collector head, this did not occur.

The two existing strategies are described below, along with three new strategies, with their relative advantages summarised as a survivability matrix. The new ideas are submitted in response to the likelihood of waves breaking in the region of the EB Frond. It should be noted that the final solution could be a variation or combination of more than one design.

6.4.1 Free to Swing

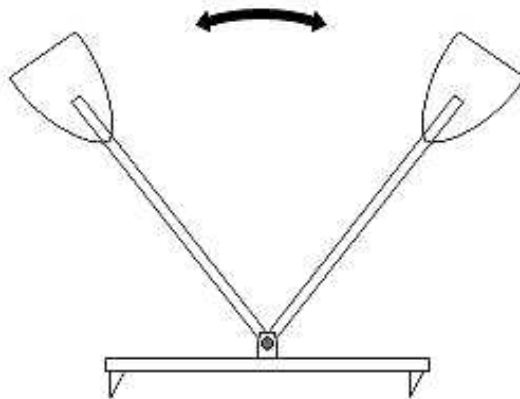


Figure 63 - EB Frond free to swing

During exceptionally large waves EB Frond is allowed to oscillate, (Figure 63) in a de-tuned mode with minimal restoring force. To prevent the EB Frond from encountering end-stops the PTO and restoring force mechanisms may be used as control devices alongside soft end-stops to prevent impact damage. This strategy is simple to implement but still exposes the collector head to the full forces of large waves. Power production by the EB Frond may still be possible.

If a wave were to break, impacting the collector head, large instantaneous forces would not be dissipated and hence local or structural damage could occur. This system does not remove the collector head from the impact of breaking waves.

An advantage of this system is that minimal control and instrumentation is required with the system defaulting to free swinging or reduced PTO should the loads on the structure exceed a set limit. Thus this system could be termed fail-safe. A disadvantage of this system is that the added cost of providing adequate reinforcement to withstand all load cases may become unacceptable.

6.4.2 Fixed to Seabed

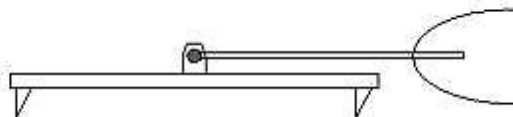


Figure 64 - Collector fixed to seabed.

If the wave monitoring system detects the potential for waves exceeding the safe operating limit the collector is lowered until in close proximity to the seabed and latched in this position, see Figure 64. Thus the EB Frond experiences the lesser

wave motions present at this depth. With the collector head fixed the structure experiences forces from the waves, which have the potential to damage or dislocate EB Frond from its foundation. Orcina has previously modelled this with a flat plate collector head, in a JONSWAP spectrum of peak period 12s and significant wave height of 7.3m, at an inclination of 10° and 30° with maximum arm bending moments of 24 and 35MN.m. This study will be repeated with the latest collector head shape.

The mechanism for lowering the collector head has not been decided upon. If the waves are monitored ahead of the EB Frond a lowering system that can react before the wave reaches the collector could reduce the chance of impacts from breaking waves. No power can be generated during the lock-down period.

As the collector head is fixed the full power capture from the collector head is transferred through to the collector arm and base. Previous analysis by Orcina shows these forces can become high and hence careful consideration of load limitation is required. Hence the free-swinging concept detailed in Section 6.4.1 is preferred.

6.4.3 Lowering Collector from Surface

If the conditions exceed operating limits the collector is lowered towards the pivot, thus reducing the wave forces upon it, see Figure 65. This could be used in collaboration with either of the above two ideas.

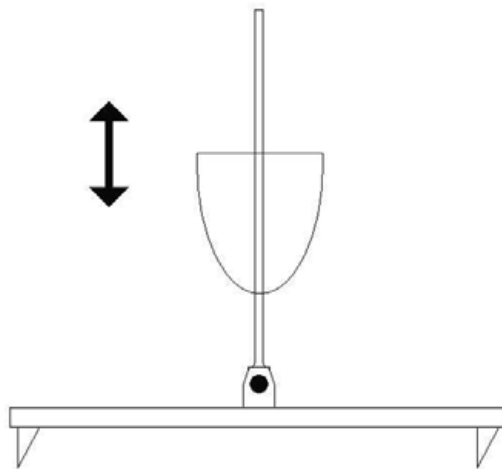


Figure 65 - Lowering collector along swing arm

A linear sliding mechanism like this will be complex and expensive to integrate into a full size machine and will reduce the overall stiffness and strength of the structure. Unlike the previous survival mechanisms, this EB Frond would be less affected by tidal variations and could potentially be kept below possible impact from breaking waves. In severe storms the angle of free movement of the collector head could be significantly hindered due to its close proximity to the base. It has clear advantages for modulating power capture over the previous suggestions, as the collector can

still operate at depths where the power in the waves is reduced. Such an EB Frond could be made to fail safe in the event of a system failure.

Ideally, for breaking waves, a forecasting mechanism is required to allow the collector head to be removed from the danger area before the wave passes over the EB Frond. This could be achieved by seabed or surface instrumentation mounted individually or in an array in front of the EB Frond.

This concept could also be achieved by hinging the collector arm about its centre, although this negates the power modulation.

6.4.4 Reduction in Collector Volume/Area

The area and or volume of the collector head could be reduced, in response to overloading wave forces, allowing EB Frond to be configured to capture less power and hence reduce structural loads. Although an active system could pre-empt high loads from occurring, a passive system could potentially be cheaper and more reliable.

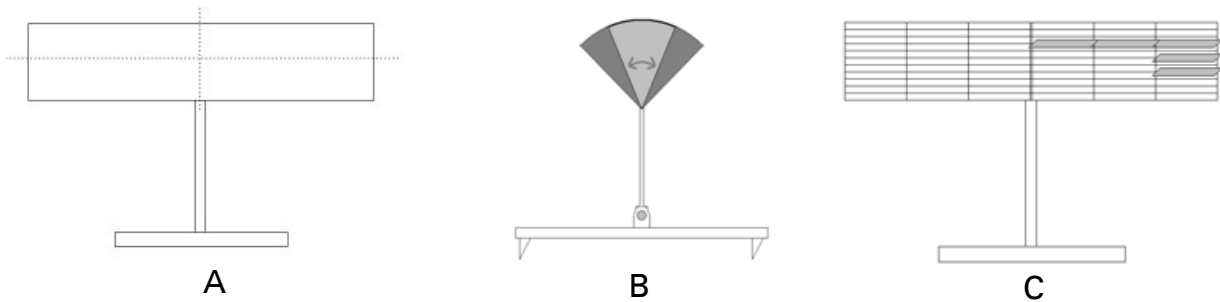


Figure 66 - Possible Folding Collectors

The method of achieving this is dependant upon the collector design, but could include hinging of the collector around the central arm (A), hinging between the collector sides (B) or allowing individual collector panels to hinge (C), see Figure 66. By incorporating passive or overload protection into the folding mechanism, impact and large wave forces can be dissipated before yielding occurs. The addition of joints and hinge mechanisms will add to the overall machine cost and reduce its structural rigidity. However the machine could operate in storm conditions with a reduced power capture.

6.4.5 Inflatable Collector

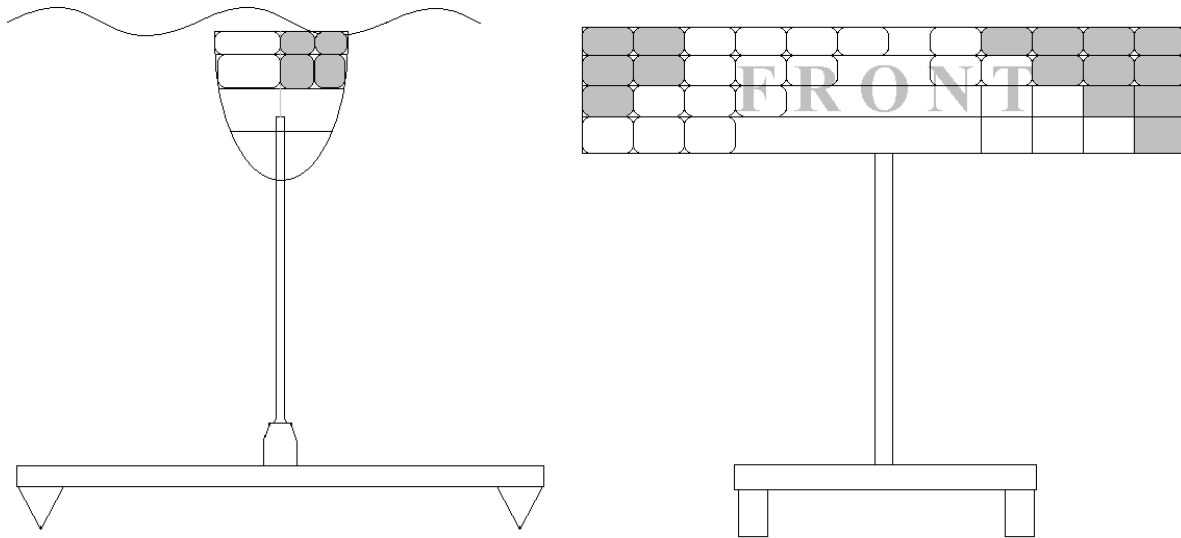


Figure 67 – Possible general arrangement for inflatable collector

In this version, the collector would be made from a series of water filled bags supported within a steel framework. Pressure relief valves on the bags allow them to deflate should loads become excessively high. During storms the bags could be deflated to reduce the collector volume to a bare minimum or by only filling half of the bags the inferred collector volume is reduced and power capture reduced. Although more equipment will be required to inflate and deflate the bags this could be offset by incorporating the restoring force required in separate air filled buoyancy bags within the collector head. The modular design of the structure may also be advantageous in terms of transport, commissioning and maintenance.

Breaking waves will deform the bags and hence overall loads and pressures are distributed. Figure 67 shows possible arrangement of inflatable bags within a framework for the collector. In essence the bags need only be placed towards the extremities of the device to allow power collection in small seas or where breaking waves are likely to impact. The bags could also be designed to be sacrificial in the event of breaking waves similar to the breakaway collector head described in Section 6.4.6.

This design has at present not been physically tested or mathematically modelled and may have significantly different power absorption characteristics from a solid collector. In addition durability of the bags is a concern. Advantages include a highly modular design and a low weight collector reducing transport and installation costs.

6.4.6 Breakaway Collector Head

Assuming that the probability of high loads is very small a pre-determined method of failure can be used to allow the device to fail in a pre-determined manner. The most common method of allowing failure is through the use of shear bolts or pins and would probably allow the collector head to detach from the arm. A slight negative buoyancy would allow the collector head to sink and hence not pose a hazard to shipping. Serious consideration would have to be given to the likely costs of recovering and reinstalling a collector head.

6.4.7 Summary of Survival Methods

Table 11 summarises the survival concepts and their relative merits. Detailed cost modelling of each solution has yet to be undertaken and the final design will be a compromise between economics against probability. The next project phase will determine these probabilities of breaking waves and the magnitude of their associated loads.

Design	Simplicity	Potential to survive breaking waves	Potential to survive freak waves	Modulated power generation possible	Relative Cost (✓✓✓=cheapest)	Notes
Free to swing	✓✓✓	✓	✓✓✓	✓	✓✓✓	Easy to achieve, if it can be built strong enough to survive all possible conditions.
Fixed to seabed	✓✓	✓	✓		✓✓	High loadings possible under storm conditions.
Lowering collector head	✓	✓✓	✓	✓✓✓	✓	Potentially difficult to design. Unmodelled.
Reduction in collector head area	✓	✓✓✓	✓✓✓	✓✓✓	✓	Potentially complex with many exposed moving components. Unmodelled.
Inflatable collector	✓	✓✓✓	✓✓✓	✓✓✓	✓	Unmodelled for power collection and durability.

Table 11 – Summary of survival modelling

6.5 Summary

Loads from green waves on the EB Frond allow the present design to remain feasible with only minimal preventative action required to keep stresses reasonable. A free swinging survival method can be designed to withstand these forces, although confirmation through modelling that this new design does not impact on the seabed is required.

Breaking waves will occur in the region of the EB Frond. Should these break on or close to the EB Frond large impact pressures will occur. For the next project phase work is planned to mathematically model and physically scale test the intricacies of breaking and freak waves in the region around EB Frond. This information will allow detailed costing analysis of device survival against overall economics to be determined.

The choice of collector head survival strategy has therefore been deferred until a more detailed analysis on breaking wave impact forces can be performed.

7 ECONOMIC MODEL

7.1 Introduction

The case for taking the EB Frond project from the present research phase to full-scale commercial exploitation can only be made if the basis of projected cost of energy generated and supplied to the electrical distribution network is fully understood. It is expected that this understanding will develop through various stages, with cost estimates being refined at each stage and in the light of changing electricity market forces.

The broad technical stages foreseen are:

- Intermediate (1/6th) scale model testing
- Manufacture and deployment of a full-scale ocean demonstrator (probably with 150kW output)
- Establishment of a pre-commercial wave energy farm (probably 10 machines each of 500kW output)
- Establishment of larger wave energy farms (possibly up to 100MW each).

Development of the technology is not yet sufficiently advanced for meaningful estimates to be made beyond the pre-commercial farm stage. The analysis which follows is concentrated on that stage.

7.2 Energy Capture Estimates

7.2.1 Machine Characteristics

In this economic modelling, a uniform machine design operating in 30m water depth is used. The machines are assumed to use a full-scale triangular cross-section collector. They are assumed to have a collector top thickness of 9.050m, a bottom thickness of 2.500m, a width of 15.750m and a draught of 7.625m.

7.2.2 Site Characteristics

The wave energy resource is generally quoted as an annual average expressed in kilowatts per metre width of wave-front. In practice, the near-shore resource (which EB Frond is designed to tap) is usually less than the deep, offshore resource. Many factors contribute to this reduction, and most are highly dependent on the specific characteristics of a particular site. These factors include:

- Local sea bed topography
- Directionality of incoming wave energy
- Refraction effects
- Tidal range
- Currents

Some possible sites could be proposed from published data, but extensive surveys will be needed to determine the most favourable locations. The cost of surveys is not known at this stage, and is not included at present.

7.2.3 Wave Resource

Measured and projected wave data for the present analysis has been taken for three sites:

- Orkney, 30m depth derived data. (Point RP30S [OS datum 320882.1, 1009187.2] in HR Wallingford report EX4471 for the European Marine Energy Centre)
- South Uist, 40m depth actual data (derived from ETSU report WV1683).
- Horns Rev, North Sea, 30m depth (taken from Annex II.2 RAMBOLL , Denmark, draft report to IEC, Feb 2002. Table 2.2)

The data has been reduced to a common format using a system of bins. The period bins are each 1 second wide and the wave height bins 0.5m in extent, as shown in Figure 68, Figure 69 and Figure 70 below.

The original data for South Uist was reduced from tabulated form without further smoothing to give the results in Figure 69.

Hs (m) (Bin Centre)	Mean Wave Period (s) (Centre of Bin)														Total Hours
	2.5	3.5	4.5	5.5	6.5	7.5	8.5	9.5	10.5	11.5	12.5	13.5	14.5	15.5	
<1	87	591	1176	621	227	95	46	22	6	1	1				2873
1.25	58	666	586	217	83	23	8	2							1645
1.75	14	233	701	218	73	28	10	2				1			1281
2.25	2	44	496	310	73	22	14	4	1						965
2.75		6	155	419	82	19	8	4	2						696
3.25			26	268	161	23	7	2	1	1					489
3.75			3	85	190	30	7	2	1						320
4.25				14	125	52	7	2	1						201
4.75				2	41	61	10	2	1						117
5.25					6	46	13	1	1						66
5.75					1	20	15	1							38
6.25						6	13	5							25
6.75						1	10	6							18
7.25							5	8							14
7.75							3	4	1						8
8.25							1	3	2						5
8.75								2	1						3
9.25									1						1
9.75										1					1
10.25															1
10.75															
11.25															
11.75															
12.25															
12.75															
Sum	87	665	2125	2589	1761	930	376	153	56	15	5	1	1		8766

Data in hours per year (rounded)

Figure 68 - Orkney RP30S Wave Data (30m depth)

Hs (m) (Bin Centre)	Mean Wave Period (s) (Centre of Bin)													Total Hours	
	2.5	3.5	4.5	5.5	6.5	7.5	8.5	9.5	10.5	11.5	12.5	13.5	14.5		15.5
<1															207
1.25				278	802	414		117							1611
1.75			369	388		1133	44	275	160	32					2400
2.25									14						14
2.75					264	769	94	266	208	25					1626
3.25					279	97			313	36					725
3.75						26	303	61							391
4.25						180	523	74	105	386					1268
4.75						182									182
5.25							30					53			82
5.75															
6.25								46							46
6.75								63	32	27	18				141
7.25															
7.75															
8.25									28						28
8.75													5		5
9.25												16			16
9.75															
10.25											24				24
10.75															
11.25															
11.75															
12.25															
12.75															
Sum			369	666	1345	2801	1057	872	855	497	24	68	5		8766

Data in hours per year (rounded)

Figure 69 - South Uist Wave Data (40m depth)

Hs (m) (Bin Centre)	Mean Wave Period (s) (Centre of Bin)													Total	
	2.5	3.5	4.5	5.5	6.5	7.5	8.5	9.5	10.5	11.5	12.5	13.5	14.5		15.5
<1	594	1504	1116	167	48	14	7	6							3456
1.25	10	870	1002	137	40	13	6	5							2083
1.75		1	318	606	13	2		2							941
2.25			317	605	13	1		1							936
2.75			1	148	269	2		1							421
3.25				148	269	1									418
3.75					104	77									181
4.25					104	77									181
4.75						52	6								58
5.25						51	6								57
5.75						1	13								14
6.25						1	13								14
6.75							2	1							3
7.25							2	1							3
7.75															
8.25															
8.75															
9.25															
9.75															
10.25															
10.75															
11.25															
11.75															
12.25															
12.75															
Sum	604	2375	2754	1810	860	292	55	17							8766

Data in hours per year (rounded)

Figure 70 - North Sea, Horns Rev, Wave Data (30m depth)

The average powers, per metre width of wavefront, are 17.0kWm^{-1} , 40.4kWm^{-1} and 10.6kWm^{-1} at the Orkney, South Uist and Horns Rev sites respectively.

Examination of predicted Orkney nearshore data showed that wave energy reduction from 50m to 30m depth was 20% where the 30m point was near a reflecting shoreline but only 6% with a gentle slope from the 30m point to the shore. There is thus some difficulty in predicting the reduction of energy from 40m to 30m at South Uist, but the assumption has been made that it would be reduced by 4% and this figure is applied later in the calculations to the annual mechanical power capture (as a constant factor of 0.96).

7.2.4 Gross Power Capture

Three different models have been used for power capture by EB Frond. All models assume that the power which can be transferred from the oscillating arm to the compression and extension of hydraulic cylinders in the PTO has an upper limit determined by the mechanical and hydraulic design, and that beyond this point the stresses and oil pressures will not increase. For the pre-commercial farm machines the limit (or power 'cap') is taken as 500kW average power, and the cost estimates are derived from this.

In all models, an energy capture 'window' is assumed within which power is generated. No power generation is assumed outside the window, which extends from 1 to 6m significant wave height and from 5 to 12 seconds mean wave period. Common to all models is the 500kW power capping in a sea with 3m significant wave height and 8 second mean wave period. In practice, the power capture window may extend beyond the 'rectangular' form shown in the tables, and machine characteristics may be adjusted to suit particular sites, but for the present the 'window' is as shown in Figure 71, Figure 72 and Figure 73.

The three models are derived from collection efficiencies.

Collection width efficiency is defined by:

$$\eta_{CW} = \frac{P_C}{P_{WF}W}$$

Where:

P_C is the mechanical power collected by EB Frond

P_{WF} is the power of incoming wave per metre width of wave-front

W is the width of EB Frond collector perpendicular to direction wave propagation

Point absorber efficiency is defined by:

$$\eta_{PC} = \frac{P_C}{P_{PA}}$$

Where:

P_C is the mechanical power collected by EB Frond

P_{PA} is the theoretical power available to a true surging point absorber

7.2.4.1 Simple Collection Width Power Flux Model

In this early model, collection width efficiency was assumed to be constant at 50%, and the energy taken from a particular modified Pierson-Moskowitz (ISSC) sea-state was assumed to be proportional to the mean wave period and proportional to the square of the significant wave height. It is recognised that this model underestimates the efficiency in less energetic spectra, but any overestimate of efficiency in more energetic conditions is removed because the power is capped. The resulting power capture table for the energy capture window is shown in Figure 71.

Hs (m) (Bin Centre)	Mean Wave Period (s) (Centre of Bin)													
	2.5	3.5	4.5	5.5	6.5	7.5	8.5	9.5	10.5	11.5	12.5	13.5	14.5	15.5
<1														
1.25				60	71	81	92	103	114	125				
1.75				117	138	160	181	202	223	245				
2.25				193	229	264	299	334	369	404				
2.75				289	341	394	446	499	500	500				
3.25				403	477	500	500	500	500	500				
3.75				500	500	500	500	500	500	500				
4.25				500	500	500	500	500	500	500				
4.75				500	500	500	500	500	500	500				
5.25				500	500	500	500	500	500	500				
5.75				500	500	500	500	500	500	500				
6.25														
6.75														

Machine Outputs in kilowatts

Figure 71 - Power output (kW) – Simplified Collection Width Model

7.2.4.2 Modified Collection Width Power Flux Model

Experimental results from physical modelling included variation of collection width efficiency in a number of sea-states, though wave height and period were not varied independently in the tests. To forecast efficiency based on collection width, two matrices were produced from the data. In one matrix the efficiency values were assumed dependent solely on wave period, and in the other dependent solely on wave height.

The two matrices were averaged to give an assumption of efficiency at each value of period and wave height. A power capture table was then produced and the outputs capped at 500kW. This is shown in Figure 72.

Hs (m) (Bin Centre)	Mean Wave Period (s) (Centre of Bin)													
	2.5	3.5	4.5	5.5	6.5	7.5	8.5	9.5	10.5	11.5	12.5	13.5	14.5	15.5
<1														
1.25				74	85	95	104	113	121	128				
1.75				140	161	180	197	213	227	239				
2.25				224	256	286	313	337	359	378				
2.75				322	368	410	448	482	500	500				
3.25				432	493	500	500	500	500	500				
3.75				500	500	500	500	500	500	500				
4.25				500	500	500	500	500	500	500				
4.75				500	500	500	500	500	500	500				
5.25				500	500	500	500	500	500	500				
5.75				500	500	500	500	500	500	500				
6.25														
6.75														

Machine Outputs in kilowatts

Figure 72 - Power output (kW) – Modified Collection Width Model

7.2.4.3 Point Absorber Model

The physical modelling results also included efficiency relative to the theoretical power resource available to a point absorber. Again, data was not collected independently for period and height, so efficiencies were estimated for all wave states. Power outputs were calculated, by applying estimations of the devices point absorber efficiencies to the point absorber resource. Power estimations were capped for the complete wave period and wave height matrix as described above for the modified collection width model. The power capture table is shown in Figure 73.

Hs (m) (Bin Centre)	Mean Wave Period (s) (Centre of Bin)													
	2.5	3.5	4.5	5.5	6.5	7.5	8.5	9.5	10.5	11.5	12.5	13.5	14.5	15.5
<1														
1.25				139	133	131	131	134	138	143				
1.75				244	226	216	212	212	214	218				
2.25				376	342	321	309	304	303	305				
2.75				500	481	446	424	411	405	403				
3.25				500	500	500	500	500	500	500				
3.75				500	500	500	500	500	500	500				
4.25				500	500	500	500	500	500	500				
4.75				500	500	500	500	500	500	500				
5.25				500	500	500	500	500	500	500				
5.75				500	500	500	500	500	500	500				
6.25														
6.75														

Machine Outputs in kilowatts

Figure 73 - Power Output (kW) – Point Absorber Model

7.2.4.4 Mechanical Energy Capture

The annual mechanical power capture for each site using each power collection model was obtained by multiplying the wave resource table by the power output table and summing the resultant bin outputs to give energy capture in kWh per year. As an example, the detailed calculation for the South Uist (40m depth) site using the point absorber power collection model was made by multiplying the values in Figure 69 by those in Figure 73. The result is shown Figure 74.

Hs (m) (Bin Centre)	Mean Wave Period (s) (Centre of Bin)													Total	
	2.5	3.5	4.5	5.5	6.5	7.5	8.5	9.5	10.5	11.5	12.5	13.5	14.5		15.5
<1															
1.25				38737	106590	54107		15737							215171
1.75				94647		244723		9293	58249	34110	6875				447896
2.25										4247					4247
2.75					126907	342682	39770	109610	84139	10253					713361
3.25					139379	48651			156473	17970					362474
3.75						13149	151652	30681							195482
4.25						89852	261665	36817	52596	192852					633782
4.75						91166									91166
5.25							14902								14902
5.75															
6.25															
6.75															
7.25															
7.75															
8.25															
8.75															
9.25															
9.75															
10.25															
10.75															
11.25															
11.75															
12.25															
12.75															
Sum				133384	372876	884331	477282	251093	331565	227950					2678481

South Uist, PA Model kWh per year

Figure 74 - Annual Energy Capture – South Uist Site, assuming point absorber model

The results for the three sites and three models are shown in Table 12 columns (a) (b) and (c). Note that units have been changed to MWh per year.

The three South Uist results have been factored to reflect the 4% reduction from 40m to 30m depth; so, for example, the point absorber model output from Figure 74, 2678481 kWh per year, has become:

$$2678 \times 0.96 = 2571 \text{ MWh per year.}$$

Site	Simple Collection Width Model (a)	Modified Collection Width Model (b)	Point Absorber Model (c)	Assumed Energy Capture (b + c) / 2 (d)
South Uist (30m)	2335	2410	2571	2491
Orkney	1231	1315	1642	1479
N Sea (Horns Rev)	776	833	1070	952

Table 12 - Gross Annual Energy Capture Results (MWh per year)

Predictions from the point absorber model are assumed to be the most valid. Physically modelled tests have shown that EB Frond collection width efficiencies greater than unity are achieved in some cases, so it is apparent that an element of point absorber effects may be present.

Predictions from the modified collection width model and point absorber model are of the same order but the strength of their agreement is site dependent and also depends on the predominant sea-states.

Taking these factors into account, the simplified collection width model results have been ignored, and the gross annual energy captured has been assumed to be the mean of the modified collection width and point absorber models shown in column (d) of Table 12.

7.2.5 Energy Losses – Marine Climate

In the gross energy capture calculations above, no allowance is made for variations in incoming wave direction, for 3-D seas (wave conditions other than long-crested and two-dimensional), or for the effects of currents and tides. These are seen as the main factors in reducing the energy available to an EB Frond installation, though long-term temporal variation in incident wave energy will also be a factor.

In the nearshore environment where EB Frond will operate, the effects of wave direction and 3-D seas will be dependent on the characteristics of a specific site. Shelter, nature of shoreline and local seabed topography will all contribute to modifying wave conditions. Since these are site specific, measurements must be

taken and any assumptions made at this stage could be misleading. These factors have therefore been ignored at this stage.

Results of studies made into the possible effects of currents and of tides are given below.

7.2.5.1 Tidal Currents

It is not intended that an EB Frond farm should be built at a site where strong currents occur, but the presence and effect of currents cannot be ignored. A study carried out in Phase one of the project showed that the superposition of a 1m/s current (which is probably the maximum that should be considered) on a wave spectrum with significant wave height 3m and peak period 6.85s reduced the output of EB Frond by 14%. Since any tidal currents will be cyclic, a 5% overall energy loss for currents has been assumed.

7.2.5.2 Tidal Range

Tidal range effects have been considered in more detail because they will affect all ocean shore sites. Tides have the potential for changing wave states in relatively shallow water, but this is seen as a minor factor compared with the depth variations they produce, which change the freeboard of the EB Frond collector. It is possible to design a system in which the collector can be moved up and down the arm to discrete positions at intervals of one or two hours, but the cost of this must be weighed against the benefits.

Physical model tests have led to a better understanding of the effects of the position of the collector relative to the still water surface on energy capture by EB Frond. Since the wave energy in the water decreases with depth, the energy available for conversion is correspondingly reduced as the collector becomes submerged. If the collector protrudes too far from the surface, the proportion of "dry" area not interacting with the water increases, so again the power reduces. For each value of wave height there will be an optimum depth of collector for energy capture.

Tidal ranges for a number of European Atlantic locations shown in Figure 75, were established from published tables and are given in Figure 76.



©Microsoft and/or its suppliers. All rights reserved.

Figure 75 - Locations of Tidal Range Data in Figure 76

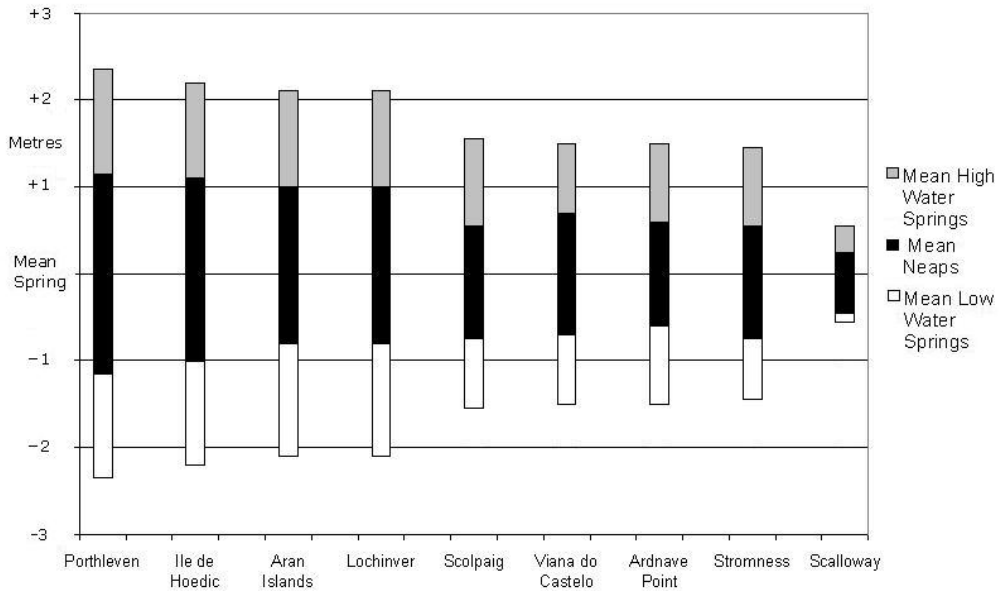


Figure 76 - Tidal Ranges, European Atlantic Coast Locations

Large tidal ranges may be accompanied by strong currents, and the combination of the two effects at a site may mean it is not an ideal location for EB Frond, though the site may not be excluded for tidal effects alone. To investigate the effect of collector freeboard and submergence on energy collection by EB Frond, it was decided that an overall range of about $\pm 1.5\text{m}$ should be considered.

A full set of tide predictions for a 6 month period was plotted for a standard port, Wick, with about $\pm 1.5\text{m}$ overall range. Water heights at 10 minute intervals in the six month period were found by sinusoidal interpolation, and these heights are shown in Figure 77. The right hand extreme of the time base has been expanded ten times to show individual tides.

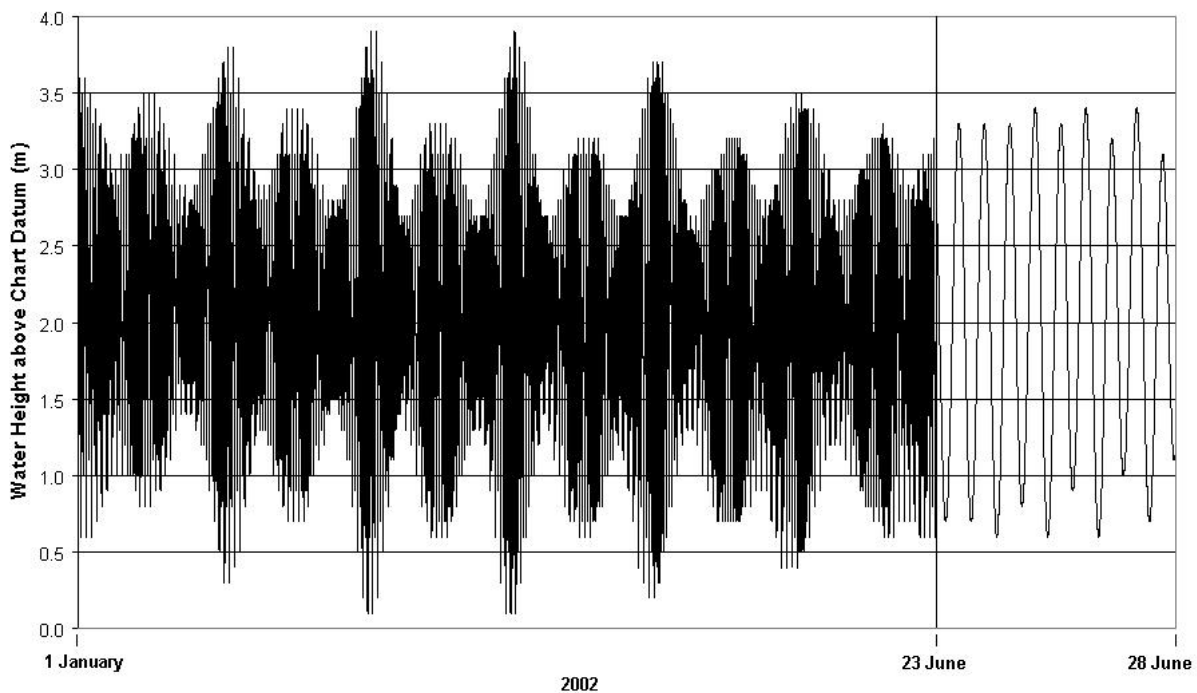


Figure 77 - Water Heights, Wick, January – June 2002

Assuming EB Frond to be operating with a fixed freeboard in a constant sinusoidal wave regime with 1.25m, 8s period waves, the power collected at the Wick site over the 6 month period was calculated for a range of freeboard settings. The power output at different freeboards was taken by linear interpolation from the results of physical modelling at Lancaster (see Figure 38). The results are shown in Figure 78. At the optimum fixed collector freeboard setting in 1.25m waves, only 85% of power is collected, representing a 15% loss.

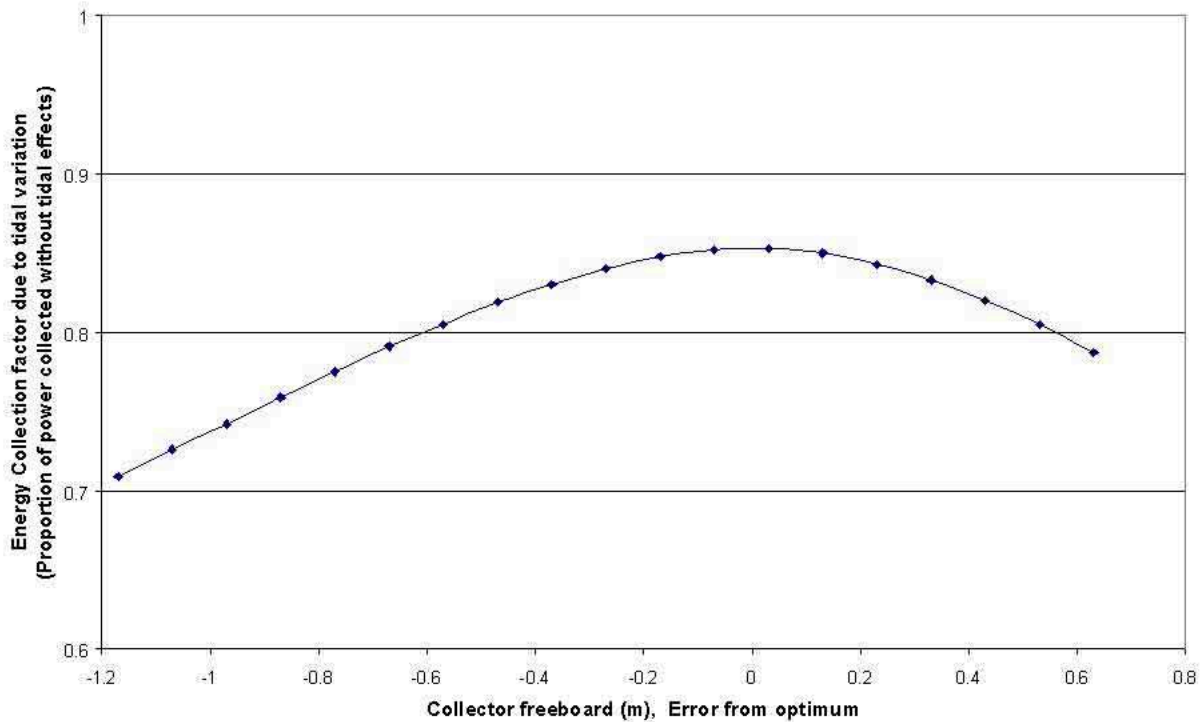


Figure 78 - Energy collection loss for tidal (depth) variation

This analysis was carried out for one wave type only. The nature of power output / freeboard variation with wave height and period is discussed in section 5.7.3.1 and the calculation above indicates that at least 15% of the energy which is potentially available for collection will be lost.

At this early stage of development, the costs of including collector height variation in the EB Frond system have not been quantified, and a 15% reduction factor in energy collection for tidal variation has been assumed. It may be that the capital cost to remove this factor is less than 15%. Tidal variation is also not the only effect on this element of the design; in particular there may be a need to lower the collector on the arm as part of the survivability design.

7.2.6 Machine and Electrical Losses

EB Frond is designed to have a hydraulic transmission, with a cylinder pivoted on the base resisting the motion of the collector arm. The restoring force on the arm will also be provided by an arrangement of hydraulic cylinders. An electric generator will be powered by the hydraulic transmission. Control power for the restoring force system will be derived from a separate power unit.

Separate control systems for each machine and for the combination of machines in a farm will each have imperfections, which will lead to losses.

EB's experience with the Stingray tidal stream generator, which uses similar systems to those envisaged for EB Frond, leads to the following estimates being made:

	Loss %
Hydraulic transmission	
Pivots, cylinders & pipework	4.0
Motor, volumetric	5.0
Motor, mechanical	5.0
Hydraulic restoring force system	
Pivots, cylinders & pipework	4.0
Electric Motor and drive losses	14.5
Control system imperfection	5.0

Taking each of these losses, converting them to efficiencies and combining them, leads to an overall proportional efficiency figure due to machine and electrical losses of 67.6%, or a proportional loss of 32.4%.

Energy consumed by a hydraulic power unit and other services on each 500kW EB Frond machine is estimated as 10kW with an 80% duty. This equates to 8kW continuous power, or $8 \times 8766 / 1000 = 70\text{MWh}$ per year.

7.2.7 Cyclic Power Variation, Multi-Machine Outputs and Power Transmission

EB Frond is an oscillating device operating almost entirely in surge, and the transfer of energy from waves to the machine will be cyclic. Whereas a combination of oscillating tidal stream energy converters can in principle be controlled so that their aggregate output variation is minimised, output from many wave energy converters including EB Frond is driven by the instantaneous wave forces acting on them. Unless smoothed by using energy storage, substantial variations may occur in the output of a combination of machines and these variations will occur within the wave period – that is over a period of a few seconds.

To simulate an array of EB Frond machines, a model was generated in which machines can be positioned at various locations within a rectangular grid. The overall size of the grid exceeds the wavelength of an incoming wave of 12s period. The spacing of machines within the grid can be varied. By summing the machine outputs in varying wavelengths of incoming waves, the change in the total output can be derived.

Results from this model with ten machines have shown that the power output during a wave cycle may vary by up to 40% due solely to the effects of machine position and wavelength. As the wavelength is not controllable and machine positions will be fixed, an optimum can be sought for the wave climate of a particular site.

Large energy storage capability may be necessary to overcome the effects of these factors altogether and so present a power delivery profile, which is acceptable for connection to the grid. As an alternative to storage, it is possible to reduce variations by using a control system to truncate machine outputs. One approach requires additional capital cost, the alternative simply reduces energy output.

With no firm data, an estimated overall reduction of 5% in energy output has been assumed to account for cyclic and multi-machine effects.

For electrical transmission and connection losses, EB's work on Stingray leads to the following estimates:

DC bus losses to shore	1.5%
Power conditioning for connection	2.0%

7.2.8 Summary – Nett Annual Energy Estimates

Taking the gross power capture from Section 7.2.4 and applying the estimates in 7.2.4 to 7.2.6 above gives the following detailed calculation for South Uist if all machines are assumed to be available 100% of the time:

	Loss %	Efficiency	Cumulative Efficiency	MWh per year
Gross capture per machine				<u>2491</u>
Less Reductions for marine climate				
Currents	5	0.95		
Tides	15	<u>0.85</u>		
Overall Marine Climate Efficiency (product)			<u>0.808</u>	
Less Reductions for Machine & Electrical losses				
Transmission: Pivots, cylinders & pipes	4	0.96		
Transmission: Motor, volumetric	5	0.95		
Transmission: Motor, mechanical	5	0.95		
Restoring Force: Pivots, Cyls & Pipes	4	0.96		
Electric Motor & Drive losses	14.5	0.855		
Control system imperfection	<u>5</u>	<u>0.95</u>		
Overall machine & electrical efficiency (product)			<u>0.676</u>	
Total collection & conversion efficiency (0.808 x 0.676)			<u>0.546</u>	
Nett capture per machine			(0.546 x 2491)	1360
Less Machine services			<u>70</u>	
Nett delivered energy per machine				<u>1290</u>
Total farm output (before conditioning)		10 machines		<u>12900</u>
Less				
Cyclic & multi-machine output reduction	5	0.95		

DC bus	1.5	0.985	
Power conditioning	2	0.98	
Overall efficiency (product)			<u>0.917</u>
Total energy delivered to grid		(0.917 x 12900)	<u>11829</u>

Similar calculations have been carried out for the Orkney and North Sea sites. The results for all sites are shown in Table 13.

Site	Predicted Energy Output (MWh per year) 5MW Farm, 100% Machine Availability
South Uist	11,829
Orkney	6,767
North Sea (Horns Rev)	4,127

Table 13 - Annual Energy Outputs

7.3 Capital and Operating Cost Estimates

The cost of building, testing and installing ten 500kW output EB Frond machines has been estimated using EB's standard system used for commercial contracts, but with minimum overhead recovery on labour rates and with no profit element included. This is the same basis as has been used by EB in the latest estimates for the Stingray tidal stream generator.

The design of EB Frond and its installation system are only just beyond the conceptual stage, and many assumptions have had to be made. In the previous Phase one study, the capital cost (including overheads and a profit element) was calculated as £13.96 million. The present calculation with minimum overheads and no profit has yielded a figure of £16.30 million, as shown in Table 14. The changes included in the table have occurred because machine complexity and weight have both increased, and there has been an increase in estimates for the installation hardware and marine costs.

Wave Farm Cost Estimates	Design & Staff Costs	Bought Out Costs	Total Cost
Totals for 10machines, each 500kW			
Fabrications and mechanical parts	170,000	4,843,000	5,013,000
Foundations	32,000	2,400,000	2,432,000
Hydraulics	110,000	1,270,000	1,380,000
Subsea electrics	88,000	325,000	413,000
Subsea drive	99,000	786,000	885,000
Topside power & control	103,000	414,000	517,000
Machine build costs	177,000	1,373,000	1,550,000
Handling system	78,000	500,000	578,000
Farm shore station	16,000	115,000	131,000
Farm connecting cables	26,000	803,000	829,000
Installation of machines	24,000	1,508,000	1,532,000
Removal of machines	19,000	772,000	791,000
Project management	45,000	210,000	255,000
Total Estimated Capital Cost	<u>987,000</u>	<u>15,319,000</u>	<u>16,306,000</u>
Annual operating cost	67,000	125,000	192,000
Annual maintenance cost	34,000	193,000	227,000
Total Estimated Annual Costs	101,000	318,000	419,000

Table 14 – Capital and Annual Operating Cost Estimates

As noted in Section 6.2.4, a reduction of 15% has been made for lower energy output due to tidal effects. By constructing the EB Frond machine so that the complete collector can be moved up or down the arm and fixed in an optimum position, this 15% factor could be removed. A further advantage of having a system which allows the collector to be moved is that this feature can form part of the survivability strategy.

At present the 15% reduction in power has been retained, and no separate cost has been shown specifically for survivability systems.

7.4 Energy Cost Modelling

The unit cost of electricity produced by EB Frond is central to the future of the project, both as a comparison with costs from other generating systems and as a means of attracting investment in the development and exploitation of the technology.

A cost model has been used in which a discounted cash flow (DCF) method is used to calculate the unit energy cost. The model is designed for use in many phases of the project, not simply the proposed 5MW farm of ten machines. Previous models have included inputs to account for assumptions on inflation, on tax allowances and

on the use of ROCs. These have been removed, and the model now has the following inputs:

- Nominal EB Frond machine output (MW)
- Number of machines installed
- Capital cost of design, manufacture and construction
- Capital Grant (if available)
- Percentage of capital cost defrayed on installation of farm
- Annual operating and maintenance costs
- Annual energy output per machine (MWh per year)
- Machine availability
- Discount rate
- Operating life

The model produces the following outputs:

- Unit cost of energy (p/kWh)
- Capital cost of installed capacity (£/MW)
- Capacity factor – the annual machine energy output (MWh per year, assuming 100% availability) divided by the nominal installed capacity (MW) multiplied by 8766 (hours per year).
- Annual farm energy production (MWh) after the effect of machine availability.

The outputs of the model for the South Uist site is shown in Figure 79, and the calculated unit costs of energy for various discount rates for the three sites are given in Table 15.

EB Frond cashflow model		Farm - 500kW machines x10	
Capital costs (£million)			
Installed cost	16.306	Note 2	
Cost per MW installed	3.261		
Capital grant %	0.0%	Note 3	
Capex on installation	95.0%		
Operating & Maintenance costs			
Percentage of installed capital cost	2.6%		
Annual O&M cost (£,000/yr)	419		
Output efficiency (%)			
Delivered Output per machine (MWh/yr)	1,183	Note 1	
Capacity Factor	27.0%		
Availability	95%		
Annual farm production (MWh)	11,238		
Capacity (MW)			
Nominal device capacity	0.5		
Number of devices	10		
TOTAL installed capacity (MW)	5		

Discount rate of	UNIT COST (p/kWh)
0%	9.53
5%	13.66
8%	16.74
10%	18.99
15%	25.09

Notes

1. Outputs from C128-03-0081.AL
2. Costs from C128-03-0082 Capital Cost 5MW farm Rev 260704
3. Capital grant is on percentage of costs incurred on installation

Figure 79 - DCF Calculation detail – South Uist site

Site	Delivered Output of Farm (MWh/yr)	Unit Cost (p/kWh) at discount rate of:-				
		15%	10%	8%	5%	0%
South Uist	11,238	25.11	19.00	16.75	13.67	9.54
Orkney	6,429	43.86	33.19	29.27	23.88	16.66
North Sea	3,924	71.86	54.39	47.95	39.13	27.30

Table 15 – Cost in pence per kWh of electricity produced at three locations, with various discount rates

7.5 Summary

Recognising that as EB Frond technology is developed the cost of electricity delivered by it can be expected to fall, the present economic analysis had as its aim the prediction of unit energy cost from a 5MW pre-commercial farm of ten EB Frond machines.

In the absence of information on the effects on output of wave direction and 3-D seas, these factors (which may have a significant effect) have been ignored.

The main conclusions that can be drawn are:

- For a high-energy wave site such as South Uist, the baseline predicted cost of energy delivered to the grid with an 8% discount rate is about 17p per kWh.
- The costs at sites with lower incoming wave energy are proportionally higher if the same design of EB Frond is used.
- It will be necessary to optimise the machine design for lower energy sites, particularly by increasing the collector width.
- For a pre-commercial demonstration farm (as the 5MW farm would be), a unit energy cost of 17p/kWh is believed to be an acceptable indicator of the potential for commercial viability. Subsequent increases in installed capacity and hence experience, investment, technological advances, etc) will result in the potential for the EB Frond unit energy costs to move down the experience curve to a level of commercial viability.

8 DEVELOPMENT ROUTE TO FULL-SCALE PRODUCTION

8.1 Limitations of Current Understanding

EB Frond has moved forward significantly from the original Frond concept developed by Lancaster University. However, there is still a lot to learn beyond the basic tank testing and rudimentary mathematical modelling undertaken to date. Specific areas where knowledge of EB Frond is known to be limited are:

- Performance in a variety of sea-states
- Predicting real sea performance without using real seas
- Benefits of collector protruding above the water surface
- Effects and survival of extreme seas – storms, limiting wave heights, breaking waves
- Physical testing of effects of tidal currents and wave directionality in realistic sea spectra
- Development of full-scale concept for a real-sea environment
- Better understanding of the real wave environment and behaviour
- Site characterisation
- Environmental and stakeholder impacts of EB Frond
- Performance at larger scales and understanding of scaling effects
- Accuracy of mathematical model for prediction of full-scale performance
- Other things that I can't think of yet
- Reliability and maintenance strategy
- Further work on deployment and recovery
- Survey, deployment and cable lay techniques in high-energy wave environments
- Effects and control of marine fouling
- Financial support – development of a mechanism whereby a concept such as EB Frond can be realised in a commercial environment

8.2 Proposed Development Route

To take the EB Frond concept through to commercial reality, the following development route is proposed:

- (i) Small-scale testing – there may be a benefit from further small-scale testing to demonstrate repeatability and check less certain data points
- (ii) Intermediate-scale modelling – ideally at least 1/6th scale, if a suitable facility is available, to check performance in extreme seas and for review of scaling effects
- (iii) Site Characterisation
- (iv) Environmental Impact Appraisal
- (v) Full-scale demonstrator – ideally grid connected, to demonstrate the full scope of an EB Frond – installation, operation and maintenance, reliability, power generation and decommissioning
- (vi) Full-scale pre-commercial demonstrator farm – grid connected

However, at this stage, EB has decided to put the development of EB Frond, and its other marine renewable generating technologies, on hold until such a time that a clear development route exists within a commercial framework.

9 CONCLUSIONS

During the course of the project EB developed and had externally verified a mathematical model of the EB Frond, which was used to predict the performance of the device with a range of different collector shapes and then to optimise its shape and dimensions. Physical model testing at 1/25th scale was carried out to confirm these predictions. These results, together with an investigation of survivability strategies in extreme wave conditions, fed into an economic model that predicted the unit energy cost of electricity produced by a pre-commercial 5MW demonstrator farm comprising ten EB Frond machines. The results of this work show that:

- In sinusoidal waves, there is good agreement between the EB time domain mathematical model predictions and physical model tests of maximum power output.
- In comparisons between the corrected linear model and the EB time domain model, agreement with the same physical tests produced a maximum power output estimation error of a 61% overestimation for the time domain model compared to an overestimation from the corrected linear model of 1556%.
- In random two dimensional waves (Pierson-Moskowitz spectra), the EB time domain model predicted average maximum power outputs, over a long period, which were less than twice the results of the physical model.
- Review of the survivability strategies could not lead to a conclusion without further physical modelling and parallel design study.
- The predicted unit cost of electricity produced by a pre-commercial 5MW demonstrator EB Frond wave farm located at a high energy wave site with 25 year machine life, assuming no contribution from ROCs, no profit element in construction, and 8% discount rate, is about 17p/kWh.
- The cost of electricity produced by EB Frond is likely to reduce in line with technology experience / cost curves published for a number of technologies.